creative commons
COMMONS DEED

저작자표시-비영리-변경금지 2.0 대한민국

이용자는 아래의 조건을 따르는 경우에 한하여 자유롭게

- 이 저작물을 복제, 배포, 전송, 전시, 공연 및 방송할 수 있습니다.

다음과 같은 조건을 따라야 합니다:

저작자표시. 귀하는 원저작자를 표시하여야 합니다.

비영리. 귀하는 이 저작물을 영리 목적으로 이용할 수 없습니다.

변경금지. 귀하는 이 저작물을 개작, 변형 또는 가공할 수 없습니다.

- 귀하는, 이 저작물의 재이용이나 배포의 경우, 이 저작물에 적용된 이용허락조건을 명확하게 나타내어야 합니다.
- 저작권자로부터 별도의 허가를 받으면 이러한 조건들은 적용되지 않습니다.

저작권법에 따른 이용자의 권리는 위의 내용에 의하여 영향을 받지 않습니다.

이것은 이용허락규약(Legal Code)을 이해하기 쉽게 요약한 것입니다.

Disclaimer

dCollection

공학박사 학위논문

로봇 매니퓰레이터의 고장 진단 및 고장 인내제어 방법 개발

DEVELOPMENT OF FAULT DIAGNOSIS AND FAULT-TOLERANT CONTROL METHODS FOR ROBOT MANIPULATORS

지도교수 강희준

이 논문을 공학 박사 학위 논문으로 제출함

2022 년 8 월

울산대학교 대학원

전기전자컴퓨터공학과

NGUYEN VAN CUONG

Nguyen Van Cuong 의 공학 박사 학위 논문을 인준함

심사위원장 김한실 (인)

심사위원 조강현 (인)

심사위원 서영수 (인)

심사위원 강현덕 (인)

심사위원 강희준 (인)

울산대학교 대학원

전기전자컴퓨터공학과

2022 년 8 월

Doctor of Philosophy

DEVELOPMENT OF FAULT DIAGNOSIS AND FAULT-TOLERANT CONTROL METHODS FOR ROBOT MANIPULATORS

The Graduate School of the University of Ulsan

Department of Electrical, Electronic and Computer Engineering

NGUYEN VAN CUONG

DEVELOPMENT OF FAULT DIAGNOSIS AND FAULT-TOLERANT CONTROL METHODS FOR ROBOT MANIPULATORS

Supervisor: Professor KANG HEE-JUN

A Dissertation

Submitted to

The Graduate School of the University of Ulsan
in partial Fulfillment of the Requirements
for the Degree of Doctor of Philosophy

by

NGUYEN VAN CUONG

Department of Electrical, Electronic and Computer Engineering

University of Ulsan, Korea

August 2022

DEVELOPMENT OF FAULT DIAGNOSIS AND FAULT-TOLERANT CONTROL METHODS FOR ROBOT MANIPULATORS

This certifies that the dissertation of NGUYEN VAN CUONG is approved

Professor Han-Sil Kim

Committee Chair

Professor Kang-Hyun Jo

Committee Member

Professor Young Soo Suh

Committee Member

Professor Hyun-Deok Kang

Committee Member

Professor Hee-Jun Kang

Committee Member

Department of Electrical, Electronic and Computer Engineering

University of Ulsan, Korea

August 2022

VITA

NGUYEN VAN CUONG was born in Thua Thien Hue province, Vietnam on October 16, 1991. He received his B.S. degree in Electronics and Telecommunications Engineering from the Danang University of Technology, Danang city, Vietnam, in 2014.

In February 2016, he began working full-time towards a Ph.D. degree in the Department of Electrical, Electronic and Computer Engineering, University of Ulsan, Ulsan, Korea under the guidance of Professor Kang Hee-Jun. His research interests include robot fault diagnosis, fault-tolerant control, sliding mode controllers/observers, intelligent control, machine learning, and deep learning-based fault diagnosis.

ACKNOWLEDGMENTS

First of all, I would like to express my gratitude to my supervisor, Professor Kang Hee-Jun, for his valuable guidance, strong belief, constant support, continuous encouragement, technical instructions, beneficial suggestions, and great patience throughout my research work.

I would like to thank my doctoral committee members for their precious time and tremendously helpful feedback to evaluate the progress of my work.

I would also thankful to my senior lab members in Intelligent Robotic System Lab, Dr. Tran Xuan Toa, Dr. Vo Anh Tuan, Dr. Hoang Duy Tang, Dr. Le Phu Nguyen, Mr. Le Quang Dan, and Mr. Truong Thanh Nguyen for their help, kindness, and enthusiasm since I first set my foot in Korea. I learned a lot from them since I was a novice in the robotic research field.

Many thanks are given to Dr. Vo Anh Dung, Mr. Nguyen Quang Huy, and all my friends at the University of Ulsan for the valuable discussion and help.

The financial support of the BK21+ and BK four programs is also gratefully acknowledged.

Further, I am particularly indebted to my father Mr. Nguyen Hoi, my mother Mrs. Nguyen Thi Thu, my brothers Mr. Pham Thanh Tu, Mr. Mai Ba Tinh, my sisters Mrs. Nguyen Thi Hang, Mrs. Nguyen Thi Minh Uyen, Ms. Nguyen Thi Hoai Thanh, and all members in my family for their encouragement, support, and love.

Many thanks are given to my uncles, Dr. Nguyen Van Vinh and Mr. Nguyen Phuong, for their valuable advice and continuous encouragement not only during my research but also throughout my life.

To my grandfathers and my grandmothers, who cannot wait to see this day.

To my love, Ms. Oanh Le, I am so blessed of having you who always stand by me through ups and downs. Thank you for your care, support, and love.

Nguyen Van Cuong

August 2022, University of Ulsan, Korea

ABSTRACT

This dissertation arm to theoretically develop fault diagnosis and fault-tolerant control methods for robot manipulator systems to keep the robot operating with good tracking performance in the presence of uncertainties and faults. The fault diagnosis in industrial processes is a challenging task that includes fault detection, isolation, and estimation problem. Early fault detection and compensation in the next stage, which is called fault-tolerant control, help robot manipulator systems are still operating in a controllable region, can help to avoid events progression and reduce the number of productivity losses during abnormal events.

In this dissertation, the fault diagnosis methods are mainly developed based on high-order sliding mode observers. Thanks to their ability not only to estimate the lumped uncertainties and faults but also to approximate the system velocities, the requirement of tachometers in robot manipulator systems is eliminated. In addition, the developed fault diagnosis method provides estimation information with fast convergence speed, high precision, low chattering phenomenon, and finite-time convergence of estimation errors.

Along with the fault diagnosis methods, fault-tolerant control schemes are developed. The proposed controllers are designed via an active fault-tolerant control method by combining the developed fault diagnosis schemes with novel non-singular fast terminal sliding mode controllers to accommodate not only system failures but also uncertainties. This combination provides robust features in dealing with the lumped uncertainties and faults, increases the control performance, reduces the chattering phenomenon, eliminates velocity measurement requirement, guarantees finite-time convergence, and provides faster reaching sliding motion. Especially, both two periods of time, before and after the convergence process takes place are carefully considered.

The stability and the finite-time convergence of the proposed controller-observer techniques are demonstrated using the Lyapunov theory. Finally, to verify the effectiveness of the proposed controller-observer methods, computer simulations on robotic manipulator systems are performed.

Contents

List of Figures

List of Tables

List of Abbreviations

FD	Fault Diagnosis
FTC	Fault-Tolerant Control
LUaF	Lumped Uncertainties and Faults
TDE	Time Delay Estimation
ESO	Extended State Observer
SOSMO	Second-Order Sliding Mode Observer
TOSMO	Third-Order Sliding Mode Observer
DO	Disturbance Observer
PFTC	Passive Fault-Tolerant Control
AFTC	Active Fault-Tolerant Control
PID	Proportional-Integral-Differential
CTC	Computed Torque Control
SMC	Sliding Mode Control
TSMC	Terminal Sliding Mode Control
FTSMC	Fast Terminal Sliding Mode Control
NTSMC	Non-singular Terminal Sliding Mode Control
NFTSMC	Non-singular Fast Terminal Sliding Mode Control
A-NFTSMC	Adaptive Non-singular Fast Terminal Sliding Mode Control
NFTS	Non-singular Fast Terminal Sliding
NN	Neural Network
DNN	Deep Neural Network

Chapter 1

Introduction

1.1 Overview of Fault Diagnosis and Fault Tolerant Control Methods

In the industrial environment, robotic manipulators are very popular. They have many special applications due to their ability to replace workers in difficult and dangerous activities such as moving heavy products, assembling mechanical structures, sheet metal cutting, material handling, milling, painting welding, and roughing etc. Moreover, they can help to improve both the product quality and quantity, thus saving the cost for manufacturers. The greater the importance of robotic manipulators in industry, the greater interest in the research field of control for robotic manipulators, which aims to make the robot tracks a desired trajectory with the greatest tracking accuracy [1, 2]. However, robot manipulator systems have highly nonlinear and very complex dynamic with coupling terms, from practical viewpoint, they are arduous or even impossible to obtain the robot's exact dynamics. Additionally, the payload changes, frictions, and external disturbances, etc. leading to model uncertainties.

Along with modern industrial applications becoming increasingly complex, unknown faults more frequently happen in the system especially in the condition of long-term operation. The faults could be actuator faults, sensor faults, or process faults. Hence, the requirement is to be able to automatically detect the faults, compensates their effects, and completes the assigned missions even in the existence of one or more faults with acceptable performance. Furthermore, for reducing the weight/size and saving the cost, in some cases, manufacturers remove the velocity sensors in the robot. They are big problems that have been challenged by many researchers. Therefore, it is necessary to develop new

Fault diagnosis (FD) and Fault-tolerant control (FTC) methods to overcome the aforementioned problems.

1.1.1 Fault Diagnosis methods

Generally, faults are considered according to the part of the system they affect including sensor fault, actuator fault, and process faults. Sensor faults are the abnormal variations in measurements, such as a systematic error abruptly affecting a position sensor value. Actuator faults are the failures on a device that influence the system dynamics, such as the bearing faults or the loss torques in the robot manipulator systems. Process faults are changes in the inner parameters of the system that modify its dynamics, such as a load change in robot dynamics. To allow the robot manipulators to continue their missions, the requirement is to identify the unknown faults in the system before they lead to a complete breakdown (failure). When faults have been detected and estimated, a natural idea is to try to compensate for their effects by modifying the control law.

FD concerns procedures for determining if a fault has occurred and prediction the level of the fault and its consequence based on available input and output signals. The FD process includes the following three tasks: 1) fault detection determines something is going wrong in a system and their times of occurrence; 2) fault isolation determines the type and location of the fault; and 3) fault estimation (or identification) is the determination the magnitude and time varying behavior of the faults.

In the present literature, various techniques to FD have been proposed to approximate the lumped uncertainties and faults [3, 4, 5, 6, 7, 8, 9], for example, neural network (NN) observer [5, 6], time delay estimation (TDE) [10, 11], extended state observer (ESO) [7], second-order sliding mode observer (SOSMO) [8, 9], and third-order sliding mode observer (TOSMO) [12, 13, 14]. With the learning ability and high accuracy estimation, the NN observer has been widely employed [5, 6, 15]. However, the learning ability makes the system more complicated and thus requires higher system configuration to use online training technique that increases the cost of devices. the TDE technique provides good estimation accuracy; however, it can only provide the ability to estimate the lumped uncertainties and faults; therefore, an additional observer is needed to estimate the system velocities [16]. It leads the system more complex and

increases the computational time. The ESO is a simple technique for online observation, which can approximate both the velocities and the lumped uncertainties and faults with quite good approximation information. Thanks to the linear characteristic of the observer element, which can strongly deal with perturbations that are very far away from the origin, the convergence speed of the ESO is very high. However, the overshoot phenomenon at the convergence stage reduces its application ability. On the contrary, the SOSMO is a finite-time observer, which has the ability to estimate both the velocities and the lumped uncertainties and faults without the overshoot phenomenon as in ESO. Although providing high precision and less chattering in the estimation signal, the convergence time of the SOSMO is a little slower compared to the ESO. In addition, a lowpass filter is needed to reconstruct the estimated lumped uncertainties and faults, which reduces its estimation accuracy. For that reason, the TOSMO that can provide a continuous equivalent output injection, has been investigated. Consequently, the required filtration in the SOSMO is eliminated. Compared with the SOSMO, the TOSMO provides the estimation of lumped uncertainties and fault with less chattering and higher estimation accuracy. Moreover, the TOSMO maintains almost all the advantages of the SOSMO. Thanks to the superior benefits, the TOSMO has been widely applied to control uncertain systems by many researchers [17, 18, 19]. Unfortunately, as a trade-off, its convergence time becomes slower than that of SOSMO. Therefore, it is necessary to design an observer which can combine the wonderful properties of both the SOSMO and the TOSMO.

1.1.2 Fault Tolerant Control methods

FTC systems are systems that can maintain an acceptable level of control even after the occurrence of the fault. Generally, FTC techniques are broadly classified into two types: passive FTC (PFTC) [20, 21] and active FTC (AFTC) [22, 23, 24]. In PFTC technique, a robust controller is designed to compensate for the effects of the lumped uncertainties and faults without requiring information feedback from a FD observer. Since the lumped uncertainties and faults' effects imposed on the nominal controller of the PFTC are heavier than that of the AFTC, the nominal controller of the PFTC requires stronger robustness against the effects of faults. On the contrary, the AFTC is constructed based on online FD technologies. Compared to the PFTC, the AFTC accommodates higher control performance when the fault information is approximated correctly. Therefore, the AFTC methods are more suitable for practical applications.

In literature, various control approaches have been developed for FTC problem of robotic manipulators, such as proportional-integral-differential (PID) control [25, 26], computed torque control (CTC) [27, 28], adaptive control [29, 30], NN control [31, 32], fuzzy logic control [33, 34, 35], and sliding mode control (SMC) [36, 37, 38]. The PID control is well-known as a simple and monotonic controller, which does not require the dynamic model of the robot systems. However, this controller cannot achieve good tracking performance. The CTC is suitable to apply to real robot system; however, its tracking accuracy tremendously depends on the exactness of robot's dynamic model. Adaptive control is an effective method to deal with matched uncertainties; however, it is not appropriate for the problem of mismatched uncertainties. Intelligent control schemes are widely employed such as the neural-network control and fuzzy control. Learning ability and good approximation of nonlinear function with arbitrary accuracy of NN controllers make them a good choice for modeling complex processes and compensating for mismatched uncertainties. However, transient performance in the presence of disturbance can be degraded due to the required online learning procedure. The fuzzy logic control method was developed based on expert knowledge and experience; however, its main disadvantages are difficulties in stability analysis and comprehensive knowledge of requirement about the system.

The SMC is one of the most powerful robust controllers which can be used in FTC problem of robot manipulators because of its fast dynamic response and effectiveness in rejecting the effects of the lumped uncertainties and faults [39, 40, 41]. In recent years, the SMC has been developed in a wide range of area by many researchers due to its simple design procedure while providing high tracking performance. It also has the ability to solve the two main crucial challenging issues in control that are stability and robustness [40, 42]. It is suitable for various types of real systems such as DC-DC converters, motors, helicopters, magnetic levitation, aircraft, and robot manipulators. Although providing wonderful control properties, some problems that reduce the applicability of the conventional SMC still exist, that are: 1) the finite-time convergence cannot be guaranteed, 2) chattering phenomenon, 3) velocity (and acceleration) measurements are required.

The terminal SMC (TSMC) has been developed by utilizing nonlinear switching functions instead of the sliding function as in the conventional SMC; therefore,

the finite-time convergence is guaranteed [43, 44, 45]. Compared with the conventional SMC, the TSMC extends two outstanding properties, that are finite-time convergence and achieving higher accuracy when parameters are carefully designed. Unfortunately, the TSMC only obtains a faster convergence when system states are near equilibrium point but slower when the system states are far from the equilibrium point. In addition, the TSMC suffers from the singularity problem. Various great research has been focused to overcome these drawbacks. Each problem has been solved by using fast TSMC (FTSMC) [46, 47, 48] and non-singular TSMC (NTSMC) [10, 49, 50], separately. In order to get rid of them simultaneously, the non-singular fast TSMC (NFTSMC) is proposed [14, 51, 52, 53, 54]. This controller has outstanding control features such as singularity removal, high tracking precision, finite-time convergence, and durability to the lumped uncertainties and faults' effects.

The chattering phenomenon is caused by the utilizing of a discontinuous term with a big and fixed gain in reaching phase. It harms the system and thus reduces the practical applicability of the SMC methods. To reduce this high-frequency oscillations, the basic idea is to use an observer to approximate the lumped uncertainties and faults and then compensates its effects in the system. By using this method, the switching gain is now chosen smaller to deal with the effects of the estimation error instead of the effects of the lumped uncertainties and faults; thus, the chattering phenomenon is reduced.

1.2 Objectives of the Thesis

The main objective of this dissertation is to develop new finite-time FD and FTC methods to deal with the lumped uncertainties and faults (LUaF) for robot manipulator systems. The FD and FTC methods are proposed based on the high-order sliding mode observers, the non-singular fast terminal sliding mode control (NFTSMC) techniques, and adaptive law. The developed controller-observer strategies fulfill the main purpose of achieving minimum tracking errors, and some/all the following purposes

1. Approximating the LUaF with high accuracy and fast convergence.
2. Eliminating/Reducing the effects of the LUaF in the system thus avoiding/eliminating/reducing the chattering phenomenon effects.

3. Increasing the convergence speed of both controller and observer methods.
4. Eliminating the need for velocity measurement in the controller designing process.
5. Eliminating the dependent on the estimation accuracy of the designed observer.
6. Considering two period of times, before and after the convergence of velocity estimation takes place.
7. The finite-time convergence and the stability of the controllers and observers can be confirmed by the Lyapunov theory.

1.3 Organization of the Thesis

The following of this thesis is organized as follows

In chapter 2, an AFTC tactic using a sliding mode controller-observer method for uncertain and faulty robotic manipulators is developed. First, a finite-time disturbance observer (DO) is proposed based on the second-order sliding mode linear observer to approximate the LUaF. The observer offers high precision, quick convergence, low chattering, and finite-time convergence of estimation information. Then, the estimated signal is employed to construct an adaptive NFTSMC (A-NFTSMC) law, in which an adaptive law is employed to approximate the switching gain. This estimation helps the controller not depend on the estimation accuracy of the proposed observer. Consequently, the combination of the proposed controller-observer approach delivers better qualities such as increased position tracking accuracy, reducing chattering effect, providing finite-time convergence, and robustness against the effect of the LUaF.

In chapter 3, an FTC method for robotic manipulators is proposed to deal with the LUaF in case of lacking tachometer sensors in the system. Different from Chapter 2, the proposed method in this chapter uses a controller-observer strategy to eliminate the requirement of velocity measurement in design process. First, the TOSMO is designed to estimate both velocity and the LUaF of the system with high accuracy, less chattering, and finite time convergence of estimation errors. Based on the estimation of velocity, a novel non-singular fast terminal sliding (NFTS) function and NFTSMC are proposed. This combination provides robust features in dealing with the LUaF, increases the control

performance, reduces the chattering phenomenon, and guarantees fast finite-time convergence. Especially, the two stages of time that before and after the convergence time, are carefully analyzed.

Chapter 4 attempts to increase the control performance of the proposed algorithm in Chapter 3 and generalize the designing process for second-order uncertain nonlinear systems. In the chapter, the estimated velocity from the TOSMO is applied to propose an integral NFTSMC for a class of second-order uncertain nonlinear systems. The proposed FTC strategy has some superior properties such as high tracking accuracy, chattering phenomenon reduction, robustness against the effects of the LUaF, velocity measurement elimination, finite-time convergence, and faster-reaching sliding motion. Further, the proposed method is applied to robot manipulator systems.

In chapter 5, a novel FTC tactic based on the combination of an NFTSMC and a novel high-speed TOSMO for robot manipulator systems using only position measurement is proposed. In the first step, a high-speed TOSMO is first time proposed to approximate both the system velocity and the LUaF with a faster convergence time compared to the TOSMO. The faster convergence speed is obtained thanks to the linear characteristic of the added elements. In the second step, the NFTSMC is constructed based on a NFTS surface and the obtained information from the proposed high-speed TOSMO. Thanks to this combination, the proposed controller-observer tactic provides excellent features such as faster convergence time, high tracking precision, chattering phenomenon reduction, robustness against the effects of the LUaF, and velocity requirement elimination. Especially, the proposed observer not only improves the convergence time of the observed signal but also increases the system dynamic response.

Finally, the conclusion of this dissertation and suggestions for further development are given in Chapter 6.

Chapter 2

An Active Fault-Tolerant Control for Robotic Manipulators Using Adaptive Non-Singular Fast Terminal Sliding Mode Control and Disturbance Observer

In this chapter, a FTC tactic using a sliding mode controller-observer method for uncertain and faulty robotic manipulators is proposed. First, a finite-time DO is proposed based on the second-order sliding mode linear observer to approximate the LUaF. The observer offers high precision, quick convergence, low chattering, and finite-time convergence estimating information. Then, the estimated signal is employed to construct an adaptive non-singular fast terminal sliding mode control law, in which an adaptive law is employed to approximate the switching gain. This estimation helps the controller automatically adapt to the LUaF. Consequently, the combination of the proposed controller-observer approach delivers better qualities such as increased position tracking accuracy, reducing chattering effect, providing finite-time convergence, and robustness against the effect of the LUaF. The Lyapunov theory is employed to illustrate the robotic system's stability and finite-time convergence. Finally, simulations using a 2-DOF serial robotic manipulator verify the efficacy of the proposed method.

2.1 Introduction

In industry, robotic manipulators are very popular. They have been employed in many applications such as material handling, milling, painting welding, and roughing. The greater the importance of robotic manipulators in industry, the greater interest in the research field of control for robotic manipulators, which aims to make the robot tracks a desired trajectory with the greatest tracking accuracy [1, 2]. However, in both theory and practice, robotic manipulators are difficult to control due to their characteristics. First, the dynamic of robotic manipulators is highly nonlinear and complicated, including the coupling effect. Furthermore, uncertainties in robot dynamics are also caused by payload fluctuations, frictions, and external disturbances, etc. Therefore, it is arduous or even impossible to correctly identify the dynamics of robots. In some special cases, with the longtime operation, unknown faults might happen. The faults could be actuator faults, sensor faults, or process faults. They are big problems that have been challenged by many researchers. A variety of approaches for dealing with both the impact of uncertainties and faults have been presented in the current literature. Authors in [55, 56, 57] proposed methods to estimate the dynamics uncertainties and faults independently. However, using two distinct observers, on the other hand, makes the methods complex, requiring resources and time for calculation. In this study, faults are regarded as extra uncertainties, and the overall impacts of the system's lumped uncertainties and faults (LUaF) are evaluated.

FTC techniques have been developed to deal with the LUaF [58, 59]. FTC techniques are broadly classified into two types: PFTC [20, 21] and AFTC [22, 23, 24]. A robust controller is built in the PFTC approach to manage the LUaF without the need for feedback input from a DO. Because the effects of LUaF imposed on the typical controller of the PFTC are greater than those imposed on the notional controller of the AFTC, the nominal controller of the PFTC has the need of more resilience to eliminate the impacts of LUaF. On the contrary, the AFTC is built using an online DO technology. Since the LUaF is appropriately estimated, the AFTC provides better control effectiveness than the PFTC. As a result, the AFTC techniques are more suited for industrial cases.

In literature, a lot of efforts have been given for FTC problem of robotic manipulators, such as CTC [27, 28], fuzzy logic control [60, 34], adaptive control [29, 30], NN control [31, 32], and SMC [36, 37, 38]. Among them, the SMC is one of the most powerful robust controllers which can be used in uncertainty

nonlinear dynamic systems. In recent years, the SMC has been developed in a wide range of area by many researchers due to its simple design procedure while providing acceptable control performance. It also has the ability to solve the two main crucial challenging issues in control that are stability and robustness [40, 42]. Although providing wonderful control properties, some problems that reduce the applicability of the conventional SMC still exist. These include the inability to ensure finite-time convergence and the chattering phenomena, which is the high-frequency oscillation of the control input signal.

To guarantee the finite-time convergence of the tracking error, a lot of efforts have been paid. In [43, 44, 45], the TSMC has been developed. As compared to the traditional SMC, the TSMC has better precision and overcomes the finite-time convergence problem, however, as a trade-off, its convergence time is slightly slower. In addition, the singularity problems are appeared in some special cases. To resolve the two disadvantages, the FTSMC [48, 47, 61] and the NTSMC [50, 49] are used. Unfortunately, the two controllers just solve the two problems separately. In order to get rid of them simultaneously, the NFTSMC is proposed [51, 52, 53, 14, 54]. This controller has outstanding control features such as singularity removal, high tracking precision, finite-time convergence, and durability to LUaF effects.

To decrease chattering caused by the adoption of a discontinuous reaching control rule with a large and fixed gain, the fundamental concept is to employ an observer to approximate the LUaF and then compensate for its impacts on the system. Using this technique, a smaller switching gain can be set to deal with the impacts of the estimated error rather than the effects of the LUaF. Therefore, the chattering phenomenon could be reduced. In the present literature, many researchers have been focusing their efforts on building an effective observer to estimate the LUaF [3, 4, 5, 62, 7, 8, 9], for example, NN observer [5, 62], ESO [7], SOSMO [8, 9]. The NN observer has been frequently used due to its learning capacity and high accuracy estimation. Nevertheless, the learning capability complicates the system and necessitates a higher system configuration in order to employ online training approaches, which raises the cost of equipment. The ESO is a simple technique for online observation, which provides quite good approximation information. Thanks to the linear characteristic of the observer element, which can strongly deal with perturbations that are very far away from the origin, the convergence speed of the ESO is very high. However, the overshoot phenomenon at the convergence stage reduces its application ability. On

the contrary, the SOSMO has the ability to estimate the LUaF without the overshoot phenomenon as in ESO, however, the convergence time is a little slower. In addition, a lowpass filter is needed to reconstruct the estimated LUaF, which reduces its estimation accuracy.

From the motivation above, this study proposed a DO to approximate the LUaF of robotic manipulator system with high accuracy and fast convergence. To attain high positional tracking accuracy and system stability under the impacts of the LUaF, an FTC technique combining the adaptive NFTSMC and the suggested DO, named A-NFTSMC-DO, is proposed. In the controller, an adaptive law is applied to estimate the switching gain to help the controller automatically adapts with the LUaF. Therefore, the combination of proposed controller-observer technique provides high tracking precision, fast convergence, less chattering effect, and finite-time convergence. The following are the main contributions of this chapter:

- Proposing a DO to approximate the LUaF with high accuracy and fast convergence,
- Proposing an FTC technique for improving the tracking performance of the robot manipulator while taking to account the overall impacts of the LUaF,
- Minimizing the phenomena of chattering in control input signals,
- Using the Lyapunov stability theory to demonstrate the system's finite-time stability.

The following is the structure of the research. Section 2.2 follows the introduction by presenting the dynamic equation of a serial robotic manipulator. Section 2.3 then depicts the suggested architecture of the DO. In Section 2.4, the A-NFTSMC-DO is designed to obtain a minimal tracking error. In Section 2.5, the simulations of the proposed algorithm are executed on a 2-DOF serial robotic manipulator. Finally, Section 2.6 gives some conclusions.

2.2 System Modeling and Problem Formulation

The following is a description of a serial robotic manipulator with a dynamic equation in Lagrangian form

$$D(q)\ddot{q} + V(q,\dot{q})\dot{q} + G(q) + F_r(\dot{q}) + \tau_d = \tau \tag{2.1}$$

where $q, \dot{q}, \ddot{q}$ are the $n \times 1$ vectors that represent robot joint angular positions, velocities, and accelerations, respectively; $D(q)$ is the $n \times n$ matrix of inertia, which is symmetric, bounded, and positive definite; $V(q, \dot{q})$ is the $n \times n$ matrix of the Coriolis and centripetal forces; τ is the $n \times 1$ vector of the control input torques; $G(q)$, $F_r(\dot{q})$, and τ_d are the $n \times 1$ vector of the gravitational forces, friction, and disturbance, respectively.

The equation (2.1) can be transformed to the below form

$$\ddot{q} = H(q, \dot{q}) + D^{-1}(q)\tau + \Delta(q, \dot{q}) \tag{2.2}$$

where $H(q, \dot{q}) = D^{-1}(q)[-V(q, \dot{q})\dot{q} - G(q)]$ and $\Delta(q, \dot{q}) = D^{-1}(q)[-F_r(\dot{q}) - \tau_d]$ represents the uncertainty terms.

Faults in a system have been growing much more common in current industrial applications as they get more sophisticated, particularly under the state of enduring implementation. As a result, this chapter supposes that the robot system operates under the impact of faults. In these cases, the robot dynamic equation (2.2) can be rewritten as

$$\ddot{q} = H(q, \dot{q}) + D^{-1}(q)\tau + \Delta(q, \dot{q}) + \Phi(q, \dot{q}, t) \tag{2.3}$$

where $\Phi(q, \dot{q}, t) = \varphi(t - T_f)\Psi(q, \dot{q}, t)$ represents the unknown faults. T_f is occurrence time and the term $\varphi(t - T_f) = diag\{\varphi_1(t - T_f), \varphi_2(t - T_f), \ldots, \varphi_n(t - T_f)\}$ denotes the time profile of faults with $\varphi_i(t - T_f) = \begin{cases} 0 & if\ t \le T_f \\ 1 - e^{-\varsigma_i(t - T_f)} & if\ t \ge T_f \end{cases}$, $\varsigma_i > 0$ denotes the evolution rate of faults.

Remark 2.1. *In robotic manipulator systems, the unknown faults can be actuator faults, sensor faults, and process faults. In this chapter, the effects of actuator faults in the system are considered. Therefore, the fault functions* $\Psi(q, \dot{q}, t)$ *are defined as faults that occur at the actuator.*

Basically, the robotic system (2.3) is reconstructed in state space as

$$\begin{aligned} \dot{x}_1 &= x_2 \\ \dot{x}_2 &= \mathrm{H}(x) + D^{-1}(x_1)u + \zeta(x, t) \end{aligned} \tag{2.4}$$

where $x_1 = q$, $x_2 = \dot{q}$, $x = \begin{bmatrix} x_1{}^T & x_2{}^T \end{bmatrix}^T$, $u = \tau$, and $\zeta(x, t) = \Delta(q, \dot{q}) + \Phi(t)$ denotes the LUaF.

The main purpose of this study is to design an FTC scheme for the robotic manipulator such that the robot can track the desired trajectory under the effect of the LUaF with minimal tracking error. The FTC scheme is constructed according to the assumptions as following.

Assumption 2.1. *The desired trajectory is bounded and is a twice continuously differentiable function respect to time.*

Assumption 2.2. *The LUaF is bounded as*

$$|\zeta(x,t)| \leq \delta \tag{2.5}$$

where δ is a positive constant.

2.3 Estimation scheme

2.3.1 Design of Disturbance Observer

The DO is developed to be used with the robot manipulator system (2.4) as.

$$\begin{aligned} \dot{\hat{x}}_2 &= H(x) + D^{-1}(x_1)u + \hat{\zeta} \\ \hat{\zeta} &= k_1|x_2 - \hat{x}_2|^{1/2} sign(x_2 - \hat{x}_2) + p_1(x_2 - \hat{x}_2) + z \\ \dot{z} &= k_2 sign(x_2 - \hat{x}_2) + p_2(x_2 - \hat{x}_2) \end{aligned} \tag{2.6}$$

where $\hat{x}_2$ is the estimator of the true state x_2, and $k_i,\ p_i,\ i = 1, 2$ represent the observer gains.

By subtracting (2.6) from (2.4), we can obtain

$$\begin{aligned} \dot{\tilde{x}}_2 &= \zeta - \hat{\zeta} \\ \hat{\zeta} &= k_1|\tilde{x}_2|^{1/2} sign(\tilde{x}_2) + p_1(\tilde{x}_2) + z \\ \dot{z} &= k_2 sign(\tilde{x}_2) + p_2(\tilde{x}_2) \end{aligned} \tag{2.7}$$

where $\tilde{x}_2 = x_2 - \hat{x}_2$ represents the state estimation errors.

The equation (2.7) can be rewritten as

$$\begin{aligned} \dot{\tilde{x}}_2 &= -k_1|\tilde{x}_2|^{1/2} sign(\tilde{x}_2) - p_1(\tilde{x}_2) + z + \zeta \\ \dot{z} &= -k_2 sign(\tilde{x}_2) - p_2(\tilde{x}_2) \end{aligned} \tag{2.8}$$

For convenience in proving the stability of the proposed DO, in this part, we suppose that the LUaF, ζ, of the system (2.4) is globally bounded by

$$|\zeta| \leq \delta_1 |x_2|^{1/2} + \delta_2 |x_2| \tag{2.9}$$

for some constants $\delta_1, \delta_2 \geq 0$. Please note that under the condition in (2.9), the assumption 2.2 still satisfies. **Theorem 2.1.** *For the robotic system given in (2.4), if the DO is designed as (2.6) and the observer gains are selected as in (2.15, 2.17), then the system is stable and the estimation error $\dot{\tilde{x}}_2$ in (2.8) will converge to zero in finite-time.* **Proof of Theorem 2.1.**

A suitable Lyapunov function is selected as

$$V(x) = 2k_2 |x_2| + p_2 {x_2}^2 + \frac{1}{2} z^2 + \frac{1}{2} \Big(k_1 |x_2|^{1/2} sign(x_2) + p_1 x_2 - z \Big)^2 \tag{2.10}$$

The Lyapunov function (10) can be written as a quadratic form $V(x) = \xi^T \Pi \xi$ where $\xi = \begin{bmatrix} |x_2|^{1/2} sign(x_2) \\ x_2 \\ z \end{bmatrix}$, and $\Pi = \frac{1}{2} \begin{bmatrix} \left(4k_2 + {k_1}^2\right) & k_1 p_1 & -k_1 \\ k_1 p_1 & \left(2p_2 + {p_1}^2\right) & -p_1 \\ -k_1 & -p_1 & 2 \end{bmatrix}$.

The time derivative of the Lyapunov function is calculated as

$$\dot{V} = -\frac{1}{|x_2|^{1/2}} \xi^T \Omega_1 \xi - \xi^T \Omega_2 \xi + \omega_1^T \xi + \frac{1}{|x_2|^{1/2}} \omega_2^T \xi \tag{2.11}$$

where

$$\Omega_1 = \frac{k_1}{2} \begin{bmatrix} \left(2k_2 + {k_1}^2\right) & 0 & -k_1 \\ 0 & \left(2p_2 + 5{p_1}^2\right) & -3p_1 \\ -k_1 & -3p_1 & 1 \end{bmatrix},$$

$$\Omega_2 = p_1 \begin{bmatrix} \left(k_2 + 2{k_1}^2\right) & 0 & 0 \\ 0 & \left(p_2 + {p_1}^2\right) & -p_1 \\ 0 & -p_1 & 1 \end{bmatrix},$$

$$\omega_1^T = \left[k_1 \left(\frac{3p_1}{2} \zeta \right) \ , \ \left({p_1}^2 + 2p_2 \right) \ \zeta, \ - p_1 \zeta \right],$$

$$\omega_2^T = \zeta \left[\left(2k_2 + \frac{k_1^2}{2} \right) \ 0 - \frac{k_1}{2} \right].$$

Using the bound (2.9) of the LUaF then

$$\frac{1}{|x_2|^{1/2}}\omega_2^T\xi \leq \frac{\delta_1}{|x_2|^{1/2}}\xi^T\Delta_1\xi + \delta_2\xi^T\Delta_1\xi \tag{2.12}$$

where

$$\Delta_1 = \begin{pmatrix} \left(2k_2 + \frac{k_1^2}{2}\right) & 0 & \frac{k_1}{4} \\ 0 & 0 & 0 \\ \frac{k_1}{4} & 0 & 0 \end{pmatrix},$$

and also

$$\omega_1^T\xi \;\leq\; \frac{1}{|x_2|^{\;1/2}}\xi^T\Delta_2\xi + \xi^T\Delta_3\xi \tag{2.13}$$

where

$$\Delta_2 = \begin{pmatrix} 0 & 0 & 0 \\ 0 & \left[k_1\frac{3p_1}{2}\delta_2 \;+\; \left({p_1}^2 + 2p_2\right)\;\delta_1\right] & 0 \\ 0 & 0 & 0 \end{pmatrix},$$

$$\Delta_3 = \begin{pmatrix} p_1\frac{3}{2}k_1\delta_1 & 0 & \frac{1}{2}p_1\delta_1 \\ 0 & \left({p_1}^2 + 2p_2\,\right)\delta_2 & \frac{1}{2}p_1\delta_2 \\ \frac{1}{2}p_1\delta_1 & \frac{1}{2}p_1\delta_2 & 0 \end{pmatrix}.$$

The derivative of the Lyapunov function can be then written as

$$\dot{V} = -\frac{1}{|x_2|^{1/2}}\xi^T\left(\Omega_1 - \Delta_2 - \delta_1\Delta_1\right)\xi - \xi^T\left(\Omega_2 - \Delta_3 - \delta_2\Delta_1\right)\xi \tag{2.14}$$

The term $(\Omega_1 - \Delta_2 - \gamma_1\Delta_1) > 0$ if

$$\begin{aligned} &k_1 > 2\delta_1 \\ &p_1 > \tfrac{3}{4}\delta_2 \\ &k_2 > k_1\frac{\delta_1 k_1 + \frac{1}{8}\delta_1^2}{2\left(\frac{1}{2}k_1 - \delta_1\right)} \\ &p_2 > \frac{k_1\left[\frac{1}{2}k_1\left(k_1 + \frac{1}{2}\delta_1\right)^2\left(2{p_1}^2 - \frac{3}{2}\delta_2 p_1\right) + \left(\frac{5}{2}{p_1}^2 + \frac{3}{2}\delta_2 p_1\right)q_1\right]}{2\left(q_1 - \frac{1}{2}k_1\left(k_1 + \frac{1}{2}\delta_1\right)^2\right)\left(\frac{1}{2}k_1 - \delta_1\right)} - \frac{1}{2}{p_1}^2 \end{aligned} \tag{2.15}$$

where $q_1 = \frac{1}{4}k_1^3 + \left(\frac{1}{2}\,k_1 - \delta_1\right)\left(2k_2 + \frac{1}{2}k_1^2\right)$.

The second term in the inequality can be written as

$$\xi^T\left(\Omega_2 - \Delta_3 - \gamma_3\Delta_1\right)\xi \;=\; \zeta^T\Gamma_1\zeta + x^T\Gamma_2 x, \tag{2.16}$$

where

$$\Gamma_1 = \begin{bmatrix} p_1\left(\left(k_2 + 2k_1^2\right) - \frac{3}{2}k_1\delta_1\right) - \left(2k_2 + \frac{k_1^2}{2}\right)\ \delta_2 & -\frac{1}{2}\left(p_1\delta_1 + \frac{1}{2}k_1\delta_2\right) \\ -\frac{1}{2}\left(p_1\delta_1 + \frac{1}{2}k_1\delta_2\right) & \frac{1}{2}p_1 \end{bmatrix}$$
$$\Gamma_2 = \begin{bmatrix} p_1\left(p_2 + {p_1}^2\right) - \left({p_1}^2 + 2p_2\right)\ \delta_2 & -p_1\left(p_1 + \frac{1}{2}\delta_2\right) \\ -p_1\left(p_1 + \frac{1}{2}\delta_2\right) & \frac{1}{2}p_1 \end{bmatrix}$$

This term is positive definite if

$$\begin{aligned} &p_1 > 2\delta_2 \\ &k_2 > \frac{\left(p_1\delta_1 + \frac{1}{2}k_1\delta_2\right)^2}{2p_1(p_1 - 2\delta_2)} + \frac{\frac{3}{2}\delta_1 k_1 p_1 - 2\left(p_1 - \frac{1}{4}\delta_2\right)k_1^2}{(p_1 - 2\delta_2)} \\ &p_2 > p_1\frac{\left[p_1(p_1 + 3\delta_2) + \frac{1}{2}{\delta_2}^2\right]}{p_1 - 2\delta_2} \end{aligned} \tag{2.17}$$

One can see that it is always possible to select $k_i > 0,\ p_i > 0,\ i = 1, 2$ so that both sets of inequalities (2.15, 2.17) are satisfied for every $\delta_i > 0,\ i = 1,\ 2$.

Under the conditions in (2.15, 2.17), the derivative of the Lyapunov function in (2.14) becomes

$$\dot{V} \leq\ -\ \frac{1}{|x_2|^{1/2}}\xi^T\left(\Omega_1 - \Delta_2 - \delta_1\Delta_1\right)\ \xi \tag{2.18}$$

According to [9], it can be concluded that the system is stable, and the estimation error $\dot{\tilde{x}}_2$ in (2.8) will approach to zero in finite-time. Accordingly, **Theorem 2.1** is clearly illustrated.

2.3.2 The LUaF Reconstruction

After the convergence time, the predicted states, $\hat{x}_2$, will approach the real states after the convergence time, x_2, thus, the estimation error (2.7) becomes

$$\dot{\tilde{x}}_2 = \zeta - \hat{\zeta} \equiv 0 \tag{2.19}$$

Therefore, the estimation of the LUaF can be reconstructed as

$$\begin{aligned} &\zeta = \hat{\zeta} = k_1|\tilde{x}_2|^{1/2}sign\left(\tilde{x}_2\right) + p_1\left(\tilde{x}_2\right) + z \\ &\dot{z} = k_2 sign\left(\tilde{x}_2\right) + p_2\left(\tilde{x}_2\right) \end{aligned} \tag{2.20}$$

Remark 2.2. *Thanks to the characteristic of linear terms, the proposed DO can obtain higher convergence speed compared to the SOSMO. This excellent property will be confirmed in the simulation part.*

Remark 2.3. *As shown in (2.20), the resulting signal is made up of an integral operator; thus, the estimated information of the suggested DO may be rebuilt directly without filtration. As a result, this observer produces a more accurate estimation signal with less chattering than the SOSMO. In the following part, this estimation information will be used to build the FTC technique.*

2.4 Design of Controller

2.4.1 The DO-based NFTSMC

We define the position tracking and velocity errors as

$$\begin{aligned} e &= x_1 - x_d \\ \dot{e} &= x_2 - \dot{x}_d \end{aligned} \tag{2.21}$$

where x_d, and $\dot{x}_d$ are the desired trajectories and velocities, respectively.

A NFTSM function is chosen as in [63]

$$\sigma = \dot{e} + \int \kappa_1 |e|^{\beta_1} sign(e) + \kappa_2 |\dot{e}|^{\beta_2} sign(\dot{e}) + \kappa_3 e + \kappa_4 e^3 \tag{2.22}$$

where constants κ_1, κ_2, κ_3, κ_4 are positive constants and β_1, β_2 can be selected as

$$\begin{aligned} \beta_1 &= (1-\varepsilon, 1), \ \varepsilon \in (0,1) \\ \beta_2 &= \tfrac{2\beta_1}{1+\beta_1} \end{aligned} \tag{2.23}$$

The control law is designed as following

$$u = -D(x_1)\left(u_{eq} + u_c + u_{sw}\right) \tag{2.24}$$

$$u_{eq} = H(x) + \kappa_1 |e|^{\beta_1} sign(e) + \kappa_2 |\dot{e}|^{\beta_2} sign(\dot{e}) + \kappa_3 e + \kappa_4 e^3 - \ddot{x}_d \tag{2.25}$$

$$\begin{aligned} u_c &= \hat{\zeta}(x,t) = k_1 |\tilde{x}_2|^{1/2} sign(\tilde{x}_2) + p_1(\tilde{x}_2) + z \\ \dot{z} &= k_2 sign(\tilde{x}_2) + p_2(\tilde{x}_2) \end{aligned} \tag{2.26}$$

The switching control law, u_{sw}, is employed to compensate for the estimation errors as follows

$$u_{sw} = (K + \mu)\, sign\,(\sigma) \tag{2.27}$$

where μ is a small positive constant and K denotes the switching gain, which is bounded as $K \geq |d\,(x,t)|$ with $d\,(x,t) = \zeta\,(x,t) - \hat{\zeta}\,(x,t)$ represents the estimation error.

Theorem 2.2. *For the uncertain and faulty robotic manipulator described in (2.4), if the proposed control law is designed as in (2.24-2.27) and the NFTSM function is selected as in (2.22), then the stability and finite-time convergence of the system are guaranteed.*

Proof of Theorem 2.2.

Taking the derivative of the sliding function (2.22) with respect to time, we obtain

$$\begin{aligned}
\dot{\sigma} &= \ddot{e} + \kappa_1 |e|^{\beta_1} sign(e) + \kappa_2 |\dot{e}|^{\beta_2} sign(\dot{e}) + \kappa_3 e + \kappa_4 e^3 \\
&= \dot{x}_2 - \ddot{x}_d + \kappa_1 |e|^{\beta_1} sign(e) + \kappa_2 |\dot{e}|^{\beta_2} sign(\dot{e}) + \kappa_3 e + \kappa_4 e^3 \\
&= -\ddot{x}_d + \mathrm{H}(x) + D^{-1}\,(x_1)\, u + \zeta\,(x,t) \; + \kappa_1 |e|^{\beta_1} sign(e) \\
&\quad + \kappa_2 |\dot{e}|^{\beta_2} sign(\dot{e}) + \kappa_3 e + \kappa_4 e^3
\end{aligned} \tag{2.28}$$

Inserting the control laws (2.24 - 2.27) into (2.28) yields

$$\dot{\sigma} = -\,(K + \mu)\, sign\,(\sigma) + d\,(x,t) \tag{2.29}$$

A candidate Lyapunov function is chosen as

$$L_1 = \frac{1}{2}\sigma^T \sigma \tag{2.30}$$

Taking the derivative of the Lyapunov function (2.30) and substituting the result from (2.29), we obtain

$$\begin{aligned}
\dot{L}_1 &= \sigma^T \dot{\sigma} \\
&= \sigma^T \left(-\,(K + \mu)\, sign\,(\sigma) + d\,(x,t)\right) \\
&= -\,(K + \mu)\,|\sigma| + d\,(x,t)\,\sigma \leq -\mu\,|\sigma| < 0, \;\; \forall \sigma \neq 0
\end{aligned} \tag{2.31}$$

Therefore, the **Theorem 2.2** is successfully proven.

Remark 2.4. *The switching gain, K, is dependent on the accuracy of the observer. In the next section, an adaptive NFTSMC will be proposed to help the controller automatically adapts with the LUaF.*

2.4.2 The DO-based Adaptive NFTSMC

An adaptive NFTSMC law is suggested as

$$u = -D\left(x_1\right)\left(u_{eq} + u_c + u_{asw}\right) \tag{2.32}$$

$$u_{eq} = H(x) + \kappa_1|e|^{\beta_1} sign(e) + \kappa_2|\dot{e}|^{\beta_2} sign(\dot{e}) + \kappa_3 e + \kappa_4 e^3 - \ddot{x}_d \tag{2.33}$$

$$\begin{aligned} u_c &= \hat{\zeta}\left(x,t\right) = k_1|\tilde{x}_2|^{1/2} sign\left(\tilde{x}_2\right) + p_1\left(\tilde{x}_2\right) + z \\ \dot{z} &= k_2 sign\left(\tilde{x}_2\right) + p_2\left(\tilde{x}_2\right) \end{aligned} \tag{2.34}$$

$$u_{asw} = \left(\hat{K} + \mu\right) sign\left(\sigma\right) \tag{2.35}$$

where $\hat{K}$ is the estimator of the ideal switching gain, K^*, and is updated by the following adaptive law

$$\dot{\hat{K}} = \rho\,|\sigma| \tag{2.36}$$

with $\rho > 0$ is the adaptation gain.

Theorem 2.3. *For the uncertain and faulty robotic manipulator described in (2.4), if the proposed DO-based adaptive NFTSMC law is designed as in (2.32-2.35) and the NFTSM function is selected as in (2.22), then the stability and finite-time convergence of the system are guaranteed.*

Proof of Theorem 2.3.

Inserting the control laws (2.32-2.35) into (2.28) yields

$$\dot{\sigma} = -\left(\hat{K} + \mu\right) sign\left(\sigma\right) + d\left(x,t\right) \tag{2.37}$$

A candidate Lyapunov function is chosen as

$$L_2 = \frac{1}{2}\sigma^T\sigma + \frac{1}{2k}\tilde{K}^T\tilde{K} \tag{2.38}$$

where $\tilde{K} = \hat{K} - K^*$.

Taking the derivative of the Lyapunov function (2.38) with respect to time, we obtain

$$\dot{L}_2 = \sigma^T\dot{\sigma} + \frac{1}{k}\tilde{K}^T\dot{\tilde{K}} \tag{2.39}$$

The derivative of $\tilde{K}$ with respect to time is taken as

$$\dot{\tilde{K}} = \dot{\hat{K}} - \dot{K}^* = \dot{\hat{K}} \tag{2.40}$$

Inserting the result from (2.37) and (2.40) into (2.39) yields

$$\dot{L}_2 = \sigma^T \left(- \left(\hat{K} + \mu \right) sign\left(\sigma \right) + d\left(x, t \right) \right) + \frac{1}{k} \left(\hat{K} - K^* \right) \dot{\hat{K}} \tag{2.41}$$

Inserting the adaptive law (2.36) into (2.41) yields

$$\begin{aligned} \dot{L}_2 &= \sigma^T \left(- \left(\hat{K} + \mu \right) sign\left(\sigma \right) + d\left(x, t \right) \right) + \tfrac{1}{k} \left(\hat{K} - K^* \right) k \left| \sigma \right| \\ &= - \left(\hat{K} + \mu \right) \left| \sigma \right| + d\left(x, t \right) \sigma + \left(\hat{K} - K^* \right) \left| \sigma \right| \\ &\leq -\mu \left| \sigma \right| < 0, \ \forall \sigma \neq 0 \end{aligned} \tag{2.42}$$

Therefore, the **Theorem 2.2** is successfully proven.

The structure of the proposed FTC strategy is described in Figure 2.1.

Remark 2.5. *Generally, the sliding motion only can archive in ideal condition, thus, the switching gain K in (2.36) keeps increasing continuously. This problem is well-known as the "parameter drift problem". To solve this problem, the following adaptive law can be utilized:*

$$\dot{\hat{K}} = \begin{cases} \rho \left| \sigma \right|, & if \ \left| \sigma \right| \geq \varepsilon \\ 0, & else \end{cases} \tag{2.43}$$

where ε is a sufficiently small constant.

2.5 Numerical Simulations

Computer simulations on a 2-DOF robotic manipulator are used to show the utility of the suggested controller-observer approach. The 2-DOF model is illustrated in Fig. 2.2, and its dynamic model is described below.

Inertia term

$$D(q) = \begin{bmatrix} D_{11} & D_{12} \\ D_{21} & D_{22} \end{bmatrix}$$

where

$$\begin{aligned} D_{11} &= m_1 {r_1}^2 + m_2 (l_1^2 + {r_2}^2 + 2 l_1 r_2 cos(q)) + I_1 + I_2 \\ D_{12} &= D_{21} = m_1 {r_2}^2 + m_2 r_2 l_1 cos(q) + I_2 \\ D_{22} &= m_2 {r_2}^2 + I_2 \end{aligned}$$

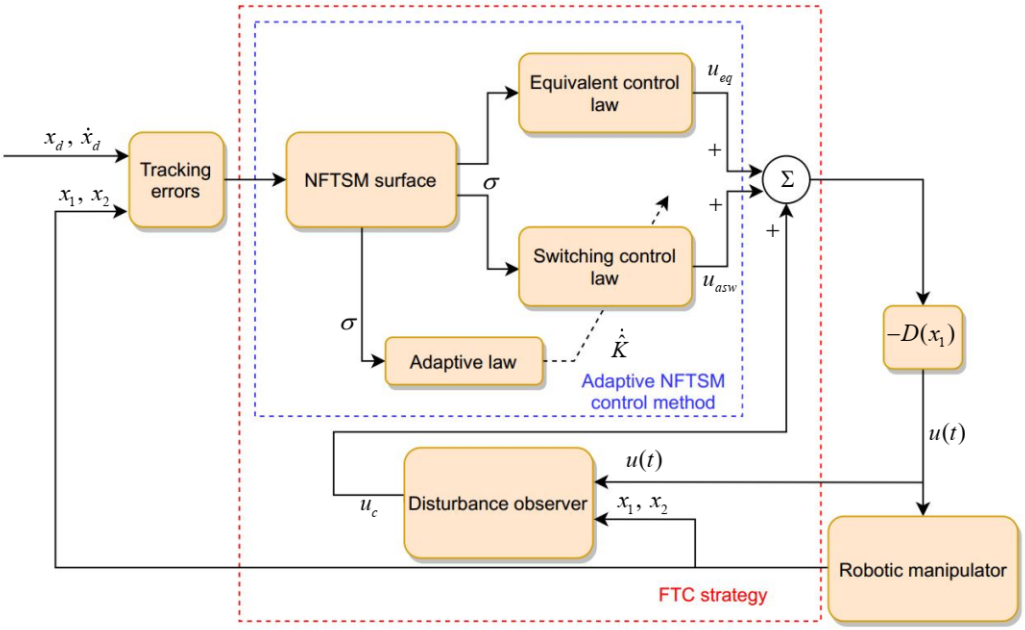

FIGURE 2.1: Structure of the proposed FTC strategy.

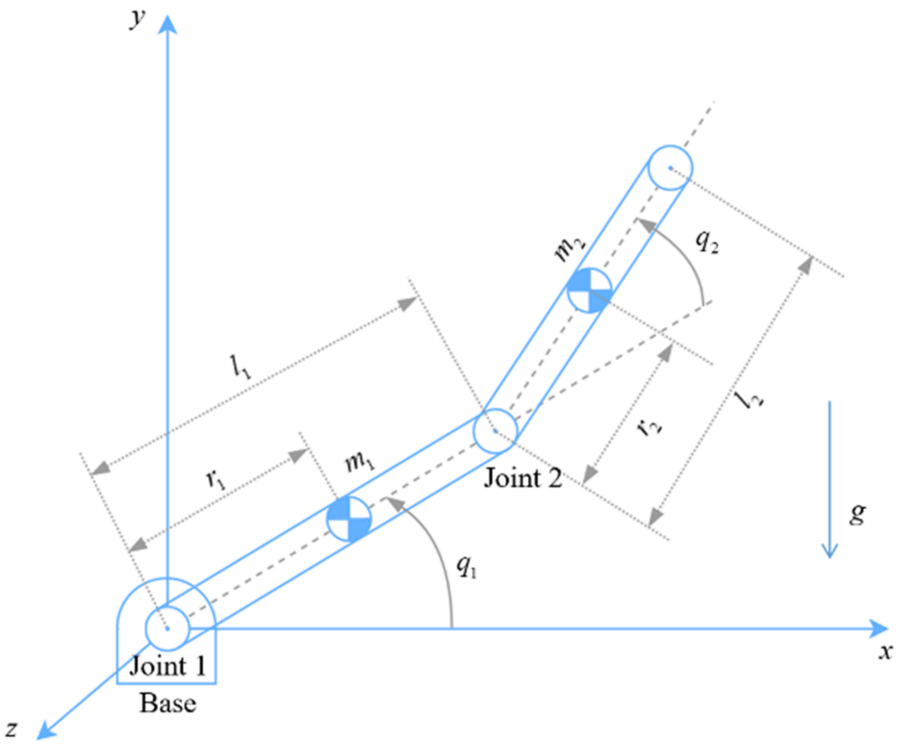

FIGURE 2.2: Configuration of the 2-DOF robotic manipulator.

TABLE 2.1: Parameters of the 2-link robot manipulator.

Parameters	Values
$m_1,\ m_2$	1.5, 1.3 (kg)
$l_1,\ l_2$	1, 0.8 (m)
$r_1,\ r_2$	0.5, 0.4 (m)
$I_1,\ I_2$	1, 0.8 ($kgNm^2$)

Coriolis and centripetal term

$$V(q,\dot{q}) = \begin{bmatrix} -2m_2 l_1 r_2 sin(q)\dot{q}_1\dot{q}_2 - m_2 l_1 r_2 sin(q_2)\dot{q}_2^2 \\ m_2 l_1 r_2 sin(q_2)\dot{q}_1^2 \end{bmatrix}$$

Gravitational term

$$G(q) = \begin{bmatrix} m_1 g r_1 \cos(q_1) + m_2 g\left(l_1 \cos(q_1) + r_2 \cos(q_1+q_2)\right) \\ m_2 r_2 g \cos(q_1+q_2) \end{bmatrix}$$

The parameters of the 2-DOF robot are given as in Table 2.1.

All simulations in this work are carried out using MATLAB/Simulink and the sampling time is $10^{-3}s$.

The desired trajectories of robot are assumed as

$$x_d = \begin{bmatrix} 1.05\cos\left(\pi t/6\right) - 1 \\ 1.2\sin\left(\pi t/7 + \pi/2\right) - 1 \end{bmatrix}$$

The friction and disturbance are respectively assumed as

$$F_r\left(\dot{q}\right) = \begin{bmatrix} 1.9\cos\left(2\dot{q}_1\right) \\ 0.53\sin\left(\dot{q}_2 + \pi/3\right) \end{bmatrix}$$

$$\tau_d = \begin{bmatrix} 1.2\sin\left(3q_1 + \pi/2\right) - \cos(t) \\ -1.14\cos\left(2q_2\right) + 0.5\sin(t) \end{bmatrix}$$

The fault is assumed to occur to joint 1 at $T_f = 15s$ and occur to joint 2 at

$$\Psi\left(q,\dot{q},t\right) = \begin{bmatrix} -3.5{q_1}^2 + 2.5\sin\left(q_2\right) + 6.1\cos(\dot{q}_1) + 4.5\dot{q}_2 + 2\sin\left(2t/\pi\right) \\ 7.5q_1 + 6.2\cos\left(q_2\right) + 8.3\sin(2\dot{q}_1) + 11.2\dot{q}_2 + 3.5\cos\left(t/\pi\right) \end{bmatrix}$$

TABLE 2.2: The values of the controller/observer's parameters.

Controller/Observer methods	Parameters	Values
DO	k_1, k_2	8, 18
	p_1, p_2	10, 10
SMC	c, δ	4, 16
NFTSMC	κ_1, κ_2	14, 10
	κ_3, κ_4	10, 5
	β_1, β_2	1/2
	δ	16
Adaptive method	ρ, ε	0.2, 0.001

The simulation is divided into two parts. First, a comparison of the proposed DO, the SOSMO [8], the ESO [7], and the DO in [64] is performed. Second, the tracking performance of the proposed A-NFTSMC-DO will be compared with the conventional SMC and the NFTSMC to show its superior control properties.

The parameters of the observer and controller are shown in the Table 2.2.

For the first part, the result of the comparison is presented in Fig. 2.3 and 2.4. The Fig. 2.3 shows the estimation results of LUaF estimation among four observers. The Fig. 2.4 shows the estimation error at each joint. As shown in the result, the ESO (the blue solid line) provides fast estimation result, however, the overshoot phenomenon at the convergence stage is the main disadvantage of the ESO. On the contrary, the SOSMO (the green solid line) provides estimation result without the overshoot phenomenon as in ESO, however, the convergence time is a little slower. In addition, a lowpass filter is needed to reconstruct the estimated LUaF. In terms of estimation accuracy, both the ESO and SOSMO provide quite good estimation result in normal operation condition, however, when faults occur the estimation errors become larger. The proposed DO (the red solid line) provides the LUaF estimation with a faster convergence speed compared to the SOSMO due to the linear characteristic of the observer elements. Compared to the ESO, the proposed DO eliminates the overshoot phenomenon. In addition, it achieves the highest estimation accuracy among three observers in both before and after faults occur. Moreover, the LUaF can be reconstructed directly without the need of a lowpass filter. Compared to the DO in [64], the proposed DO obtains almost the same estimation accuracy, however, the estimation speed is faster.

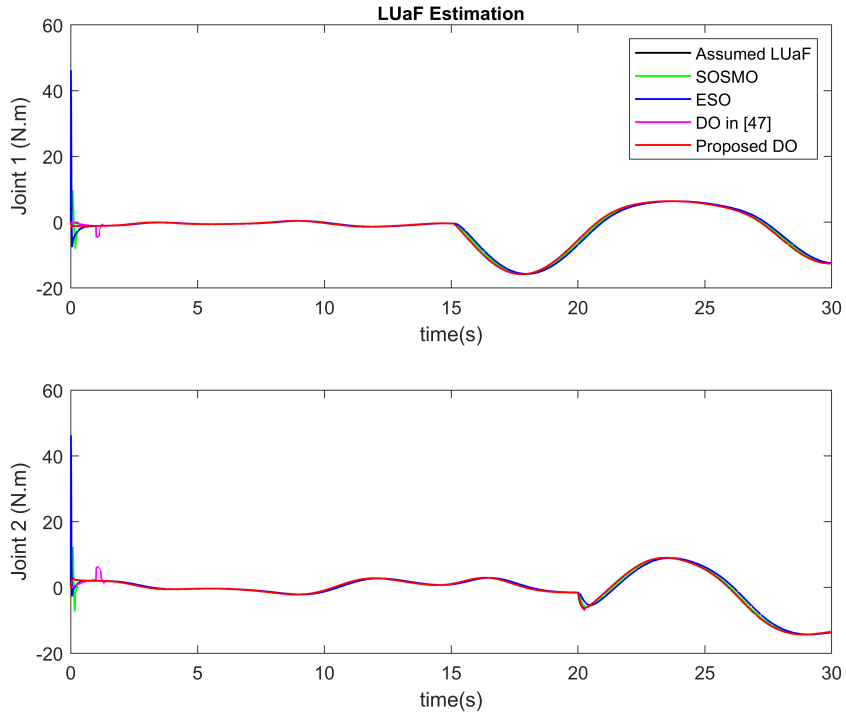

FIGURE 2.3: The estimation of LUaF among four observers.

In the second part, in order to show the effectiveness of the proposed A-NFTSMC-DO method, its control performance will be compared with the two controllers: the conventional SMC and the NFTSMC. The results are shown in Fig. 2.5, 2.6 and 2.7. The Fig. 2.5 and 2.6 show the robot end-effector tracking and the joint tracking error among three controllers. As in the results, the SMC provides acceptable tracking performance. However, compared to others, its tracking error (the blue solid line) has the lowest accuracy. In addition, in terms of convergence speed, the conventional SMC takes a longer time for convergence. On the other hand, the NFTSMC (the green solid line) offers both higher tracking accuracy and faster convergence compared to the SMC. The proposed FTC method (the red solid line) offers the tracking error with the same convergence speed as the NFTSMC, meanwhile, it provides the highest tracking accuracy compared to others. Fig. 2.7 shows the comparison of control input torque. As a result of the LUaF compensation, the switching gain parameter of the control law is now extremely small. Therefore, as we can see, the suggested A-NFTSMC-DO delivers reduced chattering control input torque. Furthermore, because of better characteristics of the adaptive law, the suggested controller can automatically adjust with the LUaF. The estimated value of the sliding gain is shown in Fig. 2.8.

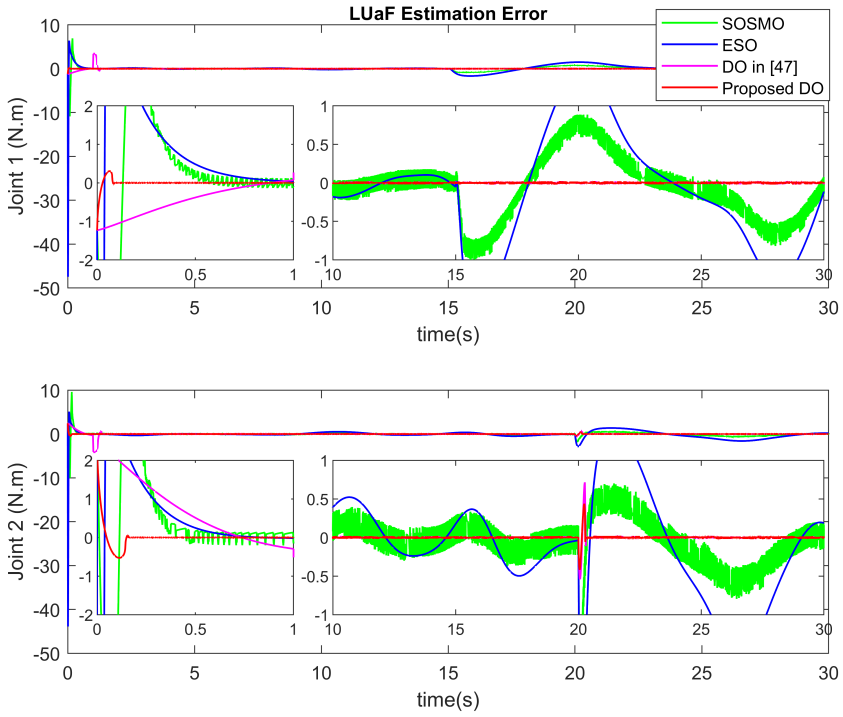

FIGURE 2.4: The LUaF estimation error at each joint.

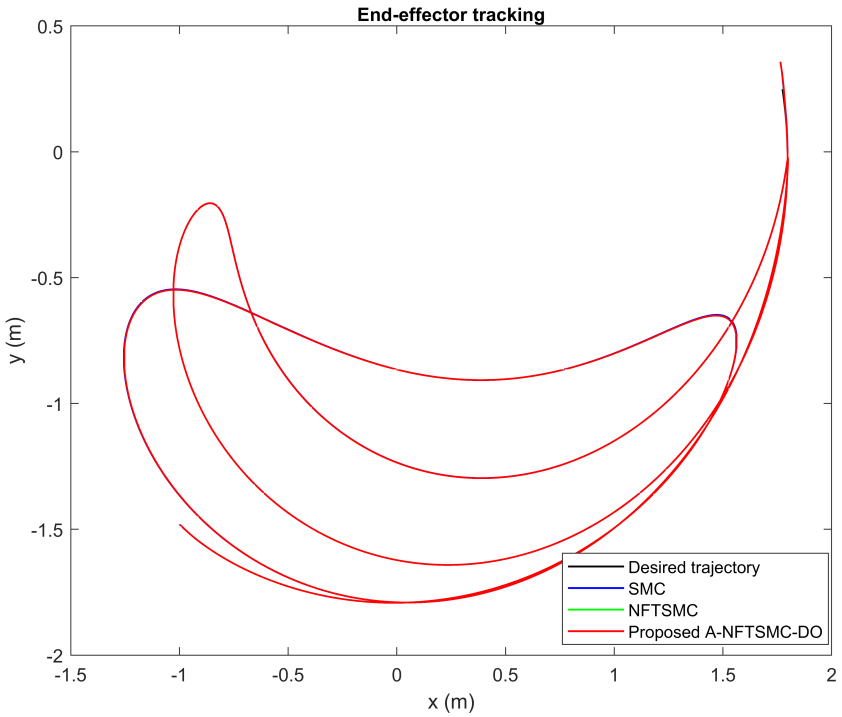

FIGURE 2.5: Robot end-effector tracking.

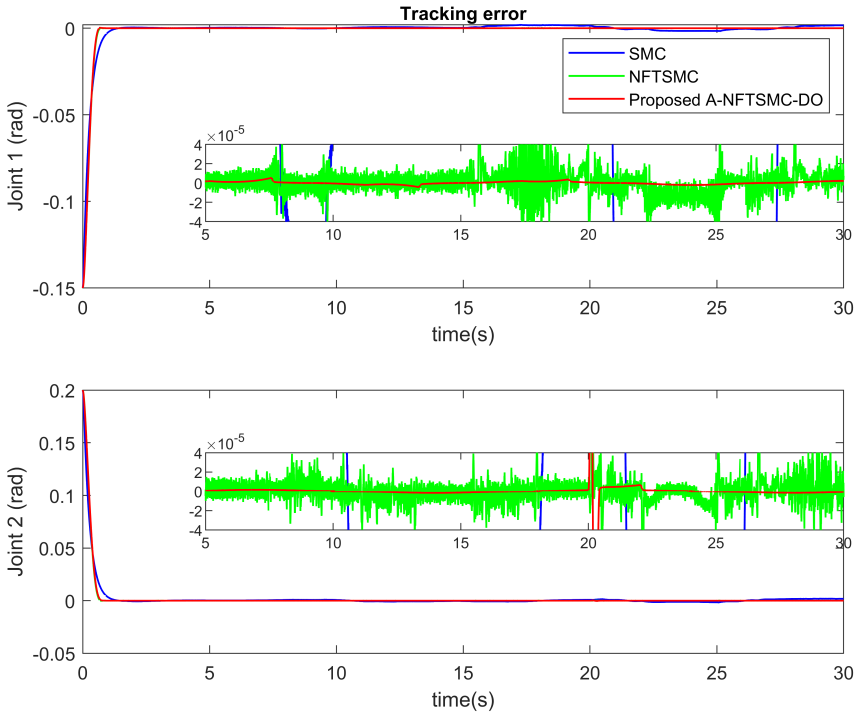

FIGURE 2.6: Tracking error at each joint.

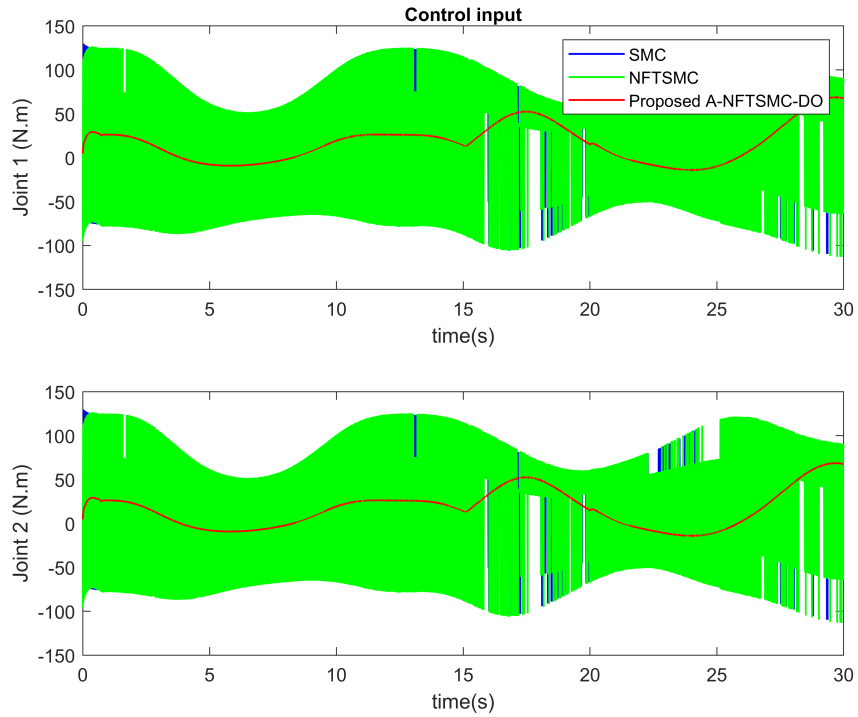

FIGURE 2.7: Control input at each joint.

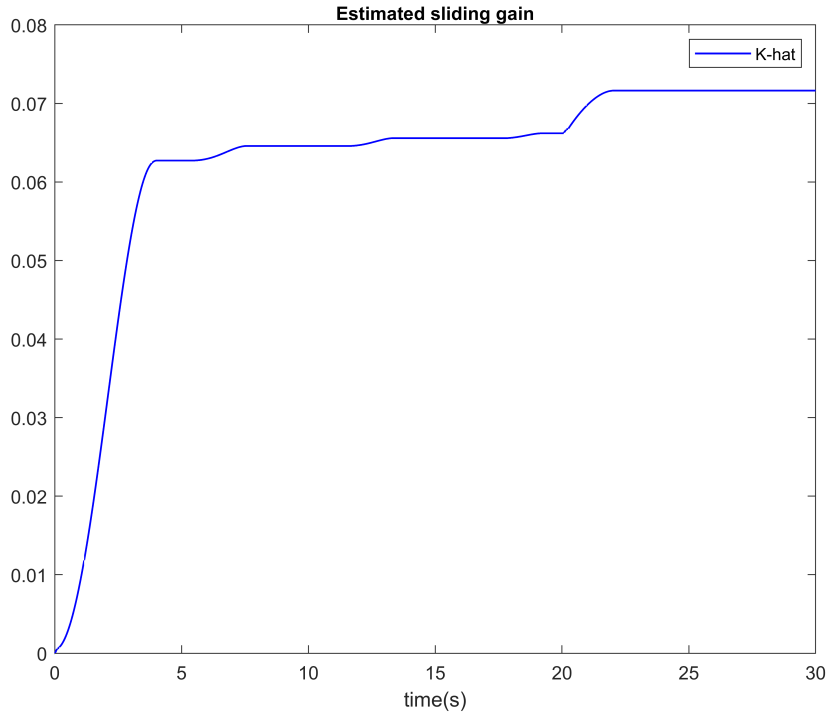

FIGURE 2.8: Estimation of sliding gain.

2.6 Conclusions

In this study, an FTC strategy using an A-NFTSMC based on a DO for uncertain and faulty robotic manipulators is proposed. The suggested observer demonstrated its capacity to estimate the LUaF with excellent accuracy, rapid convergence, and almost no chattering. They will then be used to compensate for the impacts on the system, which improves the tracking performance of the suggested FTC technique. The suggested FTC technique has advanced control characteristics of high positioning tracking accuracy with quick finite-time convergence, chattering phenomena minimization, and LUaF robustness. The use of Lyapunov theory ensures system stability and finite-time convergence. The efficacy of the suggested method has been confirmed by computer simulation on a 2-DOF robot.

Chapter 3

A Fault-Tolerant Control Using Non-Singular Fast Terminal Sliding Mode Control and Third-Order Sliding Mode Observer for Robotic Manipulators

In this chapter, a FTC method for robotic manipulators is proposed to deal with the lumped uncertainties and faults in case of lacking tachometer sensors in the system. First, the TOSMO is performed to approximate system velocities and the lumped uncertainties and faults. This observer provides estimation information with high precision, low chattering phenomenon, and finite-time convergence. Then, an FTC method is proposed based on a non-singular fast terminal switching function and the TOSMO. This combination provides robust features in dealing with the lumped uncertainties and faults, increases the control performance, reduces chattering phenomenon, and guarantees fast finite-time convergence. Especially, this chapter considers both two periods of time, in which before and after the convergence process takes place. The stability and the finite-time convergence of the proposed controller-observer technique is demonstrated using the Lyapunov theory. Finally, to verify the effectiveness of the proposed controller-observer technique, computer simulation on a serial two-link robotic manipulator is performed.

3.1 Introduction

In the industrial environment, robotic manipulators have many special applications due to their ability to replace workers in difficult and dangerous activities such as moving heavy products, assembling mechanical structures, sheet metal cutting, etc. Moreover, they can help to improve both the product quality and quantity, thus saving the cost for manufacturers. However, robotic manipulators have very complicated dynamic, from practical viewpoint, they are arduous or even impossible to obtain the robot's exact dynamics, leading to model uncertainties. They are the large challenges in both theoretical and practical control. In addition, along with modern industrial applications becoming increasingly complex, faults more frequently happen in the system especially in the condition of long-term operation. Hence, the requirement is to be able to automatically detect the faults, compensates their effects, and completes the assigned missions even in the existence of one or more faults with acceptable performance. In literature, various methods have been proposed to handle the effects of the uncertainties and faults. In some researches, the system uncertainties and faults are approximated separately [55, 56, 57, 65]. However, using two separate observers makes the algorithms cumbersome that leads to resources and time consuming for computation. In this chapter, the faults are treated as additional uncertainties, thus, the total effects of the lumped uncertainties and faults in the system are considered.

In order to deal with the lumped uncertainties and faults, FTC methods have been developed [58, 59]. In general, the FTC tactics can be divided into two categories: PFTC [20, 21] and AFTC [22, 23]. In PFTC technique, a robust controller is designed to compensate the faults without requiring information feedback from a fault diagnosis observer. Since the faults' effects imposed on the nominal controller of the PFTC are heavier than that of the AFTC, the nominal controller of the PFTC requires stronger robustness against the effects of faults. On the other hand, an AFTC is constructed based on online fault diagnosis technologies. Compared with the PFTC, the AFTC accommodates higher control performance when the fault information is approximated correctly. Therefore, the AFTC methods are more suitable for practical applications. In literature, various control approaches have been developed for FTC, such as CTC [57, 27], adaptive control [66, 67], NN control [31, 68], fuzzy logic control [34, 33, 35], and SMC [42, 54, 69, 70, 71, 72, 13, 73], etc. Compared with others, SMC stands out with superior control properties like fast convergence, high tracking precision,

and robustness against the lumped uncertainties and faults. In addition, it is pretty simple in design; therefore, the SMC has been extensively employed to control robotic manipulator system in literature. Besides the huge advantages, there still exists some big limitations that degrade the practical applicability of the conventional SMC, that are: 1) the finite-time convergence cannot be guaranteed, 2) chattering phenomenon, 3) velocity (and acceleration) measurements are required.

To overcome the first limitation – the finite-time convergence, the TSMC has been developed by utilizing nonlinear switching functions instead of the linear one [43, 74]. In addition, it can reach higher exactness by rigorously selecting parameters. The conventional TSMC, however, produces two major drawbacks, that are singularity problem and slower dynamic response compared with the conventional SMC. To overcome these limitations, the FTSMC [75, 76] and the NTSMC [49, 77] have been proposed. However, they can only handle each problem separately. In order to resolve the two problems at the same time, the NFTSMC has been investigated. In addition, the NFTSMC has the capability to obtain high tracking error precision and provide feature robustness against the influence of the lumped uncertainties and faults; therefore, this control algorithm has been extensively utilized by many researchers [16, 78, 72, 52]. Unfortunately, the last two limitations still remain. To eliminate the second limitation – chattering phenomenon, which is caused by the utilizing of a discontinuous term with a big and fixed gain in reaching phase, the basic idea is to use an observer to approximate the lumped uncertainties and faults and then compensates its effects in the system. By using this method, the switching gain is now chosen smaller to deal with the effects of the estimation error instead of the effects of the lumped uncertainties and faults; thus, the chattering phenomenon is reduced. In the literature, many researchers have been paid attention to develop an effective observer to approximate the lumped uncertainties and faults such as [5, 62, 79, 80, 15, 81, 11]. With the learning ability and high accuracy estimation, the NN observer has been widely employed [5, 62, 15]. On the other hand, the learning ability makes the system more complicated and thus requires higher system configuration to use online training technique that increases the cost of devices. The TDE method, in [81, 11], is a simpler technique; however, it needs the velocity measurement that not usually available in practical. The sliding mode observer, especially, the TOSMO, in [82], has ability to estimate the lumped uncertainties and faults with high accuracy and less

chattering. Moreover, the TOSMO provides the system velocity (and acceleration) estimation with finite-time convergence. Therefore, the third limitation of the SMC is eliminated. Thanks to the above advantages, the TOSMO has been broadly utilized in controlling theory [17, 18, 19].

In this chapter, the TOSMO is used to approximate the velocities and the lumped uncertainties and faults of robotic manipulator system. The obtained velocities are employed in the system to replace the measured velocity and the estimated uncertainties and faults are applied to reduce their effects. To achieve high position tracking precision and stability of the system, a robust control is design based on a terminal sliding function. Especially, two periods of time that before and after the convergence process takes place, are carefully considered. The proposed FTC strategy affords high tracking accuracy, low chattering phenomenon, non-singularity, robustness against the effects of the lumped uncertainties and faults, and finite-time convergence for both position tracking errors and velocity estimation.

In this chapter, the FTC method that combines the NFTSMC and the TOSMO is proposed for the robotic manipulator system to surpass the total effects of the lumped uncertainties and faults. The main contributions of this chapter are given as following:

- Proposing an NFTSM switching function based on estimated state from TOSMO,
- Proposing an FTC method to enhance the tracking performance of the robotic system under the total effect of the lumped uncertainties and faults,
- Reducing the chattering phenomenon in control input signals by estimating and compensating the lumped uncertainties and faults,
- Demonstrating the finite-time stability of the switching function and the robotic system using the Lyapunov stability theory,
- Eliminating the necessary of system velocity measurement in the design procedure,
- Considering both two periods of time, in which before and after the convergence process takes place.

This chapter is structured into six parts. Next to the introduction, the problem statement is presented in Section 3.2. Then, the TOSMO is designed for the robotic manipulator systems in Section 3.3. Section 3.4 presents the design of the

FTC algorithm using the NFTSMC and the TOSMO. In Section 3.5, computer simulations on a serial two-link robotic manipulator are presented to demonstrate the effectiveness of the proposed controller-observer algorithm. Finally, Section 3.6 gives some conclusions.

3.2 Problem Statement

3.2.1 System in Normal Operation Condition

Consider a serial n-link robotic manipulator in normal operation condition with the dynamic equation as

$$M(\theta)\ddot{\theta} + C\left(\theta,\dot{\theta}\right)\dot{\theta} + G(\theta) + F\left(\dot{\theta}\right) + \tau_d(t) = \tau(t) \tag{3.1}$$

where $\theta, \dot{\theta}, \ddot{\theta} \in \Re^n$ represent position, velocity, and acceleration of robot joints, respectively. $M(\theta) \in \Re^{n\times n}$, $C\left(\theta,\dot{\theta}\right) \in \Re^n$, and $G(\theta) \in \Re^n$ denote the inertia matrix, the Coriolis and centripetal forces, and the gravitational force term, respectively. $F\left(\dot{\theta}\right) \in \Re^n$ is the friction vector, $\tau(t) \in \Re^n$ denotes the control input torque, and $\tau_d(t) \in \Re^n$ represents the disturbance vector.

In realization, since the difference between the mathematical and practical model, the model functions of the robotic manipulator can be expressed as

$$M(\theta) = M_0(\theta) + \Delta M(\theta) \tag{3.2}$$

$$C\left(\theta,\dot{\theta}\right) = C_0\left(\theta,\dot{\theta}\right) + \Delta C\left(\theta,\dot{\theta}\right) \tag{3.3}$$

$$G(\theta) = G_0(\theta) + \Delta G(\theta) \tag{3.4}$$

where $M_0(\theta)$, $C_0\left(\theta,\dot{\theta}\right)$, and $G_0(\theta)$ represent the nominal model; the terms $\Delta M(\theta)$, $\Delta C\left(\theta,\dot{\theta}\right)$, and $\Delta G(\theta)$ are the unmodeled components.

Thus, we can rewrite the robot dynamic equation (3.1) as

$$M_0(\theta)\ddot{\theta} + C_0\left(\theta,\dot{\theta}\right)\dot{\theta} + G_0(\theta) = \tau(t) + \Theta\left(\theta,\dot{\theta},t\right) \tag{3.5}$$

where $\Theta\left(\theta,\dot{\theta},t\right) = -\Delta M(\theta) - \Delta C\left(\theta,\dot{\theta}\right) - \Delta G(\theta) - F\left(\dot{\theta}\right) - \tau_d(t)$ denotes the uncertainties of the robot system.

The equation (3.5) can be transformed to the below form

$$\ddot{\theta} = \Upsilon\left(\theta, \dot{\theta}, t\right) + {M_0}^{-1}\left(\theta\right)\tau(t) + \Pi\left(\theta, \dot{\theta}, t\right) \tag{3.6}$$

where $\Pi\left(\theta, \dot{\theta}, t\right) = {M_0}^{-1}\left(\theta\right)\Theta\left(\theta, \dot{\theta}, t\right)$ represents the uncertainty terms of the robotic system and $\Upsilon\left(\theta, \dot{\theta}, t\right) = {M_0}^{-1}\left(\theta\right)\left[-C_0\left(\theta, \dot{\theta}\right)\dot{\theta} - G_0\left(\theta\right)\right]$ represents the nominal function of the robotic system.

3.2.2 System in Fault Affected Operation Condition

Nowadays, with modern industrial applications becoming increasingly complex, faults more frequently happen in a system especially in the condition of long-term operation. Therefore, in this chapter, we assume that the robot system works under the effect of faults. Thus, the robot dynamic (3.6) becomes

$$\ddot{\theta} = \Upsilon\left(\theta, \dot{\theta}, t\right) + {M_0}^{-1}\left(\theta\right)\tau(t) + \Pi\left(\theta, \dot{\theta}, t\right) + \Psi\left(\theta, \dot{\theta}, t\right) \tag{3.7}$$

where $\Psi\left(\theta, \dot{\theta}, t\right) = \xi\left(t - T_f\right)\Phi\left(\theta, \dot{\theta}, t\right)$ represents the unknown but bounded faults that happen at time T_f. The term $\xi\left(t - T_f\right) = diag\left\{\xi_1\left(t - T_f\right), \xi_2\left(t - T_f\right), \ldots, \xi_n\left(t - T_f\right)\right\}$ represents the time profile of the unknown faults, in which $\xi_i\left(t - T_f\right) = \begin{cases} 0 & if\ t \le T_f \\ 1 - e^{-\zeta_i\left(t - T_f\right)} & if\ t \ge T_f \end{cases}$ with $\zeta_i > 0$ represent the evolution rate, $(i = 1, 2, \ldots, n)$.

Remark 3.1. *In robotic manipulator systems, faults can be actuator faults, sensor faults, and process faults. However, this chapter focuses to solve the system with actuator faults. Therefore, the fault functions $\Phi\left(\theta, \dot{\theta}, t\right)$ are defined as faults which occur in the actuator.*

In this chapter, the unknown faults will be treated as additional uncertainties, thus we consider the total effect of the lumped uncertainties and faults in the system.

By defining $x_1 = \theta$, $x_2 = \dot{\theta}$, $x = \begin{bmatrix} {x_1}^T & {x_2}^T \end{bmatrix}^T$, we transfer the robot dynamic (3.7) into the state space form as

$$\begin{aligned} \dot{x}_1 &= x_2 \\ \dot{x}_2 &= \Upsilon(x, t) + {M_0}^{-1}\left(x_1\right)\tau(t) + D(x, t) \end{aligned} \tag{3.8}$$

where $D(x, t) = \Pi\left(x, t\right) + \Psi\left(x, t\right)$ represents the lumped uncertainties and faults.

The main objective of this chapter is to design a controller-observer strategy that deals with the effects of the lumped uncertainties and faults and achieve minimum tracking errors. The proposed controller-observer method is designed based on the assumptions as following:

Assumption 3.1. *The lumped uncertainties and faults $D(x,t)$ are bounded as*

$$|D(x,t)| \leq \Delta_D \tag{3.9}$$

where Δ_D is a known positive constant.

Assumption 3.2. *There exists the time derivative of the lumped uncertainties and faults and they are bounded as*

$$\left|\frac{d}{dt}D(x,t)\right| \leq \Delta_{\dot{D}} \tag{3.10}$$

where $\Delta_{\dot{D}}$ is a known positive constant. Note that the Assumption 3.2 is realistic and was used in many researches [83, 84, 85].

3.3 Design of the Third-Oder Sliding Mode Observer

In this section, the TOSMO is designed to approximate the system velocities, which is assumed unavailable because of the lacking tachometer sensors in the system. In addition, the lumped uncertainties and faults will be reconstructed from the estimated signal and then employed to design the control in the next section.

3.3.1 Design of The Observer

The TOSMO is designed for the robotic system (3.8) as [42]

$$\begin{aligned}
\dot{\hat{x}}_1 &= \gamma_1 |x_1 - \hat{x}_1|^{2/3} sign\,(\tilde{x}_1) + \hat{x}_2 \\
\dot{\hat{x}}_2 &= \mathrm{Y}\,(\hat{x},t) + {M_0}^{-1}\,(x_1)\,\tau(t) + \gamma_2 |x_1 - \hat{x}_1|^{1/3} sign\,(x_1 - \hat{x}_1) - \hat{z} \\
\dot{\hat{z}} &= -\gamma_3 sign\,(x_1 - \hat{x}_1)
\end{aligned} \tag{3.11}$$

where $\hat{x}$ is the estimator of the true state x, and γ_i represent the observer gains, $(i = 1, 2, 3)$.

By subtracting (3.11) from (3.8), we can obtain

$$\begin{aligned}\dot{\tilde{x}}_1 &= -\gamma_1|\tilde{x}_1|^{2/3}sign\left(\tilde{x}_1\right)+\tilde{x}_2\\ \dot{\tilde{x}}_2 &= -\gamma_2|\tilde{x}_1|^{1/3}sign\left(\tilde{x}_1\right)+D(x,t)-d\left(\tilde{x},t\right)+\hat{z}\\ \dot{\hat{z}} &= -\gamma_3 sign\left(\tilde{x}_1\right)\end{aligned} \tag{3.12}$$

where $\tilde{x} = x - \hat{x}$ represent the state estimation errors and $d\left(\tilde{x},t\right) = \left[\mathrm{Y}\left(\hat{x},t\right)\right.$ $\left.+{M_0}^{-1}\left(x_1\right)\tau\right] - \left[\mathrm{Y}\left(x,t\right)+{M_0}^{-1}\left(x_1\right)\tau\right]$. We assume that the term $d\left(\tilde{x},\tau,t\right)$ and its derivative are bounded as $\left|d\left(\tilde{x},t\right)\right| \leq \Delta_d$ and $\left|\dot{d}\left(\tilde{x},t\right)\right| \leq \Delta_{\dot{d}}$.

The estimation errors (3.12) can be rewritten as follow

$$\begin{aligned}\dot{\tilde{x}}_1 &= -\gamma_1|\tilde{x}_1|^{2/3}sign\left(\tilde{x}_1\right)+\tilde{x}_2\\ \dot{\tilde{x}}_2 &= -\gamma_2|\tilde{x}_1|^{1/3}sign\left(\tilde{x}_1\right)+\hat{z}_0\\ \dot{\hat{z}}_0 &= -\gamma_3 sign\left(\tilde{x}_1\right)+\dot{\hat{\Delta}}\left(x,t\right)\end{aligned} \tag{3.13}$$

where $\hat{z}_0 = \hat{D}\left(x,t\right)+\hat{z}$ with $\hat{D}\left(x,t\right) = D\left(x,t\right)-d\left(\tilde{x},t\right)$.

The error dynamic (3.13) is in the standard form of robust exact second-order differentiator; according to [86], the stable and finite-time convergence of the differentiator has completely demonstrated. The observer gains can be selected as $\gamma_1 = \alpha_1 L^{1/3}$, $\gamma_2 = \alpha_2 L^{2/3}$, and $\gamma_3 = \alpha_3 L$ where $\alpha_1 = 2$, $\alpha_2 = 2.12$, $\alpha_3 = 1.1$, and $L = \Delta_{\dot{D}} + \Delta_{\dot{d}}$.

3.3.2 Uncertainties and Faults Reconstruction

After the convergence time, the estimated states ($\hat{x}_1$, and $\hat{x}_2$) will reach the true states (x_1, and x_2), respectively. The estimation errors (3.13) becomes

$$\begin{aligned}\dot{\tilde{x}}_1 &= -\gamma_1|\tilde{x}_1|^{2/3}sign\left(\tilde{x}_1\right)+\tilde{x}_2 \equiv 0\\ \dot{\tilde{x}}_2 &= -\gamma_2|\tilde{x}_1|^{1/3}sign\left(\tilde{x}_1\right)+\hat{z}_0 \equiv 0\\ \dot{\hat{z}}_0 &= -\gamma_3 sign\left(\tilde{x}_1\right)+\dot{\hat{\Delta}}\left(x,t\right) \equiv 0\end{aligned} \tag{3.14}$$

As a result, the estimation errors of the lumped uncertainties and faults, $d\left(\tilde{x},t\right)$, will become zero; therefore, the estimation of the lumped uncertainties and faults are reconstructed as

$$\hat{D}\left(x,t\right) = \int \gamma_3 sign\left(\tilde{x}_1\right) \tag{3.15}$$

As we can see in (3.15), the obtained signal consists of an integral operator; hence, the estimation information of the TOSMO can be reconstructed directly without filtration. Consequently, this observer provides estimation signal with higher accuracy and low chattering than that of SOSMO [12]. This estimation information will be performed to design the FTC method in the next section.

Remark 3.2. *Even if in the ideal sliding motion, we can only to get the exact estimation information after the convergence process. When employing the obtained estimation to the system, the estimation errors which appear in transient time will affect the selecting parameters of the controller. If we do not consider these components strictly, it will cause incorrect in selection of control parameters and thus affect the system stability.*

3.4 Controller Design

In this section, an FTC method using NFTSMC is designed to handle the effects of the lumped uncertainties and faults with low chattering phenomenon and high tracking performance. Especially, the control technique is designed based on the assumption that only the tachometer sensors are unavailable in the robotic system. The analysing process is divided into two periods as following.

3.4.1 Design of NFTSM Switching Function

The tracking errors and velocity errors are defined as following

$$e = x_1 - x_d \tag{3.16}$$

$$\hat{e} = \hat{x}_2 - \dot{x}_d \tag{3.17}$$

where $x_d, \dot{x}_d$ represent the desired trajectories and velocities, respectively.

In order to design the control input, an NFTSM switching function based on TOSMO is chosen as the following expression

$$\hat{s} = \hat{e} + \frac{2\kappa_1}{1+\exp(-\mu_1(|e|-\phi))}e + \frac{2\kappa_2}{1+\exp(\mu_2(|e|-\phi))}|e|^{\alpha} sign\,(e) \tag{3.18}$$

where κ_1, κ_2, μ_1, μ_2 are positive constants, $0 < \alpha < 1$ and $\phi = \left(\frac{\kappa_2}{\kappa_1}\right)^{1/(1-\alpha)}$.

Based on the SMC theory, when the system operates in the sliding mode, the following constraints are satisfied:

$$\begin{aligned} \hat{s} &= 0 \\ \dot{\hat{s}} &= 0 \end{aligned} \tag{3.19}$$

Therefore, the sliding mode dynamics can be obtained as

$$\dot{\hat{e}} = -\frac{2\kappa_1}{1+\exp(-\mu_1(|e|-\phi))}e - \frac{2\kappa_2}{1+\exp(\mu_2(|e|-\phi))}|e|^{\alpha} sign\,(e) \tag{3.20}$$

Theorem 3.1. *For the sliding mode dynamics (3.20), the origin, e, is defined as the stable equilibrium point and the state trajectories of the dynamic system (3.20) converge to zero in the finite-time.*

Proof of Theorem 3.1

We can acquire the time derivative of the tracking errors (3.16) as

$$\begin{aligned} \dot{e} &= \dot{x}_1 - \dot{x}_d \\ &= x_2 - \dot{x}_d \end{aligned} \tag{3.21}$$

According to the definition of the estimation errors in Section 3.3, the velocity errors (3.17) can be rewritten as

$$\begin{aligned} \dot{\hat{e}} &= \hat{x}_2 - \dot{x}_d \\ &= x_2 - \dot{x}_d - \tilde{x}_2 \end{aligned} \tag{3.22}$$

After the convergence estimation errors, the estimated states, $\hat{x}_2$, will reach the true states, x_2. Therefore, the velocity errors (3.22) become

$$\dot{\hat{e}} = x_2 - \dot{x}_d = \dot{e} \tag{3.23}$$

Consider the Lyapunov function candidate as

$$V_1 = \frac{1}{2}e^2 \tag{3.24}$$

Differentiating the Lyapunov function (24) with respect to time and substituting the result from (3.20), we obtain

$$\begin{aligned}\dot{V}_1 &= e\dot{e} \\ &= -\frac{2\kappa_1}{1+\exp(-\mu_1(|e|-\phi))}e^2 - \frac{2\kappa_2}{1+\exp(\mu_2(|e|-\phi))}|e|^{\alpha+1} \\ &< 0\end{aligned} \tag{3.25}$$

It is shown that $V_1 > 0$ and $\dot{V}_1 < 0$, hence, the origin, e, of the sliding mode dynamic (3.20) is stable and the state trajectories e and $\dot{e}$ converge to zero in the finite-time. Consequently, the tracking velocity errors $\hat{e}$ converge to zero in the finite-time. Therefore, the theorem 3.1 is completely demonstrated.

3.4.2 Design of FTC Method

A - Before The Convergence Time

To achieve the control objective for the robotic system (3.8), a controller-observer technique is described in Theorem 3.2.

Theorem 3.2. *For the robotic manipulator system (3.8), if the control input signal is designed as (3.26-3.28), then the system is stable, and the tracking error converges to zero in finite time.*

The control law is designed as below

$$\tau = -M_0(x_1)\left(\tau_{eq} + \tau_{sw}\right) \tag{3.26}$$

with the equivalent control law, τ_{eq}, and the switching control law, τ_{sw}, are designed as following

$$\begin{aligned}\tau_{eq} = &-\ddot{x}_d + \Upsilon(x,t) + \gamma_2|\tilde{x}_1|^{1/3}sign\left(\tilde{x}_1\right) + \int \gamma_3 sign(\tilde{x}_1) \\ &+\dot{e}\left[\begin{array}{l}\frac{2\kappa_1}{1+\exp(-\mu_1(|e|-\phi))} + \frac{2\kappa_1\mu_1 sign(e)\exp(-\mu_1(|e|-\phi))}{[1+\exp(-\mu_1(|e|-\phi))]^2} \\ +\frac{2\kappa_2\alpha}{1+\exp(\mu_2(|e|-\phi))}|e|^{\alpha-1} - \frac{2\kappa_2\mu_2\exp(\mu_2(|e|-\phi))}{[1+\exp(\mu_2(|e|-\phi))]^2}|e|^{\alpha}\end{array}\right]\end{aligned} \tag{3.27}$$

$$\tau_{sw} = (\Delta_d + \mu)sign\left(\hat{s}\right) \tag{3.28}$$

where μ is a small positive constant.

Proof of Theorem 3.2

We can acquire the time derivative of the switching function (3.18) as

$$\dot{\hat{s}} = \frac{d}{dt}\hat{\hat{e}} + \dot{e} \begin{bmatrix} \frac{2\kappa_1}{1+\exp(-\mu_1(|e|-\phi))} + \frac{2\kappa_1\mu_1 sign(e)\exp(-\mu_1(|e|-\phi))}{[1+\exp(-\mu_1(|e|-\phi))]^2} \\ +\frac{2\kappa_2\alpha}{1+\exp(\mu_2(|e|-\phi))}|e|^{\alpha-1} - \frac{2\kappa_2\mu_2\exp(\mu_2(|e|-\phi))}{[1+\exp(\mu_2(|e|-\phi))]^2}|e|^{\alpha} \end{bmatrix} \tag{3.29}$$

Taking the time derivative of velocity errors and substituting the second equation of the TOSMO (3.11) yields

$$\begin{aligned} \tfrac{d}{dt}\hat{\hat{e}} &= \dot{\hat{x}}_2 - \ddot{x}_d \\ &= -\ddot{x}_d + \mathrm{Y}(\hat{x},t) + {M_0}^{-1}(x_1)\,\tau \\ &\quad +\gamma_2|\tilde{x}_1|^{1/3} sign(\tilde{x}_1) + \int \gamma_3 sign(\tilde{x}_1) \\ &= -\ddot{x}_d + \mathrm{Y}(x,t) + {M_0}^{-1}(x_1)\,\tau + d(\tilde{x},t) \\ &\quad +\gamma_2|\tilde{x}_1|^{1/3} sign(\tilde{x}_1) + \int \gamma_3 sign(\tilde{x}_1) \end{aligned} \tag{3.30}$$

Substituting (3.29) into (3.30) yields

$$\begin{aligned} \dot{\hat{s}} = &-\ddot{x}_d + \mathrm{Y}(x,t) + {M_0}^{-1}(x_1)\,\tau + d(\tilde{x},t) \\ &+\gamma_2|\tilde{x}_1|^{1/3} sign(\tilde{x}_1) + \int \gamma_3 sign(\tilde{x}_1) \\ &+\dot{e} \begin{bmatrix} \frac{2\kappa_1}{1+\exp(-\mu_1(|e|-\phi))} + \frac{2\kappa_1\mu_1 sign(e)\exp(-\mu_1(|e|-\phi))}{[1+\exp(-\mu_1(|e|-\phi))]^2} \\ +\frac{2\kappa_2\alpha}{1+\exp(\mu_2(|e|-\phi))}|e|^{\alpha-1} - \frac{2\kappa_2\mu_2\exp(\mu_2(|e|-\phi))}{[1+\exp(\mu_2(|e|-\phi))]^2}|e|^{\alpha} \end{bmatrix} \end{aligned} \tag{3.31}$$

Employing the control input (3.26-3.28) into (3.31), we achieve

$$\dot{\hat{s}} = -(\Delta_d + \mu) sign(\hat{s}) + d(\tilde{x},t) \tag{3.32}$$

Consider the Lyapunov function candidate as

$$V_2 = \frac{1}{2}\hat{s}^T\hat{s} \tag{3.33}$$

Differentiating the Lyapunov function (3.33) with respect to time and substituting the result from (3.32), we obtain

$$\begin{aligned} \dot{V}_2 &= \hat{s}^T\dot{s} \\ &= \hat{s}^T\left(-(\Delta_d+\mu) sign(\hat{s}) + d(\tilde{x},t)\right) \\ &= -(\Delta_d+\mu)\sum_{i=1}^{n}|\hat{s}_i| + d(\tilde{x},t)^T\hat{s} \le -\mu\sum_{i=1}^{n}|\hat{s}_i| \\ &\le -\mu\,\|\hat{s}\| = -\sqrt{2}\mu {V_2}^{1/2} < 0,\ \forall \hat{s} \neq 0 \end{aligned} \tag{3.34}$$

According to the stability theory in [87], it can be concluded that the robotic system (3.8) is stable and the tracking error converges to zero after finite time. Thus, the Theorem 3.2 is completely demonstrated.

B - After The Convergence Time

In this part, we consider the control law after the convergence process. After the convergence time, the term $\gamma_2|\tilde{x}_1|^{1/3}sign\left(\tilde{x}_1\right)$ in the equivalent control law (3.27) converts to zero; therefore, the control law (3.26-3.28) will become

$$\tau = -M_0(x_1)\left(\tau_{eq} + \tau_{sw}\right) \tag{3.35}$$

$$\begin{aligned}\tau_{eq} = &-\ddot{x}_d + \Upsilon(x,t) + \int \gamma_3 sign(\tilde{x}_1) \\ &+\dot{e}\left[\begin{array}{l} \frac{2\kappa_1}{1+\exp(-\mu_1(|e|-\phi))} + \frac{2\kappa_1\mu_1 sign(e)\exp(-\mu_1(|e|-\phi))}{[1+\exp(-\mu_1(|e|-\phi))]^2} \\ +\frac{2\kappa_2\alpha}{1+\exp(\mu_2(|e|-\phi))}|e|^{\alpha-1} - \frac{2\kappa_2\mu_2\exp(\mu_2(|e|-\phi))}{[1+\exp(\mu_2(|e|-\phi))]^2}|e|^{\alpha} \end{array}\right]\end{aligned} \tag{3.36}$$

$$\tau_{sw} = (\Delta_d + \mu)sign\left(\hat{s}\right) \tag{3.37}$$

Generally, the control law in (3.35-3.37) is employed to the system; however, the missing of the component $\gamma_2|\tilde{x}_1|^{1/3}sign\left(\tilde{x}_1\right)$ leads to incorrect in selecting parameters and may affect the operation of the system at the initial stage and when faults happen. Therefore, this chapter performs the control law in (3.26-3.28) instead of the control law in (3.35-3.37). The proposed controller-observer technique provides some superior control properties such as high tracking control precision with finite-time convergence, faster dynamic response, low chattering phenomenon, non-singularity, velocity measurement elimination and robustness against the lumped uncertainties and faults. Its efficiency will be demonstrated in the simulation part.

3.5 Numerical Simulations

To demonstrate the effectiveness of the proposed FTC technique, computer simulations are performed on a serial two-link robotic manipulator which is presented in Fig. 3.1. The detailed dynamic model of the two-link robot is given as following Inertia term

$$M(\theta) = \left[\begin{array}{cc} M_{11} & M_{12} \\ M_{21} & M_{22} \end{array}\right] \tag{3.38}$$

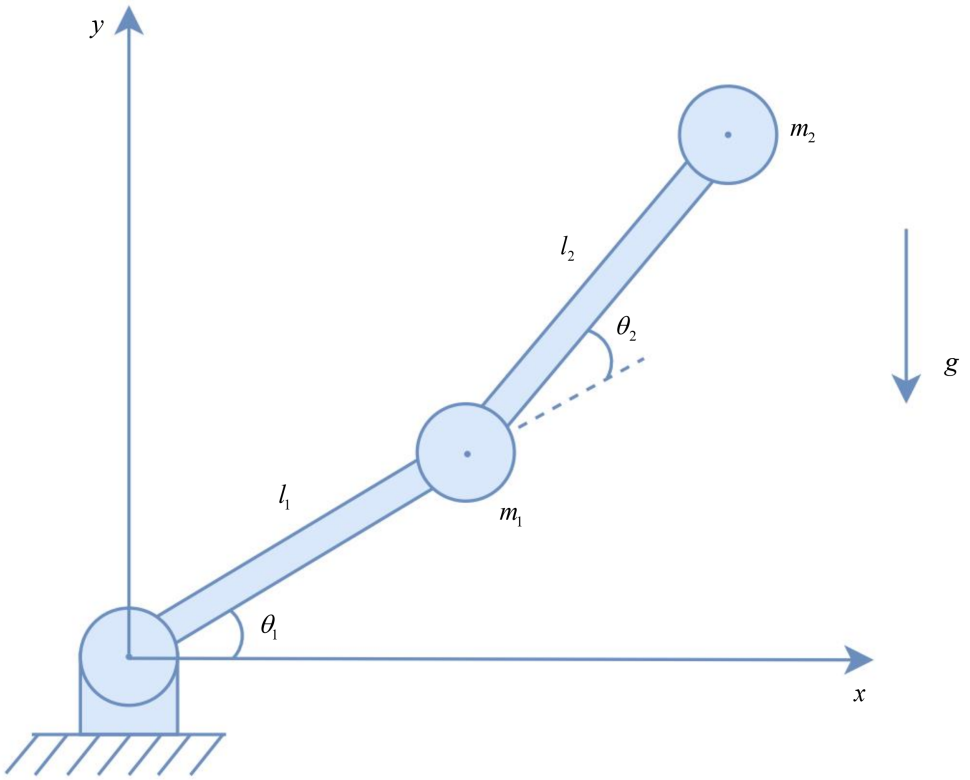

FIGURE 3.1: Two-link robotic manipulator

where

$$M_{11} = m_1 {l_{c1}}^2 + m_2(l_1^2 + {l_{c2}}^2 + 2l_1 l_{c2} cos(\theta)) + I_1 + I_2$$

$$M_{12} = M_{21} = m_1 {l_{c2}}^2 + m_2 l_{c2} l_1 cos(\theta) + I_2$$

$$M_{22} = m_2 {l_{c2}}^2 + I_2$$

Coriolis and centripetal term

$$C(\theta, \dot{\theta}) = \begin{bmatrix} -2m_2 l_1 l_{c2} sin(\theta)\dot{\theta}_1\dot{\theta}_2 - m_2 l_1 l_{c2} sin(\theta_2)\dot{\theta}_2^2 \\ m_2 l_1 l_{c2} sin(\theta_2)\dot{\theta}_1^2 \end{bmatrix} \tag{3.39}$$

Gravitational term

$$G(\theta) = \begin{bmatrix} m_1 g l_{c1} \cos(\theta_1) + m_2 g \left(l_1 \cos(\theta_1) + l_{c2} \cos(\theta_1 + \theta_2)\right) \\ m_2 l_{c2} g \cos(\theta_1 + \theta_2) \end{bmatrix} \tag{3.40}$$

with the values of parameters are given in Table 3.1.

TABLE 3.1: Parameters of the 2-link robot

Parameters	Values
$m_1,\ m_2$	1.5, 1.3 (kg)
$l_1,\ l_2$	1, 0.8 (m)
$l_{c1},\ l_{c2}$	0.5, 0.4 (m)
$I_1,\ I_2$	1, 0.8 ($kgNm^2$)

All simulation in this chapter is accomplished by employing the MATLAB/Simulink with the sampling time $10^{-3}s$. The desired trajectories of robot are assumed as

$$\theta_d = \begin{bmatrix} 1.2\cos(t/7) - 0.7 \\ \sin(t/6 + \pi/2) - 0.4 \end{bmatrix} \tag{3.41}$$

The robot frictions and disturbances are assumed as

$$F(\dot{\theta}) = \begin{bmatrix} 1.9\cos(2\dot{q}_1) \\ 1.05\cos(\dot{q}_2) \end{bmatrix} \tag{3.42}$$

$$\tau_d = \begin{bmatrix} 2.5\sin(t) + 0.4\cos(\pi t) \\ \cos(t) + 0.6\sin(t/\pi) \end{bmatrix} \tag{3.43}$$

To validate the property in handling the fault effects, two cases of faults are assumed to impact the robot system. Firstly, simple faults Φ_1 are assumed to be occurred to joint 1 at $T_f = 10s$ and to joint 2 at $T_f = 20s$. Secondly, complex faults Φ_2 are assumed to be occurred to both joints at $T_f = 10s$.

$$\Phi_1 = \begin{bmatrix} -9.7\cos(\pi t/7 + \pi/5) \\ 8.2\cos(\pi t/5 + \pi/4) \end{bmatrix} \tag{3.44}$$

$$\Phi_2 = \begin{bmatrix} -3.02{\theta_1}^2 + \sin(\theta_2) + 6.1\cos(\dot{\theta}_1) + 4.5\dot{\theta}_2 + 0.7\sin(2t/\pi) \\ 1.5\theta_1 + 3.2\cos(\theta_2) + 2.3\sin(2\dot{\theta}_1) + 9.2\dot{\theta}_2 + 0.5\cos(t/\pi) \end{bmatrix} \tag{3.45}$$

The selected parameters of the controller and observer methods in the simulations are shown in Table 3.2.

In the first part of simulation, a comparison of the estimation results between the TOSMO and the SOSMO is performed. In Fig. 3.2 and Fig. 3.3, the achieved

TABLE 3.2: Parameters of the controller/observer methods

Controller/Observer methods	Parameters	Values
TOSMO	L	9
SMC	c	2
	Δ_d, μ	0.5, 0.01
NFTSMC	β_1, β_2, λ, α	1.5, 0.4, 0.7, 0.3
	Δ_d, μ	0.5, 0.01
Proposed controller	μ_1, μ_2, α	1.2, 1.4, 0.6
	Δ_d, μ	0.5, 0.01

velocity estimation errors when faults Φ_1 and Φ_2 occur, are presented, respectively. The results show that the TOSMO provides the estimation information with higher accuracy than that of the SOSMO. According to [12], the SOSMO needs a lowpass filter to rebuild the estimated signal of the lumped uncertainties and faults. This filtration process causes time delay and estimation errors, that reduce the estimation performance of the SOSMO. Fortunately, this limitation is removed in the TOSMO. The estimation results of the lumped uncertainties and faults are presented from Fig. 3.4 to Fig. 3.7. In both two cases of faults, the TOSMO provides higher estimation performance and less chattering than that of the SOSMO. However, the time response of the TOSMO is slower. This is also the main limitation of the TOSMO that needs to improve.

In the second part, a comparison of the proposed FTC algorithm with the control law in (3.35-3.37) and the control techniques which are designed based on the conventional SMC (Appendix A) and the NTSMC (Appendix B) is performed to demonstrate its superior control properties. The tracking position and the tracking error at each joint when the simple faults Φ_1 occur are displayed in Fig. 3.8 and Fig. 3.10, respectively. As in the results, the real trajectories provided by the proposed FTC method track the desired trajectories with higher accuracy than the FTC methods that are designed based on the conventional SMC and the NTSMC. Compared with the control law in (3.35-3.37), the tracking performance that provided by the proposed controller is similar after the convergence process. However, by performing the additional term $\gamma_2|\tilde{x}_1|^{1/3}sign\,(\tilde{x}_1)$, the proposed FTC method provides faster response at the initial stage and when faults happen. For the case of the complex faults Φ_2, the similar results are obtained and shown in the Fig. 3.9 and Fig. 3.11.

The additional term $\gamma_2|\tilde{x}_1|^{1/3}sign\,(\tilde{x}_1)$ also influences to the convergence of the

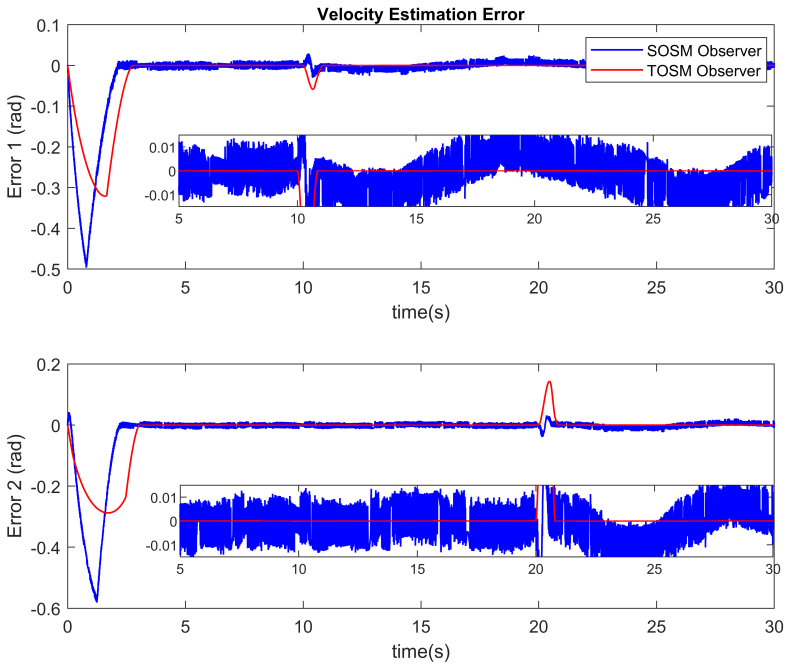

FIGURE 3.2: The velocity estimation errors are supplied by SOSMO and TOSMO at each joint when faults Φ_1 occur

switching function. As shown in the Fig. 3.12 and Fig. 3.13, the switching function of the proposed FTC method converges to zero faster compared with other controllers in both cases of faults. In other words, the sliding motion can be faster reached. In term of the control input torque, the simulation results for both cases of faults of controllers at each joint are presented in Fig. 3.14 and Fig. 3.15, respectively. As shown in the figures, by using the proposed FTC algorithm, the chattering phenomenon in the control inputs are reduced due to the compensation of the estimated uncertainties and faults.

3.6 Conclusions

In this chapter, an FTC method using the NFTSMC and the TOSMO for the robotic manipulator system is proposed. The TOSMO showed its capability to estimate system velocities; thus, the need of tachometers in the system is eliminated. In addition, the obtained lumped uncertainties and faults are utilized to compensate their effects to the system, thus the tracking performance of the proposed controller-observer method is improved. Moreover, the two stages of time that before and after the convergence time, are carefully analyzed. The

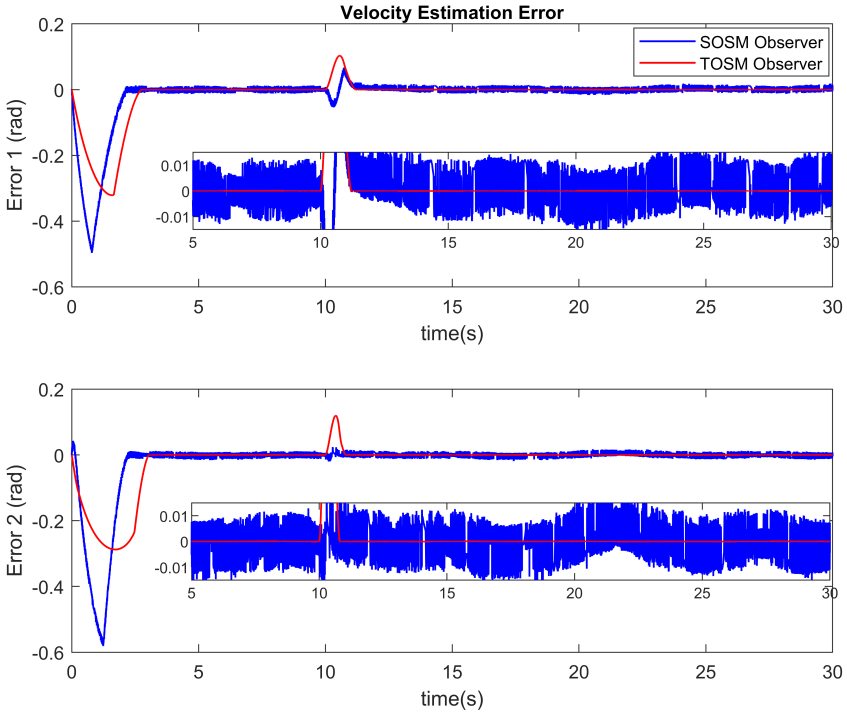

FIGURE 3.3: The velocity estimation errors are supplied by SOSMO and TOSMO at each joint when faults Φ_2 occur

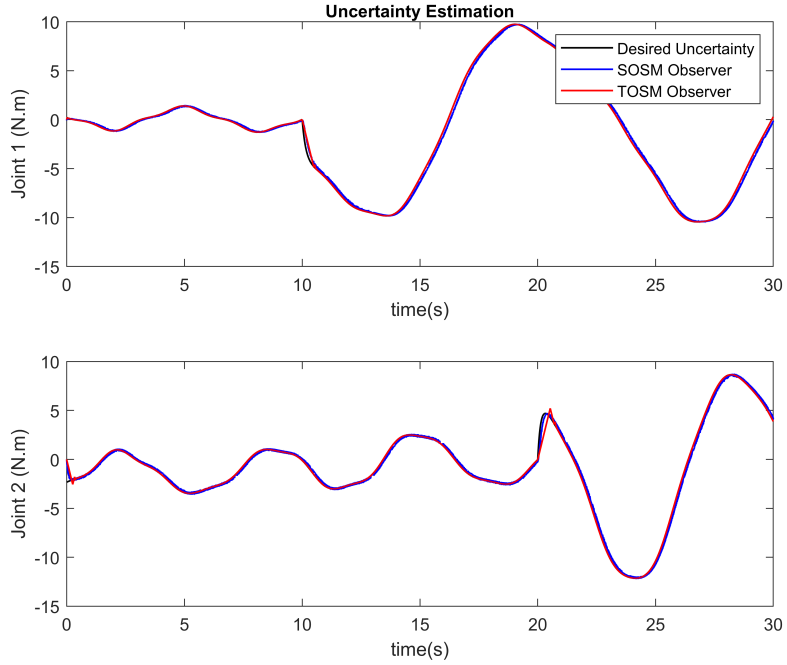

FIGURE 3.4: The estimation of the lumped uncertainties and faults are supplied by SOSMO and TOSMO at each joint when faults Φ_1 occur

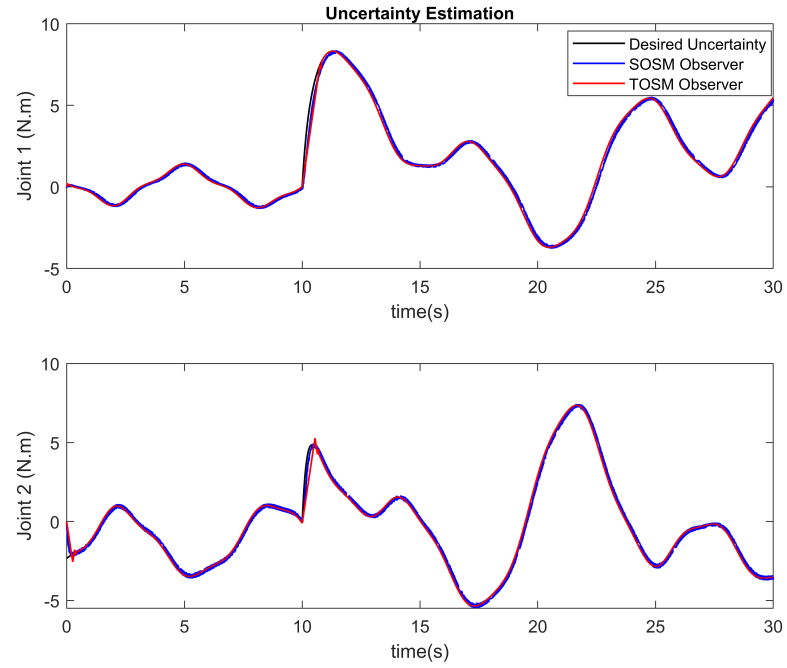

FIGURE 3.5: The estimation of the lumped uncertainties and faults are supplied by SOSMO and TOSMO at each joint when faults Φ_2 occur

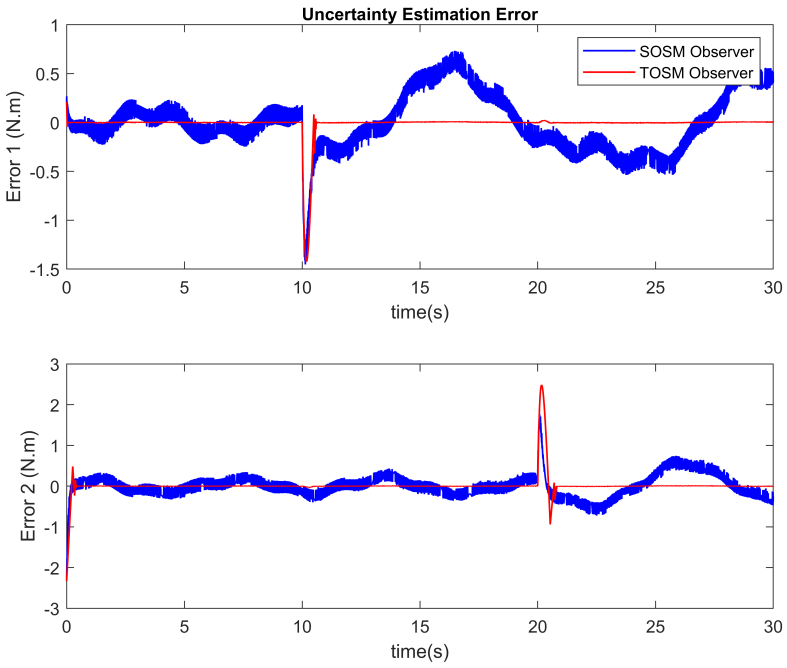

FIGURE 3.6: The estimation errors of the lumped uncertainties and faults are supplied by SOSMO and TOSMO at each joint when faults Φ_1 occur

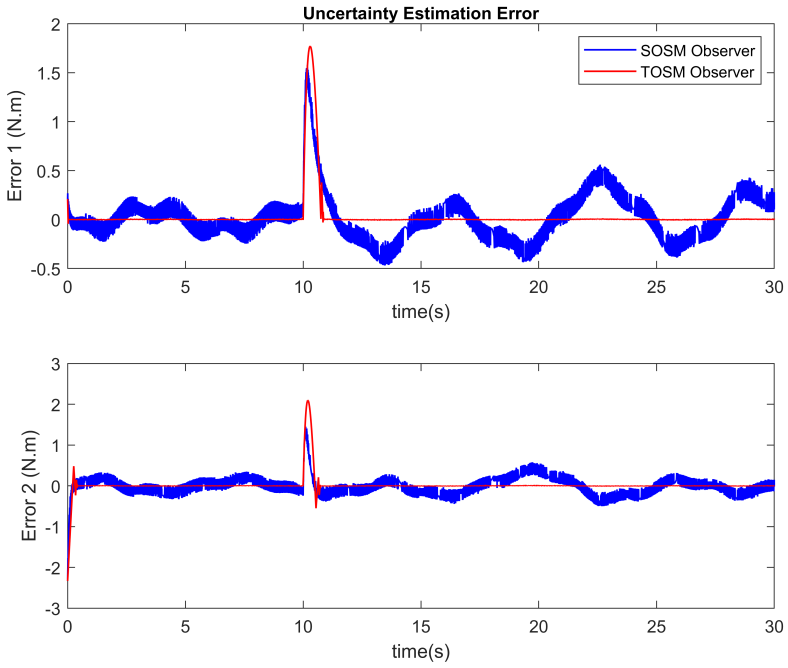

FIGURE 3.7: The estimation errors of the lumped uncertainties and faults are supplied by SOSMO and TOSMO at each joint when faults Φ_2 occur

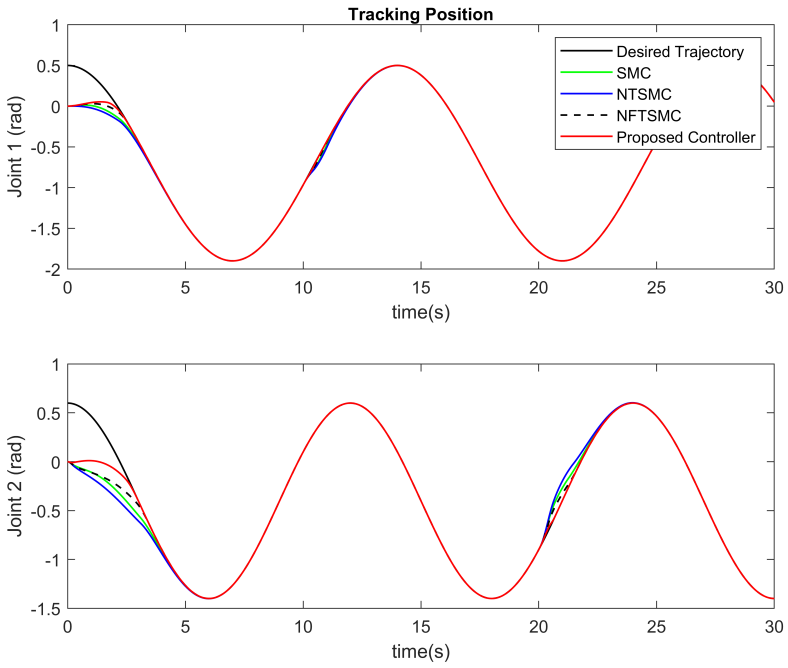

FIGURE 3.8: Desired trajectories and joint angles are supplied by SMC, NTSMC, NFTSMC, and the proposed controller-observer technique at each joint when faults Φ_1 occur

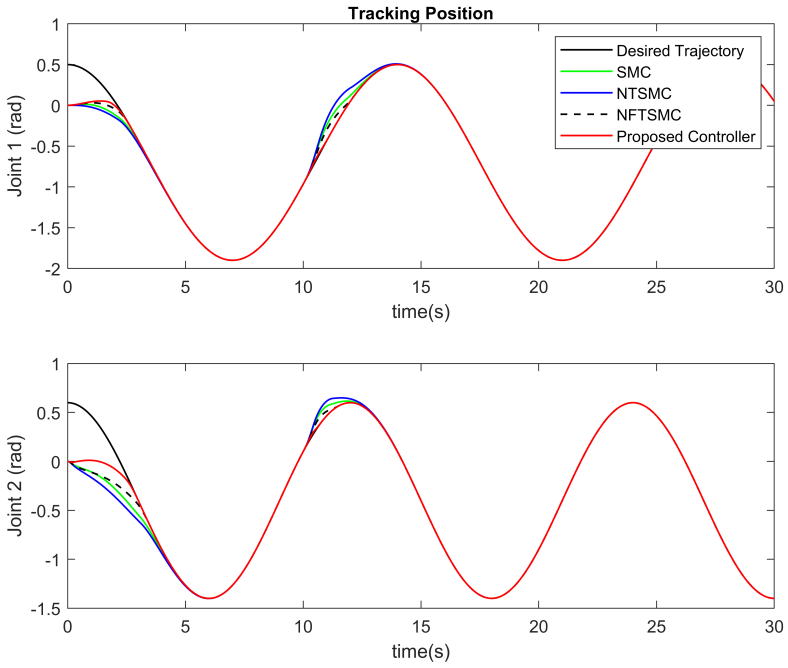

FIGURE 3.9: Desired trajectories and joint angles are supplied by SMC, NTSMC, NFTSMC, and the proposed controller-observer technique at each joint when faults Φ_2 occur

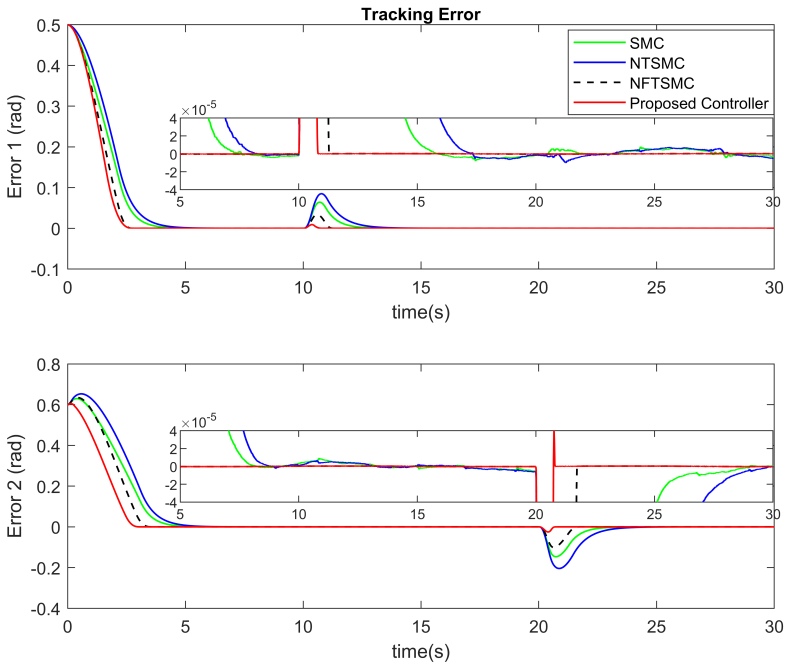

FIGURE 3.10: Tracking errors are supplied by SMC, NTSMC, NFTSMC, and the proposed controller-observer technique at each joint when faults Φ_1 occur

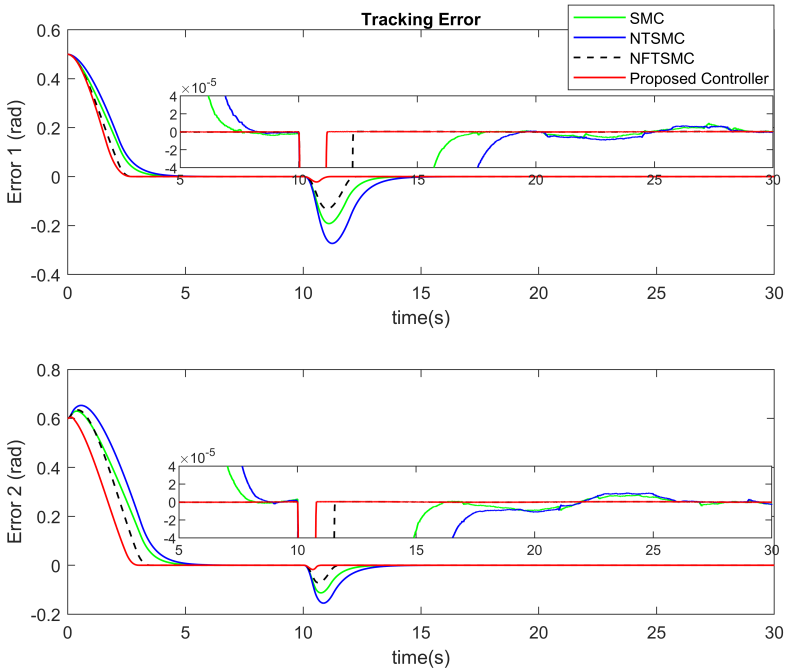

FIGURE 3.11: Tracking errors are supplied by SMC, NTSMC, NFTSMC, and the proposed controller-observer technique at each joint when faults Φ_2 occur

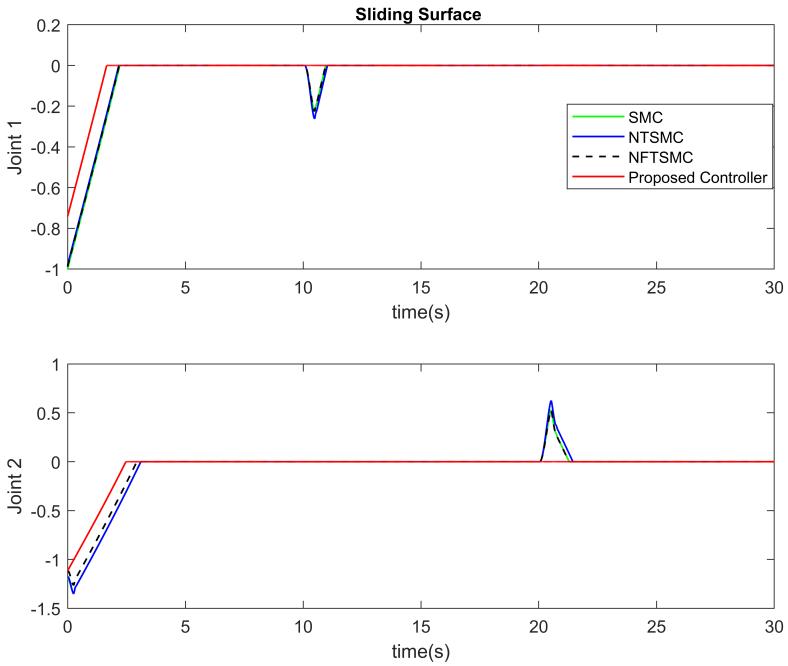

FIGURE 3.12: Switching functions are supplied by SMC, NTSMC, NFTSMC, and the proposed controller-observer technique at each joint when faults Φ_1 occur

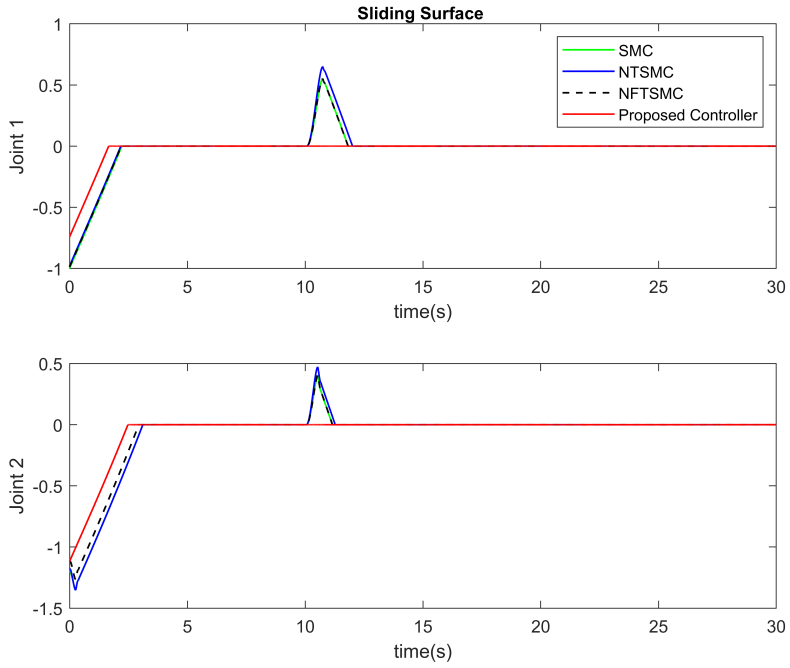

FIGURE 3.13: Switching functions are supplied by SMC, NTSMC, NFTSMC, and the proposed controller-observer technique at each joint when faults Φ_2 occur

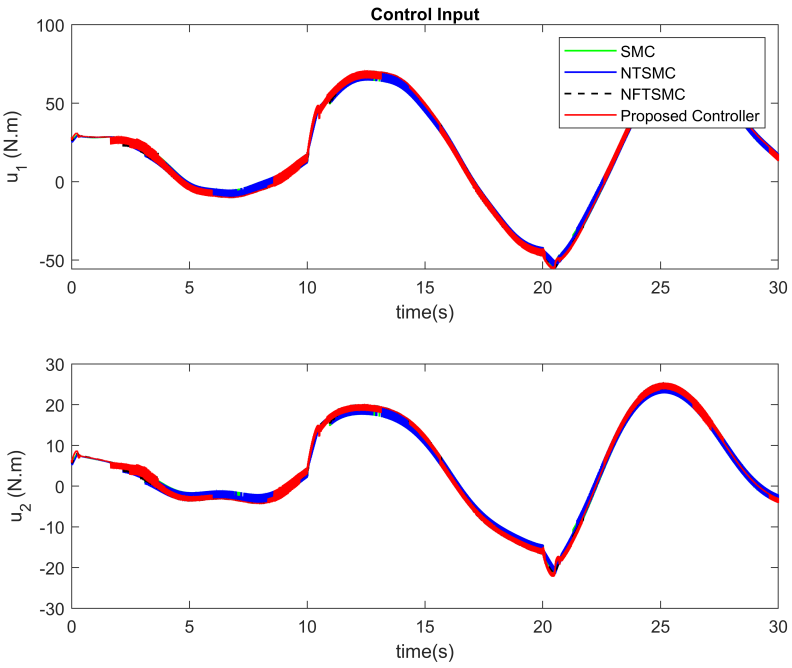

FIGURE 3.14: Control inputs are supplied by SMC, NTSMC, NFTSMC, and the proposed controller-observer technique at each joint when faults Φ_1 occur

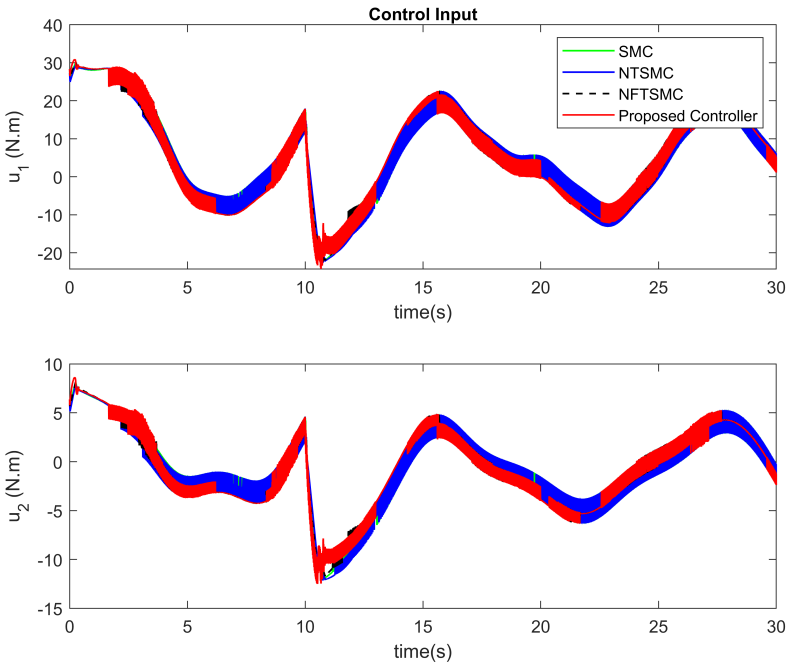

FIGURE 3.15: Control inputs are supplied by SMC, NTSMC, NFTSMC, and the proposed controller-observer technique at each joint when faults Φ_2 occur

proposed FTC method provides advanced control features such as high position tracking precision with fast finite-time convergence, less chattering phenomenon, and robustness against the effects of the lumped uncertainties and faults. The superior control properties of the proposed controller-observer algorithm are fully demonstrated by the simulation results. Further, the proposed method can be applied to the systems that have form of the second-order dynamic systems.

Appendix

A - DESIGN OF CONVENTIONAL SMC

With the position and velocity errors are described in (3.16-3.17), the conventional switching function based on the TOSMO is chosen as

$$\hat{s} = \hat{\dot{e}} + ce \tag{3.46}$$

where c is a positive constant.

The control law is designed as below

$$\tau = -M_0(x_1)\left(\tau_{eq} + \tau_{sw}\right) \tag{3.47}$$

$$\tau_{eq} = -\ddot{x}_d + \mathrm{Y}(x,t) + \int \gamma_3 sign(\tilde{x}_1) + c\dot{e} \tag{3.48}$$

$$\tau_{sw} = (\Delta_d + \mu) sign\left(\hat{s}\right) \tag{3.49}$$

where μ is a small positive constant.

B - DESIGN OF NTSMC

With the position and velocity errors are described in (3.16-3.17), the non-singular terminal switching function based on TOSMO is chosen as in [88]

$$\hat{s} = \hat{\dot{e}} + \beta_1 e + \beta_2 \exp(-\lambda t)\left(e^T e\right)^{-\alpha} e \tag{3.50}$$

where $\beta_1,\ \beta_2$ are positive constants, $0 < \alpha < 1$, and $\lambda > 0$.

The control law is designed as below

$$\tau = -M_0(x_1)\left(\tau_{eq} + \tau_{sw}\right) \tag{3.51}$$

$$\tau_{eq} = -\ddot{x}_d + \mathrm{Y}(x,t) + \int \gamma_3 sign(\tilde{x}_1) + \beta_1\dot{e} + \beta_2 A \tag{3.52}$$

$$\tau_{sw} = (\Delta_d + \mu) sign\left(\hat{s}\right) \tag{3.53}$$

where μ is a small positive constant and the term $A = [(-\lambda)\exp(-\lambda t)\left(e^T e\right)^{-\alpha} e + (-2\alpha)\exp(-\lambda t)\left(e^T e\right)^{-\alpha-1}\left(e^T\dot{e}\right)e + \exp(-\lambda t)\left(e^T e\right)^{-\alpha}\dot{e}]$.

Chapter 4

A Non-Singular Fast Terminal Sliding Mode Control Based on Third-Order Sliding Mode Observer For A Class of Second-Order Uncertain Nonlinear Systems and Its Application To Robot Manipulators

This chapter proposes a controller-observer strategy for a class of second-order uncertain nonlinear systems with only available position measurement. The TOSMO is first introduced to estimate both velocities and the lumped uncertain terms of system with high accuracy, less chattering, and finite time convergence of estimation errors. Then, the proposed controller-observer strategy is designed based on NFTSMC and proposed observer. Thanks to this combination, the proposed strategy has some superior properties such as high tracking accuracy, chattering phenomenon reduction, robustness against the effects of the lumped uncertain terms, velocity measurement elimination, finite time convergence, and faster reaching sliding motion. Especially, two period times, before and after the convergence of the velocity estimation takes place, are considered. The finite time stability of proposed controller-observer method is proved by using the Lyapunov stability theory. Final, the proposed strategy is applied to robot manipulator system and its effectiveness is verified by simulation results, in which a PUMA560 robot manipulator is employed.

4.1 Introduction

In the past decades, controlling uncertain nonlinear systems have been a topic that attracts attention from many researchers theoretically [89, 90, 91]. This topic is also crucial in practical because almost real-world systems have nonlinear dynamic characteristics. Generally, the dynamic model of the system is not clearly known because of the unknown uncertainties and/or external disturbances - in this chapter, for more convenience and avoiding duplication, we will treat it as the lumped uncertainties. They affect directly to the control signal thus reduce the accuracy of the system. This problem has been a big challenge in control theory. To deal with the lumped uncertainties, numerous control strategies have been proposed by researchers, such as PID control [25, 26], adaptive control [92, 93, 94], fuzzy logic control [95, 96], NN control [97, 98], and SMC [42, 69, 70, 71, 72], etc. Among them, the SMC has been widely used in controlling uncertain system by many researchers because of its attractive properties such as fast dynamic response, robustness against the lumped uncertainties and a quite simple design procedure. It is suitable for various types of real systems such as DC-DC converters, motors, helicopters, magnetic levitation, aircraft, and robot manipulators. Besides the great benefits, the utilization of a linear sliding function in conventional SMC causes the finite-time convergence of system state error cannot be guaranteed. To overcome this limitation, the TSMC has been proposed, in which nonlinear sliding functions are utilized instead of the linear sliding function in design procedure [43, 44, 74]. By carefully designing parameters, TSMC provides higher accuracy and finite-time convergence; unfortunately, the conventional TSMC generates two main limitations: 1) slower convergence time comparing to SMC; 2) singularity problem. Various great researches have been focused to overcome these drawbacks. Each problem has been solved by using FTSMC [48, 47, 46] and NTSMC [50, 49, 10], separately. To handle both problems simultaneously, NFTSMC has been developed [51, 53, 71, 99, 16]. Thanks to the superior properties of the NFTSMC such as finite-time convergence, singularity elimination, high tracking error performance, and robustness against the lumped uncertainties, this controller has been extensively utilized to a variety of systems. However, both conventional SMC and NFTSMC still utilize a switching element in reaching phase with a big fixed sliding gain against the effects of the lumped uncertainties leads to the chattering phenomenon. It harms the system and thus reduces the practical applicability of both control methods. On the other hand, the design procedure requires real velocity information which is not usually available in a practical system because of saving cost and

reducing the size of the device.

In order to reduce or eliminate the chattering phenomenon, the basic idea is to reduce the sliding gain in the switching element. Accordingly, the lumped uncertainties must be completely or partially estimated and applied to the control signals to compensate for its effects. Consequently, the switching element is now used to handle the effects of the uncertainty's estimation error instead of the lumped uncertainties; therefore, the sliding gain will be selected smaller than the original method to guarantee the sliding mode can be reached. As a result, the chattering phenomenon will be reduced depending on the precision of the estimation method. In the literature, various model-based techniques have been developed to estimate the lumped uncertainties such as TDE [16, 100], NN observer [101, 6], SMSMO [8, 9, 102, 13], TOSMO [42, 102, 82, 12, 103]. Among them, the TDE technique can only provide the ability to estimate unknown inputs; therefore, an additional observer is needed to estimate the system velocities [16]. It leads the system more complex and increases the computational time. Thanks to the learning capability and excellent approximation, the NN observer can supply an arbitrary accuracy of estimation information. Especially, it can not only have the capability to approximate the lumped uncertainties but also the system velocities. Therefore, only one observer is employed in the system. However, the drawback of using learning techniques is that the transient performance in the existence of external disturbance can be reduced because of the requirement of the online learning procedure. Moreover, the complex training process of neural weights requires a large computation of the system thus degrades the implementation ability in a practical system. Compared to others, the SOSMO stands out due to its capability to approximate both system velocities and the lumped uncertainties with the finite-time convergence of estimation error. Although providing high precision and less chattering in the estimation of velocities, the equivalent output injection of SOSMO which is used to obtain the estimation of the lumped uncertainties is a discontinuous term that causes an undesired chattering phenomenon. Therefore, a lowpass filter is needed to reconstruct the lumped uncertainties from the equivalent output injection. However, it causes the estimation delay and error thus reduces the estimation accuracy of the SOSMO. For that reason, the TOSMO which has the ability to provide a continuous equivalent output injection, has been investigated. Consequently, the required filtration in the SOSMO is eliminated. Compared with the SOSMO, the TOSMO provides the estimation of lumped uncertainties with

less chattering and higher estimation accuracy. Moreover, the TOSMO maintains almost all the advantages of the SOSMO. Thanks to the superior benefits, the TOSMO has been widely applied to control uncertain systems by many researchers [17, 18, 19]. In [17], the TOSMO has been employed to estimate system velocities; however, the author did not consider the ability to approximate the lumped uncertainties of the observer. In contrast, an SMC combined with the TOSMO is presented in [18]. Unfortunately, only the estimation of lumped uncertainties is considered to eliminate its effects. A combination of the two algorithms above, both obtained velocities and lumped uncertainties from the TOSMO is applied to design a conventional SMC, in [19]. However, the actual velocity signal of the system is replaced by the estimated velocity which is after the convergence takes place instead of the original one. This makes the controller design simpler but leads to some components in the control signal not being clearly considered. Consequently, the system is sometimes unstable due to the incorrect selection of control parameters, especially, in the period before the convergence occurs.

In this chapter, the TOSMO is first designed to estimate not only system velocities but also the lumped uncertainties for the class of second-order uncertain nonlinear systems without any filtration. Based on the obtained information, an NFTSMC is proposed for position tracking trajectory without the requirement of system velocities. With this control strategy, we can obtain a control law that provides high accuracy, nonsingularity, robustness against the lumped uncertainties, low chattering, and finite-time convergence without the need of velocity measurement. In summary, the major contributions of this chapter are as follow:

- Proposing a NFTSMC law based on the obtained information from the TOSMO;
- Proving the global stability of the system when combining controller and observer by using the Lyapunov stability theory;
- Reducing the chattering phenomenon in control output signal by compensating the lumped uncertainties;
- Eliminating the requirement of velocity measurement in the system;
- Obtaining higher performance of the NFTSM controller by using higher accuracy compensation method.

This chapter is constructed into seven sections. After the introduction, Section 4.2 declares the problem statement. In Section 4.3, the design of the TOSMO is presented, followed by the design method of the NFTSMC for the class of second-order uncertain nonlinear systems is proposed in Section 4.4. The application of the controller-observer strategy for robotic manipulators is presented in Section 4.5. In Section 4.6, numerical simulations on a PUMA560 robot manipulator are shown to prove the effectiveness of the proposed method. Finally, some conclusions are provided in Section 4.7.

4.2 Problem Statement

Consider the following second-order nonlinear control systems with dynamic uncertainties and/or external disturbances as

$$\begin{aligned} \dot{x}_1 &= x_2 \\ \dot{x}_2 &= f(x,t) + g(x,t)u(t) + \Delta(x,u,t) \end{aligned} \tag{4.1}$$

where $x_1 \in \mathbb{R}^n$ and $x_2 \in \mathbb{R}^n$, $x = \left[{x_1}^T \ {x_2}^T\right]^T$ denote the system state vectors, $f(x,t) \in \mathbb{R}^n$ and $g(x,t) \in \mathbb{R}^{n\times n}$ are given nonlinear functions, $g(x,t)$ is invertible, $\Delta(x,u,t) \in \mathbb{R}^n$ presents lumped uncertainties which includes the dynamic uncertainties and/or external disturbances, and $u(x,t) \in \mathbb{R}^n$ denotes the control input.

The main purpose of this chapter is to design a controller-observer strategy which can eliminate the effects of the lumped uncertainties without the requirement of velocity measurement. This control method is designed based on the following assumptions:

Assumption 4.1. *The system states are bounded at all time.*

Assumption 4.2. *The lumped uncertainties $\Delta(x,u,t)$ of the system (4.1) are bounded as*

$$\|\Delta(x,u,t)\| \leq \Lambda \tag{4.2}$$

where Λ is a positive constant.

Assumption 4.3. *The first-time derivative lumped uncertainties $\Delta(x,u,t)$ exist and are bounded as*

$$\left\| \frac{d}{dt}\Delta(x,u,t) \right\| \leq \bar{\Lambda} \tag{4.3}$$

where $\bar{\Lambda}$ is a positive constant.

4.3 State Observer Design and Uncertainty Identification

First, the TOSMO is introduced to estimate both system velocities and the lumped uncertainties. Then, the estimated information will be applied to design the control signal.

4.3.1 State Observer Design

Based on system (4.1), the TOSMO is designed as [25]

$$\begin{aligned}\dot{\hat{x}}_1 &= \gamma_1|x_1-\hat{x}_1|^{2/3}sign\,(x_1-\hat{x}_1)+\hat{x}_2\\ \dot{\hat{x}}_2 &= f(\hat{x},t)+g(\hat{x},t)u(t)+\gamma_2|x_1-\hat{x}_1|^{1/3}sign\,(x_1-\hat{x}_1)-\hat{z}\\ \dot{\hat{z}} &= -\gamma_3 sign\,(x_1-\hat{x}_1)\end{aligned} \tag{4.4}$$

where $\hat{x}$ denotes the estimation of x and γ_i denote the observer gains. Subtracting (4.1) to (4.4), we can get the estimation errors as

$$\begin{aligned}\dot{\tilde{x}}_1 &= -\gamma_1|\tilde{x}_1|^{2/3}sign\,(\tilde{x}_1)+\tilde{x}_2\\ \dot{\tilde{x}}_2 &= -\gamma_2|\tilde{x}_1|^{1/3}sign\,(\tilde{x}_1)+\Delta(x,u,t)-d\,(x,\tilde{x},u,t)+\hat{z}\\ \dot{\hat{z}} &= -\gamma_3 sign\,(\tilde{x}_1)\end{aligned} \tag{4.5}$$

where $\tilde{x} = x-\hat{x}$ denote the system state's estimation errors and the estimation errors of the lumped uncertainties are described as $d\,(x,\tilde{x},u,t) = \{f(\hat{x},t) + g(\hat{x},t)u(t)\} - \{f(x,t)+g(x,t)u(t)\}$. Based on the **Assumption 1**, the estimation errors, $d\,(x,\tilde{x},u,t)$, are bounded as $\|d\,(x,\tilde{x},u,t)\| \leq \Xi$.

Denoting the estimation of the lumped uncertainties, $\Delta\,(x,u,t)$, as $\hat{\Delta}\,(x,\hat{x},u,t) = \Delta\,(x,u,t) - d\,(x,\tilde{x},u,t)$, the estimation errors (4.5) can be rewritten as follow

$$\begin{aligned}\dot{\tilde{x}}_1 &= -\gamma_1|\tilde{x}_1|^{2/3}sign\,(\tilde{x}_1)+\tilde{x}_2\\ \dot{\tilde{x}}_2 &= -\gamma_2|\tilde{x}_1|^{1/3}sign\,(\tilde{x}_1)+\hat{\Delta}\,(x,\hat{x},u,t)+\hat{z}\\ \dot{\hat{z}} &= -\gamma_3 sign\,(\tilde{x}_1)\end{aligned} \tag{4.6}$$

Now, let define $\hat{z}_0 = \hat{\Delta}\,(x,\hat{x},u,t)+\hat{z}$, the system (4.6) becomes

$$\begin{aligned}\dot{\tilde{x}}_1 &= -\gamma_1|\tilde{x}_1|^{2/3}sign\,(\tilde{x}_1)+\tilde{x}_2\\ \dot{\tilde{x}}_2 &= -\gamma_2|\tilde{x}_1|^{1/3}sign\,(\tilde{x}_1)+\hat{z}_0\\ \dot{\hat{z}}_0 &= -\gamma_3 sign\,(\tilde{x}_1)+\dot{\hat{\Delta}}\,(x,\hat{x},u,t)\end{aligned} \tag{4.7}$$

The estimation errors (4.7) is in the standard form of second-order robust exact differentiator and its finite-time stability has successfully proved in literature [86]. Therefore, by selecting suitable observer gains, the estimation errors, $\tilde{x}_1$, $\tilde{x}_2$, and $\hat{z}_0$ will converge to zero in finite time.

Remark 4.1. *The observer gains of (4.4) could be selected based on [86] as* $\gamma_1 = \alpha_1 L^{1/3}$, $\gamma_2 = \alpha_2 L^{2/3}$, *and* $\gamma_3 = \alpha_3 L$ *where* $\alpha_1 = 2$, $\alpha_2 = 2.12$, *and* $\alpha_3 = 1.1$ *with* $L = \Lambda + \Xi$.

4.3.2 Uncertainty Identification

After the convergence process, the differentiators will converge to zero. In other words, the estimated states will achieve the real states ($\hat{x}_1 = x_1$, $\hat{x}_2 = x_2$) after finite time. Thus, the uncertainty estimation errors will be equal to zero, $d(x, \tilde{x}, u, t) = 0$. The third equation of system (4.7) turn into

$$\dot{\hat{z}}_0 = -\gamma_3 sign(\tilde{x}_1) + \dot{\hat{\Delta}}(x, \hat{x}, u, t) \equiv 0 \tag{4.8}$$

The lumped uncertainties can be reconstructed as

$$\hat{\Delta}(x, \hat{x}, u, t) = \int \gamma_3 sign(\tilde{x}_1) \tag{4.9}$$

Since the estimation of lumped uncertainties in (4.9) include integral element; therefore, it can be reconstructed immediately from the output injection term without requirement of lowpass filter. Thanks to this preeminent feature, the TOSMO can provide higher estimation accuracy than that of SOSMO, which is designed in Appendix A. Moreover, the finite time convergence of both system velocities and the lumped uncertainties is guaranteed. The obtained lumped uncertainties can also be utilized for fault detection and applied to the FTC. The estimated velocities are used in the control design procedure instead of the measured velocities in the next Section.

Remark 4.2. *It is worth noting that when applying the estimation states from the observer to the closed-loop controlling system, the exact estimation of system states can only achieve after some transient time. In another word, there exists additional errors in the period before the convergence occurs. These errors will affect in choosing the parameters of the controller. If it is not carefully considered, it will lead to a wrong selection of control parameters. Consequently, the system will be unstable in some cases.*

4.4 Design of Observer-Based NFTSMC Algorithm

In this part, a NFTSMC algorithm is proposed for the class of second-order uncertain nonlinear systems (4.1) to handle the effect of the lumped uncertainties with low chattering and minimum tracking errors. Especially, only position measurements are required. The design method is expressed in the two following steps.

4.4.1 Design of Sliding Function

The tracking errors and velocity errors are defined as

$$\begin{aligned} e &= x_1 - x_d \\ \dot{e} &= x_2 - \dot{x}_d \end{aligned} \tag{4.10}$$

where$x_d, \dot{x}_d$ denote the desired trajectories and velocities, respectively.

A terminal sliding function is chosen as the following expression [59]

$$s = \dot{e} + \int_0^t \left(\kappa_2 |\dot{e}|^{\alpha_2} sign\left(\dot{e}\right) + \kappa_1 |e|^{\alpha_1} sign\left(e\right)\right) dt \tag{4.11}$$

where constants κ_1, κ_2 denote sliding gains which can be chosen such that the polynomial $\kappa_2 p + \kappa_1$ is Hurwitz and α_1, α_2 can be selected as

$$\begin{aligned} \alpha_1 &= (1-\varepsilon, 1), \ \varepsilon \in (0,1) \\ \alpha_2 &= \tfrac{2\alpha_1}{1+\alpha_1} \end{aligned} \tag{4.12}$$

Generally, for saving the cost and reducing the weight of devices, the tachometers in the devices will be cut off by manufacturers. Therefore, in this article, we assume that only the position measurements are available in the system (4.1). Consequently, the variables $\dot{e}$ in sliding functions, s, in (4.11), are not available. To achieve applicable sliding functions, we define the tracking errors and estimation of velocity errors as

$$e = x_1 - x_d \tag{4.13}$$

$$\hat{\dot{e}} = \hat{x}_2 - \dot{x}_d \tag{4.14}$$

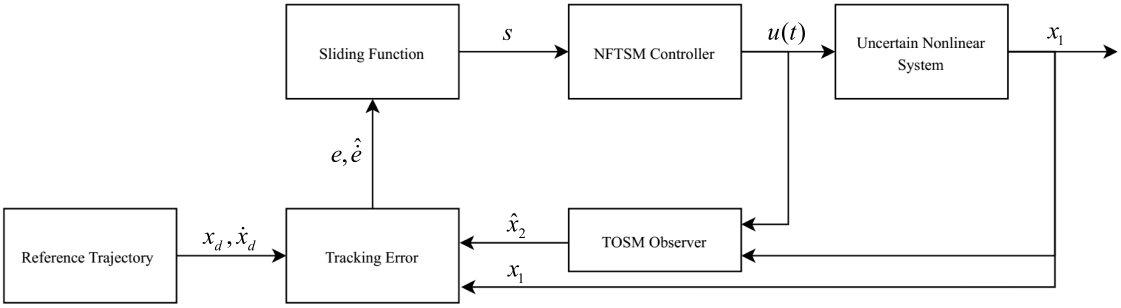

FIGURE 4.1: Block diagram of the proposed controller-observer strategy.

With the above defining, the estimation of sliding function (4.11) can be obtained as

$$\hat{s} = \hat{e} + \int_0^t \left(\kappa_2 |\hat{e}|^{\alpha_2} sign\left(\hat{e}\right) + \kappa_1 |e|^{\alpha_1} sign\left(e\right) \right) dt \tag{4.15}$$

4.4.2 Design of Controller

In order to obtain the control signal for the uncertain nonlinear system (4.1), an NFTSMC based on TOSMO as described in Fig. 4.1 is proposed. The control law is proposed as below

$$u = -g(x,t)^{-1} \left(u_{eq} + u_{sw} \right) \tag{4.16}$$

In (4.16), the equivalent control law, u_{eq}, holds the trajectory of the error state on the sliding surface, is designed as

$$\begin{aligned} u_{eq} = {} & f(x,t) + \gamma_2 |\tilde{x}_1|^{1/3} sign\left(\tilde{x}_1\right) \\ & + \int \lambda_3 sign(\tilde{x}_1) + \kappa_2 |\hat{e}|^{\alpha_2} sign\left(\hat{e}\right) + \kappa_1 |e|^{\alpha_1} sign\left(e\right) - \ddot{x}_d \end{aligned} \tag{4.17}$$

The switching control law, u_{sw}, is constructed to compensate for the estimation errors as follows

$$u_{sw} = (\Xi + \mu) sign\left(\hat{s}\right) \tag{4.18}$$

where μ is a small positive constant.

The control design method for the system is described in Theorem below.

Theorem 4.1. *Consider the class of second-order uncertain nonlinear systems given by (4.1), if the NFTSMC input is designed as (4.16-4.18), then the origin of the sliding function (4.15) is globally finite-time stable equilibrium point and the sliding function (4.15) will converge to zero in finite time defined by* $T_r = \frac{\|\hat{s}(0)\|}{\mu}$.

Proof of Theorem 4.1

Taking the first-time derivative of the estimated sliding function (4.15) yields

$$\dot{\hat{s}} = \frac{d}{dt}\hat{e} + \kappa_2 \left|\hat{e}\right|^{\alpha_2} sign\left(\hat{e}\right) + \kappa_1 |e|^{\alpha_1} sign\left(e\right) \tag{4.19}$$

We can obtain the first-time derivative of tracking velocity errors (4.14) as follows

$$\frac{d}{dt}\hat{e} = \dot{\hat{x}}_2 - \ddot{x}_d \tag{4.20}$$

Substituting the second equation of observer (4.4) into (4.20), we can get

$$\begin{aligned} \tfrac{d}{dt}\hat{e} &= -\ddot{x}_d + f(\hat{x},t) + g(\hat{x},t)u(t) \\ &\quad +\gamma_2 |\tilde{x}_1|^{1/3} sign\left(\tilde{x}_1\right) + \textstyle\int \gamma_3 sign\left(\tilde{x}_1\right) \\ &= -\ddot{x}_d + f(x,t) + g(x,t)u(t) + d\left(x,\tilde{x},u,t\right) \\ &\quad +\gamma_2 |\tilde{x}_1|^{1/3} sign\left(\tilde{x}_1\right) + \textstyle\int \gamma_3 sign\left(\tilde{x}_1\right) \end{aligned} \tag{4.21}$$

Substituting (4.21) into (4.20), we can obtain

$$\begin{aligned} \dot{\hat{s}} &= -\ddot{x}_d + f(x,t) + g(x,t)u(t) + d\left(x,\tilde{x},u,t\right) \\ &\quad +\gamma_2 |\tilde{x}_1|^{1/3} sign\left(\tilde{x}_1\right) + \textstyle\int \gamma_3 sign\left(\tilde{x}_1\right) \\ &\quad +\kappa_2 \left|\hat{e}\right|^{\alpha_2} sign\left(\hat{e}\right) + \kappa_1 |e|^{\alpha_1} sign\left(e\right) \end{aligned} \tag{4.22}$$

Employing the control input from (4.16) to (4.18) into (4.22) yields

$$\dot{\hat{s}} = -(\Xi + \mu) sign\left(\hat{s}\right) + d\left(x,\tilde{x},u,t\right) \tag{4.23}$$

Define the Lyapunov function as following

$$V = \frac{1}{2}\hat{s}^T\hat{s} \tag{4.24}$$

Taking the first-time derivative of Lyapunov function (4.24) and substituting the result from (4.23) yields

$$\begin{aligned} \dot{V} &= \hat{s}^T\dot{\hat{s}} \\ &= \hat{s}^T\left(-(\Xi+\mu) sign\left(\hat{s}\right) + d\left(x,\tilde{x},u,t\right)\right) \\ &= -(\Xi+\mu)\sum_{i=1}^{n}|\hat{s}_i| + d(x,\tilde{x},u,t)^T\hat{s} \leq -\mu\sum_{i=1}^{n}|\hat{s}_i| \\ &\leq -\mu\left\|\hat{s}\right\| = -\sqrt{2}\mu V^{1/2} < 0,\ \forall \hat{s} \neq 0 \end{aligned} \tag{4.25}$$

As a result, according to [87], we can conclude that the origins $s_i = 0, i = 1, 2, ..., n$ of sliding function (4.15) are globally finite-time stable equilibrium points and the sliding function will converge to zero in finite time $T_r = \frac{\|\hat{s}(0)\|}{\mu}$. **Theorem 4.1** is successful proved.

The proposed controller-observer method provides high position tracking accuracy, non-singularity, and robustness against the lumped uncertainties, low chattering, and finite-time convergence without the need of velocity measurement. Its effectiveness will be illustrated by the simulation results.

Remark 4.3. *We can see that the estimation of the lumped uncertainties term, $\int \gamma_3 sign(\tilde{x}_1)$, which is obtained from the TOSMO (4.4), contains in the equivalent control signal (4.17). Accordingly, in the switching control law, only a small value of sliding gain, Ξ, is selected to compensate the effects of the lumped uncertainties' estimation errors, $d(x, \tilde{x}, u, t)$. By using this way, the chattering is significantly reduced in control input torque.*

Remark 4.4. *It is worth noting that there exists an additional component, $\gamma_2 |\tilde{x}_1|^{1/3} sign(\tilde{x}_1)$, in the equivalent control signal (4.17) compared with the control signal (60), in which the converged estimation velocities is used in controller design procedure, see Appendix D. After the convergence time, this term will be equal to zero; however, the presence of this component ensures the proper functioning of the system when a steady state has not been established.*

4.5 Application to Robot Manipulators

The controller-observer method is designed for the class of second-order uncertain nonlinear systems; therefore, it can be applied to many systems which have the same characteristic such as motors, helicopters, aircraft, and robot manipulators. In this part, the proposed controller-observer strategy is employed for tracking trajectory a serial n-link robotic manipulator with the dynamic equation is given in Lagrange form as

$$M(\theta)\ddot{\theta} + C\left(\theta, \dot{\theta}\right)\dot{\theta} + G(\theta) + F\left(\dot{\theta}\right) = \tau(t) + \tau_d(t) \tag{4.26}$$

where $\theta, \dot{\theta}, \ddot{\theta} \in \mathbb{R}^n$ denote position, velocity, and acceleration of robot joints, respectively. $\tau(t) \in \mathbb{R}^n$ represents the control input torque, $M(\theta) \in \mathbb{R}^{n \times n}$ represents the inertia matrix, $C\left(\theta, \dot{\theta}\right) \in \mathbb{R}^n$ represents the Coriolis and centripetal

forces, $G(\theta) \in \mathbb{R}^n$ represents the gravitational force term. $F(\dot{\theta}) \in \mathbb{R}^n$denotes the friction vector, $\tau_d(t) \in \mathbb{R}^n$ denotes the disturbance vector.

Generally, because of the different between the mathematical and practical model, there exist uncertain component of the model of the robot manipulators as

$$M(\theta) = M_0(\theta) + \Delta M(\theta) \tag{4.27}$$

$$C(\theta, \dot{\theta}) = C_0(\theta, \dot{\theta}) + \Delta C(\theta, \dot{\theta}) \tag{4.28}$$

$$G(\theta) = G_0(\theta) + \Delta G(\theta) \tag{4.29}$$

where $M_0(\theta)$, $C_0(\theta, \dot{\theta})$, and $G_0(\theta)$ denote the nominal terms; and $\Delta M(\theta)$, $\Delta C(\theta, \dot{\theta})$, and $\Delta G(\theta)$ denote the uncertain terms. Therefore, the robot dynamic equation (4.26) becomes

$$M_0(\theta)\ddot{\theta} + C_0(\theta, \dot{\theta})\dot{\theta} + G_0(\theta) = \tau(t) + \Upsilon(\theta, \dot{\theta}, t) \tag{4.30}$$

where $\Upsilon(\theta, \dot{\theta}, t) = -\Delta M(\theta) - \Delta C(\theta, \dot{\theta}) - \Delta G(\theta) - F(\dot{\theta}) + \tau_d(t)$.

The robot dynamic equation (4.30) can be converted to the below form

$$\ddot{\theta} = {M_0}^{-1}(\theta)\left[\tau(t) - C_0(\theta, \dot{\theta})\dot{\theta} - G_0(\theta) + \Upsilon(\theta, \dot{\theta}, t)\right] \tag{4.31}$$

For simply in designing, the robot dynamic (4.31) can be rewritten in state space form as

$$\begin{aligned} \dot{x}_1 &= x_2 \\ \dot{x}_2 &= f^*(x) + g^*(x)u(t) + \Delta^*(x, t) \end{aligned} \tag{4.32}$$

where $x_1 = \theta$, $x_2 = \dot{\theta}$, $x = \begin{bmatrix} {x_1}^T & {x_2}^T \end{bmatrix}^T$, $u(t) = \tau(t)$, $f^*(x) = {M_0}^{-1}(\theta)\left[-C_0(\theta, \dot{\theta})\dot{\theta} - G_0(\theta)\right]$, $g^*(x) = {M_0}^{-1}(\theta)$, and $\Delta^*(x, t) = {M_0}^{-1}(\theta)\Upsilon(\theta, \dot{\theta}, t)$.

It can be shown that the robot dynamic system (4.28) is in the same form as (4.1). Thus, the proposed controller-observer algorithm, which are designed in Section 4.3 and Section 4.4, can be applied directly.

4.6 Numerical Simulations

In this section, a PUMA560 robot manipulator (the last three joints are blocked) as shown in Fig. 4.2 is used for computer simulation to demonstrate the significance and applicability of the proposed controller-observer method. The

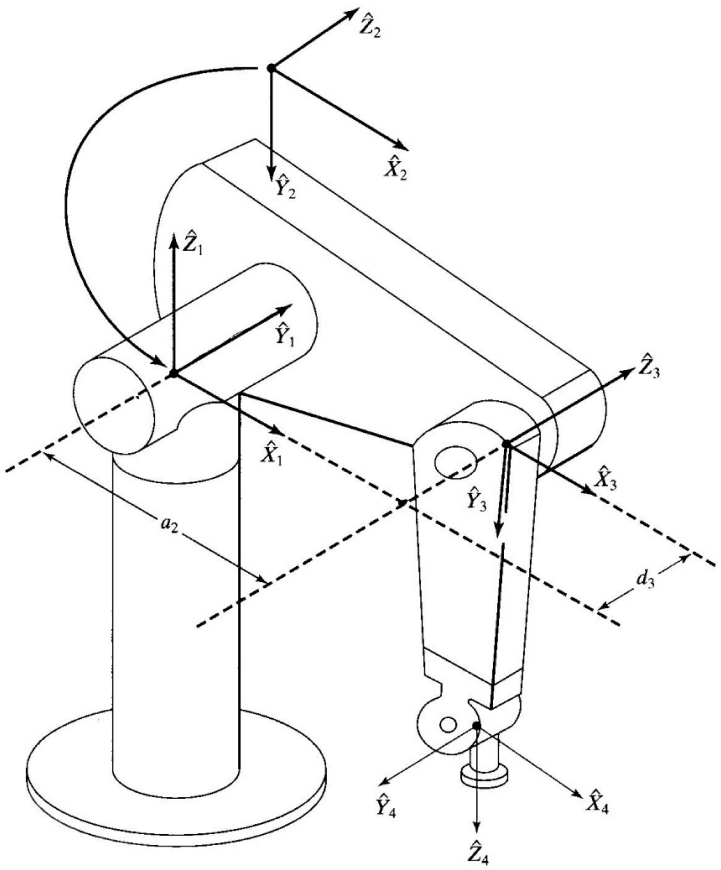

FIGURE 4.2: PUMA560 robot manipulator.

specific dynamic model with required parameter values of PUMA560 robot are provided in [104]. In this chapter, the simulation analysis is performed by using the MATLAB/Simulink program and the sampling time is $10^{-3}s$.

In this work, it is assumed that the desired trajectories to be tracked are

$$\theta_d = \begin{bmatrix} \theta_{d_1} \\ \theta_{d_2} \\ \theta_{d_3} \end{bmatrix} = \begin{bmatrix} 2\cos(\pi t/6) - 1 \\ 3\sin(\pi t/7 + \pi/2) - 1 \\ 1.5\sin(\pi t/5 + \pi/2) - 1 \end{bmatrix} \tag{4.33}$$

The initial states are chosen as $\theta_1(0) = \theta_2(0) = \theta_3(0) = -0.5$ and $\dot{\theta}_1(0) = \dot{\theta}_2(0) = \dot{\theta}_3(0) = 0$.

The dynamic uncertainties, friction, and external disturbances are assumed as

$$\Delta = \begin{bmatrix} \Delta_1 \\ \Delta_2 \\ \Delta_3 \end{bmatrix} = \begin{bmatrix} -1.1\dot{q}_1 + 1.2\sin(3q_1 + \pi/2) - \cos(t) \\ 1.65\dot{q}_2 - 2.14\cos(2q_2) + 0.5\sin(t) \\ -0.5\dot{q}_3 + 1.3\sin(2.5q_3 - \pi/2) + 0.7\sin(0.5t) \end{bmatrix} \tag{4.34}$$

$$F(\dot{\theta}) = \begin{bmatrix} F_1 \\ F_2 \\ F_3 \end{bmatrix} = \begin{bmatrix} 1.9\cos(2\dot{q}_1) \\ 2.03\sin(\dot{q}_2 + \pi/2) - 1 \\ 1.76\cos(0.9\dot{q}_3) \end{bmatrix} \tag{4.35}$$

$$\tau_d = \varsigma\left(t - T_f\right) \begin{bmatrix} \tau_{d_1} \\ \tau_{d_2} \\ \tau_{d_3} \end{bmatrix} = \varsigma\left(t - T_f\right) \begin{bmatrix} -12.5\sin(\pi t/4 + \pi/3) \\ 13.7\cos(\pi t/5 + \pi/2) \\ 7.5\sin(\pi t/3) \end{bmatrix} \tag{4.36}$$

where T_f denotes the time of occurrence and $\varsigma\left(t - T_f\right) = diag\left\{\varsigma_1\left(t - T_f\right), \varsigma_2\left(t - T_f\right), \ldots, \varsigma_n\left(t - T_f\right)\right\}$ represents the time profile of the of the external disturbances. With $\varsigma_i\left(t - T_f\right) = \begin{cases} 0 & if\ t \le T_f \\ 1 - e^{-\sigma_i\left(t - T_f\right)} & if\ t \ge T_f \end{cases}$ and $\sigma_i > 0$ denote the evolution rate.

In this simulation, the external disturbances occur at $T_f = 20s$. The parameters of the controllers using in this simulation are chosen as $L = 9$, $\alpha_1 = 1/2$, $\alpha_2 = 2/3$, $\Xi = 1$, $\kappa_1 = diag\,(15, 15, 15)$, $\kappa_2 = diag\,(10, 10, 10)$.

The simulation consists three parts. First, the estimation results of the TOSMO is compared with that of the SOSMO - which is designed in Appendix A. Second, the proposed NFTSM controller-observer method is compared with NFTSM

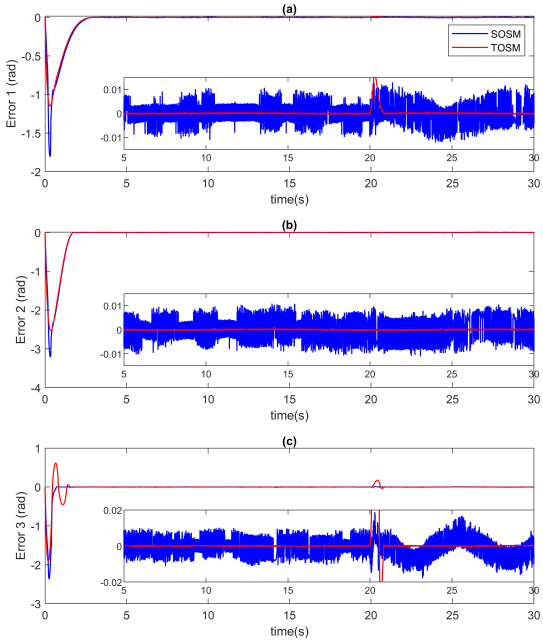

FIGURE 4.3: Velocity estimation errors of the TOSMO compared with the SOSMO.

controllers with and without compensating the estimation of lumped uncertainties – which are designed in Appendix B, C, and D. Finally, we will compare the proposed controller-observer strategy with the NFTSM controller with compensation of obtained lumped uncertainties from TOSMO, which is designed in Appendix D, in term of changing value of the switching gain.

For the first part of the simulation, the comparison results between the TOSMO and the SOSMO are shown in Fig. 4.3, Fig. 4.4, and Fig. 4.5. Fig. 4.3 shows the obtained estimation error of velocity, as we can see that the TOSMO can estimate the system velocity with higher precision whereas the SOSMO provides a larger chattering in the estimation signal. In term of the estimation of lumped uncertainties, the SOSMO requires a lowpass filter to reconstruct the estimation information that is the cause of time delay reducing the precision of this observer. On the contrary, the TOSMO can construct the lumped uncertainties directly without the need of using lowpass filter. The simulation results of the estimation of lumped uncertainties and estimation errors in Fig. 4.4 and Fig. 4.5 indicate that the TOSMO can obtain higher estimation accuracy than that of the SOSMO. However, as a trade-off, the convergence time is little slower. It is worth noting that the more accurate the estimation information, the higher the control performance.

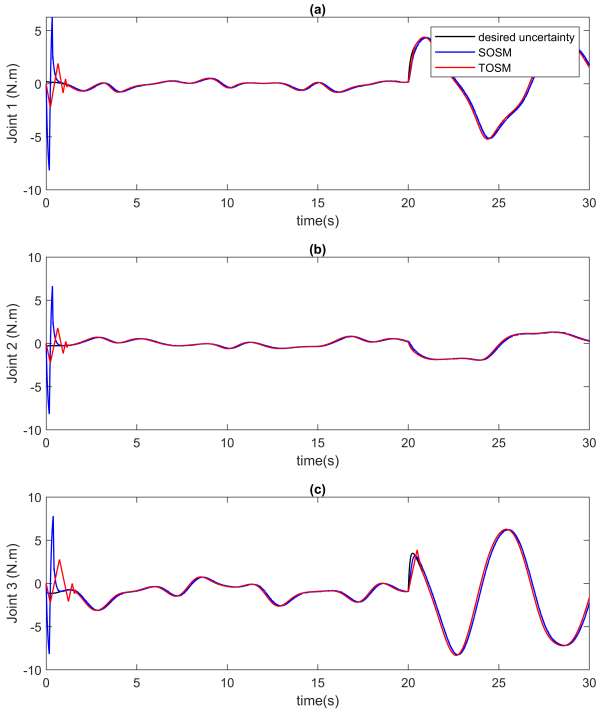

FIGURE 4.4: Uncertainty estimation of the TOSMO compared with the SOSMO.

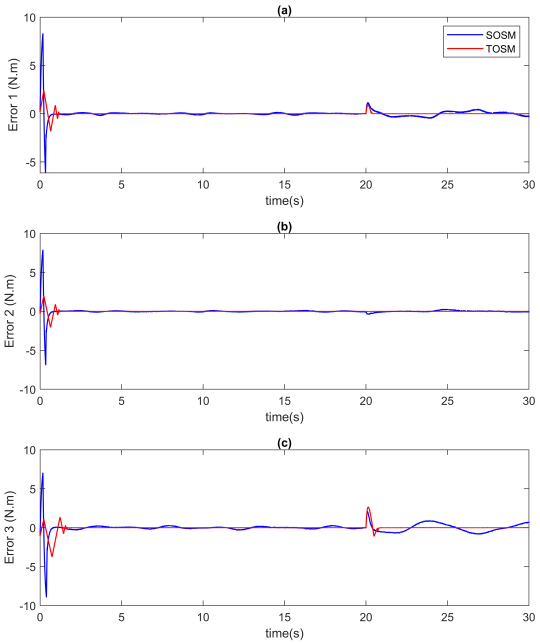

FIGURE 4.5: Uncertainties estimation error of the TOSMO compared with the SOSMO.

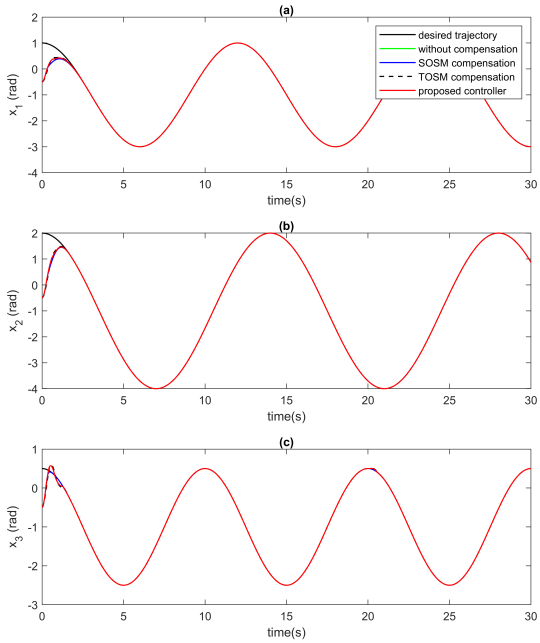

FIGURE 4.6: Tracking position of the proposed controller-observer method compared with the NFTSMC with and without uncertainty compensation.

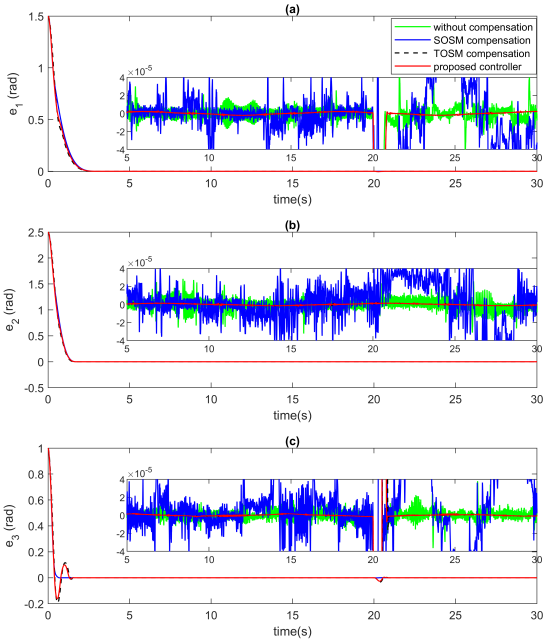

FIGURE 4.7: Tracking error of the proposed controller-observer method compared with the NFTSMC with and without uncertainty compensation.

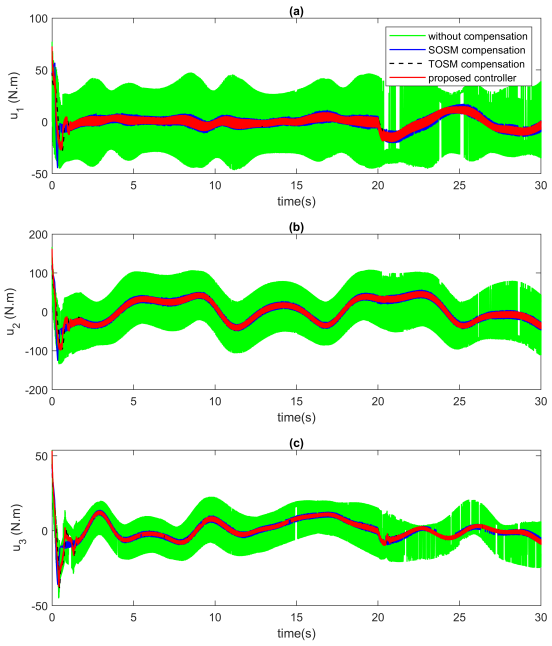

FIGURE 4.8: Control input of proposed controller-observer method compared with the NFTSMC with and without uncertainty compensation.

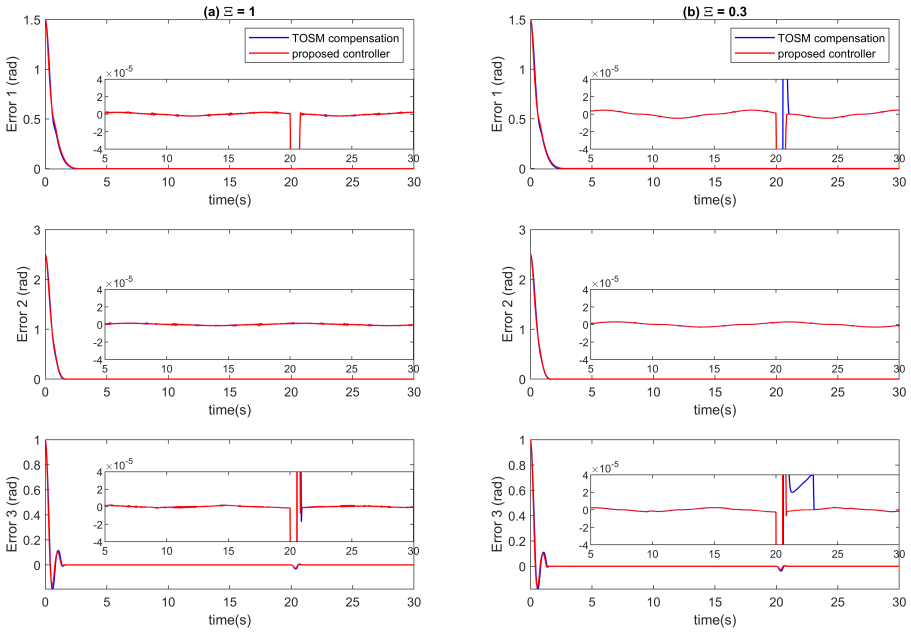

FIGURE 4.9: Position tracking error of the controller-observer control method compared with NFTSMC-TOSMO: a) $\Xi = 1$, b) $\Xi = 0.3$.

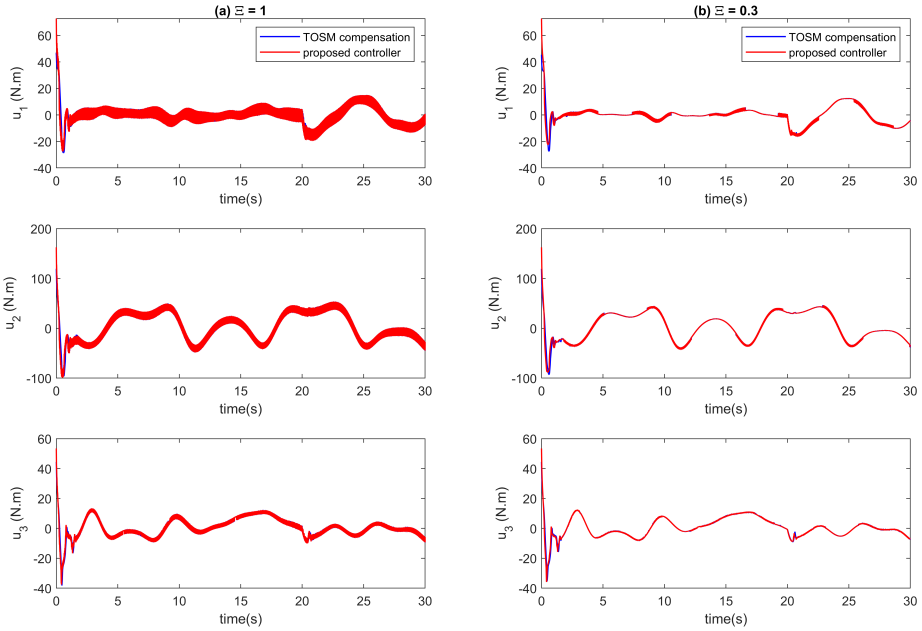

FIGURE 4.10: Control input of the proposed controller-observer method compared with NFTSMC-TOSMO: a) $\Xi = 1$, b) $\Xi = 0.3$.

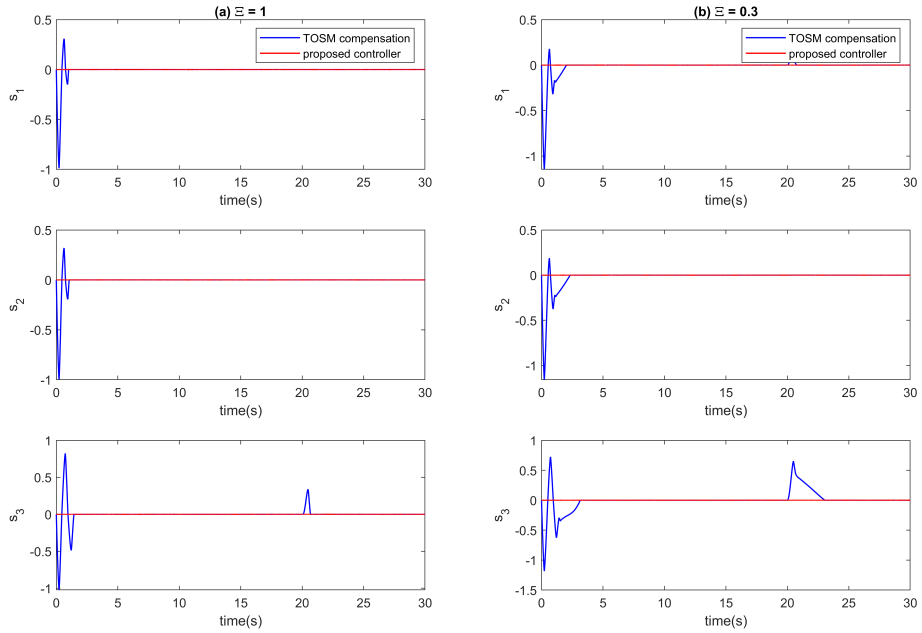

FIGURE 4.11: Sliding function of the proposed controller-observer method compared with NFTSMC-TOSMO: a) $\Xi = 1$, b) $\Xi = 0.3$.

For the second part of the simulation, the comparison results among the proposed controller-observer strategy in Eq. 4.16 - 4.18, the NFTSM controller without the uncertainties compensation in Eq. 4.43 - 4.45, the NFTSM controller with SOSMO compensation (NFTSMC-SOSMO) in Eq. 4.50 - 4.53, and the NFTSM controller with TOSMO compensation (NFTSMC-TOSMO) in Eq. 4.58 - 4.61 are presented in Fig. 4.6, Fig. 4.7 and Fig. 4.8. The tracking position and the tracking error among three joints are shown in Fig.4.6 and Fig. 4.7, respectively. Fig. 4.8 presents the control input of controllers among three joints. As shown in the figures, the proposed controller-observer strategy can provide higher tracking precision and less chattering in control input compared with others, except for the NFTSMC-TOSMO.

In order to show the superior properties of the proposed controller-observer strategy compared with the NFTSMC-TOSMO, we go into the third part of the simulation in which the switching gain, Ξ, of the switching control law, u_{sw}, is changed. The comparison of position tracking error between the proposed control method and the NFTSMC-TOSMO is show in Fig. 4.9. The results show that when the switching gain, $\Xi = 1$, the proposed controller-observer method and the NFTSMC-TOSMO can provide almost the same position tracking performance. However, when reducing the switching gain Ξ to 0.3, the NFTSMC-TOSMO provides a slower convergence time. This happened because the switching gain, Ξ, in the proposed controller-observer strategy is only used against the effect of the uncertainties' estimation error whereas in the NFTSMC-TOSMO, this gain is used to handle the effect of both the uncertainties' estimation error and its overshooting. It is worth mentioning that the smaller the selected switching gain, Ξ, the lower the chattering in the control input signal, which is presented in Fig. 4.10. The comparison of sliding function is illustrated in Fig. 4.11. As we can see that the proposed controller-observer method can provide fast convergence of sliding function for both cases. On the contrary, the convergence of sliding function of the NFTSMC-TOSMO increases when the value of switching gain, Ξ, is reduced. It means that the sliding mode will reach slower.

4.7 Conclusions

This chapter has proposed an effective controller-observer method for the class of second-order uncertain nonlinear systems. The ability to approximate system velocities of the TOSMO eliminates the requirement of tachometer in the

system thus the device's cost and size can be reduced. Moreover, the obtained lumped uncertainties with high accuracy increases the controller performance when applying the estimated information to compensate the uncertainties' effects. The proposed NFTSMC method provides high tracking accuracy, fast response time, low chattering phenomenon, robustness against the lumped uncertainties, faster reaching to the sliding motion and finite-time convergence of the system states. The finite-time stability of both observer and controller have been demonstrated in theory. The proposed controller-observer algorithm has been successfully applied to robot manipulator and its effectiveness has been verified by simulation results.

Appendix

A - DESIGN OF SOSMO

Based on system (4.1), the SOSMO is designed in [44] as

$$\begin{aligned} \dot{\hat{x}}_1 &= \hat{x}_2 + k_1|x_1 - \hat{x}_1|^{1/2} sign\,(x_1 - \hat{x}_1) \\ \dot{\hat{x}}_2 &= f(\hat{x}, t) + g(\hat{x}, t)u(t) + k_2 sign\,(x_1 - \hat{x}_1) \end{aligned} \tag{4.37}$$

where $\hat{x}$ denotes the estimation of x and k_i denote the observer gains.

By subtracting (4.1) to (4.33) we can obtain the estimation error as

$$\begin{aligned} \dot{\tilde{x}}_1 &= -k_1|\tilde{x}_1|^{1/2} sign\,(\tilde{x}_1) + \tilde{x}_2 \\ \dot{\tilde{x}}_2 &= -k_2 sign\,(\tilde{x}_1) + \Delta(x, u, t) - d\,(x, \tilde{x}, u, t) \end{aligned} \tag{4.38}$$

where $\tilde{x} = x - \hat{x}$ and $d\,(x, \tilde{x}, u, t) = \{f(\hat{x}, t) + g(\hat{x}, t)u(t)\} - \{f(x, t) + g(x, t)u(t)\}$.

After the convergence process, the differentiators will converge to zero, thus the estimated states will reach the real states ($\hat{x}_1 = x_1$, $\hat{x}_2 = x_2$) and the lumped uncertainties' estimation will be equal to zero, $d\,(x, \tilde{x}, u, t) = 0$. The lumped uncertainties can be reconstructed as

$$\hat{\Delta}\,(x, u, t) = k_2 sign\,(\tilde{x}_1) \tag{4.39}$$

As we can see, the equivalent output injection of SOSMO is the result of the discontinuous terms $k_2 sign\,(\tilde{x}_1)$, which cause the chattering phenomenon in estimation signal. For that reason, a lowpass filter is required to reconstruct the estimation of the lumped uncertainties.

The observer gains in (4.38) could be selected based on [86] as $k_1 = \alpha_1 L^{2/3}$, and $k_2 = \alpha_2 L$ where $\alpha_1 = 2.12$, and $\alpha_2 = 1.1$.

B - DESIGN OF NFTSMC WITHOUT UNCERTAINTIES COMPENSATION

The tracking errors and velocity errors as (4.10), the terminal sliding function is selected as (4.11). The control law is designed as follows:

$$u = -g(x,t)^{-1}\left(u_{eq} + u_{sw}\right) \tag{4.40}$$

$$u_{eq} = f(x,t) + \kappa_2|\dot{e}|^{\alpha_2} sign\left(\dot{e}\right) + \kappa_1|e|^{\alpha_1} sign\left(e\right) - \ddot{x}_d \tag{4.41}$$

$$u_{sw} = \left(\Lambda + \mu\right) sign\left(s\right) \tag{4.42}$$

After substituting the estimation of system velocities from the TOSMO (4.4), the control law becomes

$$u = -g(\hat{x},t)^{-1}\left(u_{eq} + u_{sw}\right) \tag{4.43}$$

$$u_{eq} = f(\hat{x},t) + \kappa_2|\hat{\dot{e}}|^{\alpha_2} sign\left(\hat{\dot{e}}\right) + \kappa_1|e|^{\alpha_1} sign\left(e\right) - \ddot{x}_d \tag{4.44}$$

$$u_{sw} = \left(\Lambda + \mu\right) sign\left(\hat{s}\right) \tag{4.45}$$

The switching control law here is used to compensate for the lumped uncertainties.

C - DESIGN OF NFTSMC WITH SOSMO COMPENSATION

The tracking errors and velocity errors as (4.10), the terminal sliding function is selected as (4.11). The control law is designed as follows:

$$u = -g(x,t)^{-1}\left(u_{eq} + u_{sw} + u_c\right) \tag{4.46}$$

$$u_{eq} = f(x,t) + \kappa_2|\dot{e}|^{\alpha_2} sign\left(\dot{e}\right) + \kappa_1|e|^{\alpha_1} sign\left(e\right) - \ddot{x}_d \tag{4.47}$$

$$u_{sw} = \left(\Xi + \mu\right) sign\left(s\right) \tag{4.48}$$

$$u_c = k_2 sign\left(\tilde{x}_1\right) \tag{4.49}$$

Substituting the estimation of system velocities from the SOSMO (4.37), the control law becomes

$$u = -g(\hat{x},t)^{-1}\left(u_{eq} + u_{sw} + u_c\right) \tag{4.50}$$

$$u_{eq} = f(\hat{x}, t) + \kappa_2 \left|\hat{\dot{e}}\right|^{\alpha_2} sign\left(\hat{\dot{e}}\right) + \kappa_1 |e|^{\alpha_1} sign\left(e\right) - \ddot{x}_d \tag{4.51}$$

$$u_{sw} = \left(\Xi + \mu\right) sign\left(\hat{s}\right) \tag{4.52}$$

$$u_c = k_2 sign\left(\tilde{x}_1\right) \tag{4.53}$$

The switching control law here is used to compensate for the uncertainty's estimation error of the SOSMO and the compensation element, u_c, is obtained from (4.39).

D - DESIGN OF NFTSMC WITH TOSMO COMPENSATION

The tracking errors and velocity errors as (4.10), the terminal sliding function is selected as (4.11). The control law is designed as follows:

$$u = -g(x, t)^{-1} \left(u_{eq} + u_{sw} + u_c\right) \tag{4.54}$$

$$u_{eq} = f(x, t) + \kappa_2 |\dot{e}|^{\alpha_2} sign\left(\dot{e}\right) + \kappa_1 |e|^{\alpha_1} sign\left(e\right) - \ddot{x}_d \tag{4.55}$$

$$u_{sw} = \left(\Xi + \mu\right) sign\left(s\right) \tag{4.56}$$

$$u_c = \int \gamma_3 sign\left(\tilde{x}_1\right) \tag{4.57}$$

Substituting the estimation of system velocities from the TOSMO (4.4), the control law becomes

$$u = -g(\hat{x}, t)^{-1} \left(u_{eq} + u_{sw} + u_c\right) \tag{4.58}$$

$$u_{eq} = f(\hat{x}, t) + \kappa_2 \left|\hat{\dot{e}}\right|^{\alpha_2} sign\left(\hat{\dot{e}}\right) + \kappa_1 |e|^{\alpha_1} sign\left(e\right) - \ddot{x}_d \tag{4.59}$$

$$u_{sw} = \left(\Xi + \mu\right) sign\left(\hat{s}\right) \tag{4.60}$$

$$u_c = \int \gamma_3 sign\left(\tilde{x}_1\right) \tag{4.61}$$

The switching control law here is used to compensate for the uncertainty's estimation error of the TOSMO and the compensation element, u_c, is obtained from (4.9).

Chapter 5

A Novel High-Speed Third-Order Sliding Mode Observer for Fault-Tolerant Control Problem of Robot Manipulators

In this chapter, a novel FTC tactic for robot manipulator systems using only position measurement is proposed. The proposed algorithm is constructed based on the combination of a NFTSMC and a novel high-speed TOSMO. In the first step, the high-speed TOSMO is first time proposed to approximate both the system velocity and the lumped unknown input with faster convergence time comparing to the TOSMO. The faster convergence speed is obtained thanks to the linear characteristic of the added elements. In the second step, the NFTSMC is constructed based on a NFTS surface and the obtained information from the proposed high-speed TOSMO. Thanks to this combination, the proposed controller-observer tactic provides excellent features such as fast convergence time, high tracking precision, chattering phenomenon reduction, robust against the effects of the lumped unknown input, and velocity requirement elimination. Especially, the proposed observer not only improves the convergence time of observed signal but also increases the system dynamic response. The system stability has been proved using Lyapunov theory. Finally, to validate the efficiency of the proposed strategy, simulations on the PUMA560 robot manipulator are performed.

5.1 Introduction

In industry, robotic manipulators are employed widely with various applications such as material handling, milling, painting welding, and roughing. Along with the growth of robot manipulator applications, the interest in robotic control, which has the purpose of making the robot tracks the desired trajectories to further improve the tracking precision, has been increased [105, 106, 107]. However, robot manipulators are difficult to control in both theoretical and practical due to some characteristics as follows. First, robot manipulator systems have highly nonlinear and very complex dynamic with coupling terms. Additionally, the payload changes, frictions, and external disturbances etc. lead to robot dynamic uncertainty. Therefore, getting the robot's correct dynamics is arduous or even impossible. In some special cases, with the long-time operation, fault can be happened when the robot is operating, which can be actuator fault or sensor fault. Furthermore, for reducing the weight/size and saving the cost, in some cases, manufacturers remove the velocity sensors in the robot. They are big problems that have been challenged by many researchers. To simplify the presentation and avoid the duplication, in this article, the dynamic uncertainty, and unknown fault will be treated and abbreviated as lumped unknown input.

To deal with the aforementioned lumped unknown input, many control methods have been developed, such as PID control [25, 108], adaptive control [109], fuzzy control [110], NN control [111], SMC [42, 112]. Among above controllers, the SMC has been widely utilized in FTC problem of robot manipulators because of its effectiveness in rejecting the effects of the lumped unknown input [40, 39, 41]. Besides, its design procedure is not complicated and quite popular in literature [37, 43, 113]. Unfortunately, conventional SMC uses a linear sliding surface that causes the finite-time convergence cannot be guaranteed. In order to achieve the finite-time convergence, nonlinear sliding surface is utilized instead of a linear one in design process of the controller, this technique is well-known as TSMC [45, 114]. Compared with the conventional SMC, the TSMC extends two outstanding properties, that are finite-time convergence and achieving higher accuracy when parameters are carefully designed. Unfortunately, the TSMC only obtains a faster convergence when system states are near equilibrium point but slower when the system states are far from the equilibrium point. In addition, the TSMC suffers from the singularity problem. The two problems have been handled separately using the FTSMC [61, 46] and the NTSMC [49, 115]. In order to solve both problems at the same time, NFTSMC

has been developed [52, 54, 116]. Due to the excellent control features such as providing finite-time convergence, eliminating singularity elimination, achieving high position tracking precision, and robustness against the lumped unknown input, the NFTSMC has been applied widely in literature. However, the same as the SMC and TSMC, utilizing a discontinuous switching element with a big and fixed sliding gain to handle the effects of the lumped unknown input in designing process of the NFTSMC is the root of high-frequency oscillations, which is so-called chattering [117]. This phenomenon harms to the system, therefore, decreases the practical applicability of SMC. In addition, the design procedure of NFTSMC involves the real velocity information, which is sometimes unavailable in practical systems.

To resolve the chattering problem, the elementary idea is reducing the sliding gain in the switching control component. In this approach, the lumped unknown input is first completely or partially estimated. After that, the estimated unknown input is applied in controller designing as compensator to reduce the lumped unknown input effects. Therefore, the switching control component is now utilized to carry out the impacts of the estimation error instead of the lumped unknown input in original controller. As a result, the sliding gain is chosen with a smaller value and the chattering phenomenon would be reduced. In the literature, various techniques to fault diagnosis have been proposed to approximate the lumped unknown input such as neural network observer [101, 6], adaptive observer [118, 119], time delay estimation [10, 11], linear extended state observer (LESO) [120, 121], SOSMO [96], and TOSMO [14, 13, 12]. Among them, the SOSMO and the TOSMO stands out with the capability to estimate not only the lumped unknown input but also the velocity information; therefore, the requirement of the tachometer is eliminated without the need of an additional state observer. In comparison of the above two observers, the main advantage of the SOSMO is providing a faster approximation speed. In contrast, the TOSMO can provide the estimation signals with higher estimation accuracy, and less chattering without any filtration. Unfortunately, as a trade-off, its convergency time becomes slower than that of SOSMO. Therefore, it is necessary to design an observer which can combine the wonderful properties of both the SOSMO and the TOSMO.

Motivated by all the above discussion, this chapter first proposes a novel high-speed TOSMO for the robot manipulator systems by adding additional terms to the original TOSMO. This observer can not only maintain the remarkable

benefits of original TOSMO but also obtain a faster convergence time. The estimated velocity and unknown input are then applied to design a FTC based on the NFTSMC. The major contributions of this chapter are summarized as following:

- Proposing a novel high-speed TOSMO which can obtain a faster convergence speed whereas maintains the high estimation accuracy of the TOSMO.
- Proposing a FTC law based on the NFTSMC and the proposed high-speed TOSMO which handles the effects of the lumped unknown input.
- Archiving faster convergence, higher tracking accuracy, finite-time convergence, non-singularity, and low chattering without velocity measurement.
- Proving system finite-time stability when combining controller and observer.

This chapter is organized into six parts. Following the introduction, the mathematical dynamics model of robot manipulators and problem formulation are presented in Section 5.2. In Section 5.3, the design of the high-speed TOSMO is presented, followed by the design procedure of the FTC law based on the NFTSMC for the robot manipulators is shown in Section 5.4. To confirm the efficiency of the proposed method, computer simulations on a PUMA560 robot manipulator are shown in Section 5.5. Finally, Section 5.6 gives some conclusions.

5.2 Mathematical dynamics model of robot manipulators and problem formulation

5.2.1 Robot dynamics

Let we consider a serial n-link robotic manipulators under the effects of dynamic uncertainty and unknown fault as following

$$\ddot{q} = M(q)^{-1}\left[\tau(t) - C(q,\dot{q})\,\dot{q} - G(q) - F_r(\dot{q}) - \tau_d(t)\right] + \Omega(q,\dot{q},t) \tag{5.1}$$

where $q, \dot{q}, \ddot{q} \in R^n$ correspondingly represent robot joints' position, velocity, and acceleration vectors; $M(q) \in R^{n\times n}$ represents the inertia matrix, which is symmetric and positive definite, hence, it is invertible; $C(q,\dot{q}) \in R^n$, $G(q) \in R^n$,

and $F_r(\dot{q}) \in R^n$ denote the Coriolis and centripetal forces, gravitational vector, and friction vector, respectively; $\tau_d(t) \in R^n$ denotes the disturbance vector; $\tau(t) \in R^n$ denotes the control input signal; and $\Omega(q, \dot{q}, t) = \omega\left(t - T_f\right)\Phi(q, \dot{q}, t)$ denotes the unknown but bounded fault with the time profile $\omega\left(t - T_f\right) = diag\left\{\omega_1\left(t - T_f\right), \omega_2\left(t - T_f\right), \ldots, \omega_n\left(t - T_f\right)\right\}$, where $\omega_i\left(t - T_f\right) = \begin{cases} 0 & if\, t \leq T_f \\ 1 - e^{-\zeta_i\left(t - T_f\right)} & if\, t \geq T_f \end{cases}$. The unknown fault function $\Phi(q, \dot{q}, t)$ occurs at time T_f with evolution rate $\zeta_i > 0$, $(i = 1, 2, \ldots, n)$.

By defining $u = \tau(t)$, and $x = \begin{bmatrix} x_1{}^T & x_2{}^T \end{bmatrix}^T$ with $x_1 = q$, $x_2 = \dot{q}$, we can transfer the system (5.1) into the state space form as

$$\begin{aligned} \dot{x}_1 &= x_2 \\ \dot{x}_2 &= \Psi(x) + M(x_1)^{-1}u + \Delta(x, t) \end{aligned} \tag{5.2}$$

where $\Psi(x) = M(q)^{-1}\left[-C(q, \dot{q})\dot{q} - G(q)\right]$ represents the nominal model of robot manipulators and $\Delta(x, t) = M(q)^{-1}\left[-F_r(\dot{q}) - \tau_d\right] + \Omega(q, \dot{q}, t)$ denotes the lumped unknown but bounded dynamic uncertainty, and unknown fault.

Remark 5.1. *In this chapter, the unknown fault is considered as additional dynamic uncertainty, therefore, their total effects in the system will be carried out. We can simply name them as the lumped unknown input.*

5.2.2 Problem formulation

Let $x_d \in R^n$ be an expected trajectory of robot's joint, the tracking error is defined as

$$e = x_1 - x_d \tag{5.3}$$

The central purpose of this chapter is divided to two parts. First, a novel high-speed TOSMO is first time proposed to estimate both the system states and the lumped unknown input with high precision and fast response time. Second, based on the achieved information from the proposed observer, a FTC approach using NFTSMC is then designed for system (5.2) to ensure that the joint positions x_1 track the desired trajectory x_d with high accuracy even in presence of the lumped unknown input and absence of the velocity measurement. In addition, the controller further demonstrates effectiveness of the proposed high-speed TOSMO. The proposed algorithm is constructed based on assumptions as follows

Assumption 5.1. *The desired trajectory x_d is a twice continuously differentiable function respect to time t.*

Assumption 5.2. *The lumped unknown input $\Delta(x,t)$ is bounded by a positive constant Δ_D as*

$$|\Delta(x,t)| \leq \Delta_D \tag{5.4}$$

Assumption 5.3. *The derivative of the lumped unknown input $\Delta(x,t)$ respect to time is existed and bounded by a positive constant $\Delta_{\dot{D}}$ as*

$$\left|\frac{d}{dt}\Delta(x,t)\right| \leq \Delta_{\dot{D}} \tag{5.5}$$

5.3 Design of Observer

5.3.1 High-speed third-order sliding mode observer

In this section, a novel high-speed TOSMO is proposed to approximate both velocity and the lumped unknown input with high estimation precision. Especially, the slow convergence characteristic of the TOSMO is improved thanks to the linear characteristic of the adding terms.

Based on the system (5.2), the novel high-speed TOSMO is proposed as following

$$\begin{aligned}
\dot{\hat{x}}_1 &= k_1|x_1 - \hat{x}_1|^{2/3} sign\,(x_1 - \hat{x}_1) + \hat{x}_2 + \Gamma\,(x_1 - \hat{x}_1) \\
\dot{\hat{x}}_2 &= \Psi(\hat{x}) + M(x_1)^{-1}u + k_2|x_1 - \hat{x}_1|^{1/3} sign\,(x_1 - \hat{x}_1) + \Gamma\left(\dot{\hat{x}}_1 - \hat{x}_2\right) - \hat{z} \\
\dot{\hat{z}} &= -k_3 sign\,(x_1 - \hat{x}_1)
\end{aligned} \tag{5.6}$$

where $\hat{x}$ is the estimation of x, $k_i\ (i = 1,\ 2,\ 3)$ denotes the sliding gains, and Γ is positive constant.

Theorem 5.1. *For the robot manipulator system given by (5.2) with the high-speed TOSMO (5.6), if the sliding gains of the observer is chosen as Remark 5.3, then the proposed observer is stable and the estimation states $(\hat{x}_1,\ \hat{x}_2)$ will achieve the real states $(x_1,\ x_2)$ in finite time.*

Proof of Theorem 5.1

By subtracting (5.6) from (5.2), we obtain the estimation errors as

$$\begin{aligned}
\dot{\tilde{x}}_1 &= -k_1|\tilde{x}_1|^{2/3} sign\,(\tilde{x}_1) + \tilde{x}_2 - \Gamma\tilde{x}_1 \\
\dot{\tilde{x}}_2 &= -k_2|\tilde{x}_1|^{1/3} sign\,(\tilde{x}_1) - \Gamma\left(\dot{\hat{x}}_1 - \hat{x}_2\right) + \Delta(x,t) - \delta(x,\tilde{x}) + \hat{z} \\
\dot{\hat{z}} &= -k_3 sign\,(\tilde{x}_1)
\end{aligned} \tag{5.7}$$

where $\tilde{x}_1 = x_1 - \hat{x}_1$ and $\tilde{x}_2 = x_2 - \hat{x}_2$ represent the position and velocity estimation errors, respectively. The estimation error $\delta(x,\tilde{x}) = \Psi(\hat{x}) - \Psi(x)$. To facilitate in the next design approach, in this phase, we assume that $|\delta(x,\tilde{x})| \leq \Delta_\delta$, and $\left|\dot{\delta}(x,\tilde{x})\right| \leq \Delta_{\dot{\delta}}$, where Δ_δ and $\Delta_{\dot{\delta}}$ are positive constants.

Substituting the first term of (5.6) into (5.7), we obtain

$$\begin{aligned}
\dot{\tilde{x}}_1 &= -k_1|\tilde{x}_1|^{2/3} sign\,(\tilde{x}_1) + \tilde{x}_2 - \Gamma\tilde{x}_1 \\
\dot{\tilde{x}}_2 &= -k_2|\tilde{x}_1|^{1/3} sign\,(\tilde{x}_1) + \Delta(x,t) - \delta(x,\tilde{x}) + \hat{z} \\
&\quad -\Gamma k_1|\tilde{x}_1|^{2/3} sign\,(\tilde{x}_1) - \Gamma^2\tilde{x}_1 \\
\dot{\hat{z}} &= -k_3 sign\,(\tilde{x}_1)
\end{aligned} \tag{5.8}$$

By defining the new variable $\bar{x} = \tilde{x}_2 - \Gamma\tilde{x}_1$, the estimation errors in (5.8) are rewritten as

$$\begin{aligned}
\dot{\tilde{x}}_1 &= -k_1|\tilde{x}_1|^{2/3} sign\,(\tilde{x}_1) + \bar{x} \\
\dot{\bar{x}} &= -k_2|\tilde{x}_1|^{1/3} sign\,(\tilde{x}_1) + \Delta(x,t) - \delta(x,\tilde{x}) + \hat{z} \\
&\quad -\Gamma k_1|\tilde{x}_1|^{2/3} sign\,(\tilde{x}_1) - \Gamma^2\tilde{x}_1 \\
&\quad \underbrace{+\Gamma k_1|\tilde{x}_1|^{2/3} sign\,(\tilde{x}_1) + \Gamma^2\tilde{x}_1 - \Gamma\tilde{x}_2}_{-\Gamma\dot{\tilde{x}}_1} \\
\dot{\hat{z}} &= -k_3 sign\,(\tilde{x}_1)
\end{aligned} \tag{5.9}$$

Letting $\hat{\Delta}(x,t) = \Delta(x,t) - \delta(x,\tilde{x}) + L$, the system (5.9) becomes

$$\begin{aligned}
\dot{\tilde{x}}_1 &= -k_1|\tilde{x}_1|^{2/3} sign\,(\tilde{x}_1) + \bar{x} \\
\dot{\bar{x}} &= -k_2|\tilde{x}_1|^{1/3} sign\,(\tilde{x}_1) + \hat{\Delta}(x,t) + \hat{z} \\
\dot{\hat{z}} &= -k_3 sign\,(\tilde{x}_1)
\end{aligned} \tag{5.10}$$

where $L = -\Gamma\tilde{x}_2$ with the assumptions are that $|L| \leq \Delta_L$ and $\left|\frac{d}{dt}L\right| \leq \Delta_{\dot{L}}$.

By defining $\tilde{x}_3 = \hat{z} + \hat{\Delta}(x,t)$, the system in (5.10) can be rewritten in the same form of the second-order sliding mode differentiator [80] as

$$\begin{aligned} \dot{\tilde{x}}_1 &= -k_1|\tilde{x}_1|^{2/3} sign\,(\tilde{x}_1) + \bar{x} \\ \dot{\bar{x}} &= -k_2|\tilde{x}_1|^{1/3} sign\,(\tilde{x}_1) + \tilde{x}_3 \\ \dot{\tilde{x}}_3 &= -k_3 sign\,(\tilde{x}_1) + \dot{\hat{\Delta}}(x,t) \end{aligned} \tag{5.11}$$

Equation (5.11) is also well-known as the TOSMO [82]. By selecting the candidate Lyapunov function V_0 and using the same demonstrating process as in [82], it can be concluded that the system (5.11) is stable and the differentiators $\tilde{x}_1$, $\bar{x}$, and $\tilde{x}_3$ the converge to zero in finite-time. Thus, the system (5.7) is stable and the estimation errors $\tilde{x}_1$, $\tilde{x}_2$ converge to zero in finite-time.

Remark 5.2. *The proposed high-speed TOSMO in (5.6) is designed based on the original TOSMO in [52]. The linear characteristics of added terms are utilized to increase the convergence speed of estimated signals.*

Remark 5.3. *The observer gains of (5.6) are selected according to [80] as* $k_1 = \alpha_1 \bar{\Delta}^{1/3}$, $k_2 = \alpha_2 \bar{\Delta}^{2/3}$, *and* $k_3 = \alpha_3 \bar{\Delta}$ *where* $\alpha_1 = 2$, $\alpha_2 = 2.12$, *and* $\alpha_3 = 1.1$ *with* $\bar{\Delta} = \Delta_D + \Delta_{\dot{\delta}} + \Delta_L$.

5.3.2 Unknown input identification

After the convergence time, the estimated velocity reaches the real velocity, $\hat{x}_2 = x_2$, thus, the term $L = -\Gamma\tilde{x}_2$ converges to zero. The third term of system (5.11) becomes

$$\dot{\tilde{x}}_3 = -k_3 sign\,(\tilde{x}_1) + \dot{\hat{\Delta}}(x,t) \equiv 0 \tag{5.12}$$

Notably, because the velocity estimation error $\tilde{x}_2$ converges to zero, the auxiliary unknown input term $\hat{\Delta}(x,t) = \Delta(x,t) - \delta(x,\tilde{x}) + L$ converges to $\Delta(x,t)$.

The lumped unknown input terms can be rebuilt as

$$\hat{\Delta}(x,t) = \int k_3 sign\,(\tilde{x}_1) \tag{5.13}$$

Since the estimated unknown input in (5.13) includes integral operation, the lumped unknown input terms can be rebuilt directly from the output injection term and the chattering of the obtained function is partially eliminated without the need of lowpass filter. In addition, the proposed observer in (5.6) not only

maintains the advantages of conventional TOSMO such as finite-time convergence and high estimation accuracy for both velocity and the lumped unknown input but also provides faster convergence time than that of the TOSMO. The outstanding features of the proposed high-speed TOSMO will be verified in the simulation part.

Remark 5.4. *The obtained lumped unknown input can be used for fault detection and fault isolation and also can be applied to the FTC to eliminate its effect to the system. The estimated velocity can be employed to the controller design process instead of the real measured velocity.*

5.4 Design of Control Algorithm

In this section, a FTC tactic using NFTSMC algorithm is proposed to carry out the effects of the lumped unknown input of system (5.2). In addition, in some special cases, the tachometers in robot will be cut off by manufacturers to save the cost and reduce the weight. For that reason, this chapter assumes that the tachometers are not existed. The estimated velocity, $\hat{x}_2$, which is obtained from the proposed observer in Section 5.3 is utilized, therefore, the requirement of the real measured velocity is eliminated.

5.4.1 Design of non-singular fast terminal sliding surface

Let defining the estimated velocity error as

$$\hat{e} = \hat{x}_2 - \dot{x}_d \tag{5.14}$$

where $\dot{x}_d$ describes the desired velocity.

A NFTS surface is selected as in [63]

$$\hat{s} = \hat{e} + \int \beta_1 |e|^{\gamma_1} sign\,(e) + \beta_2 |\hat{e}|^{\gamma_2} sign\,(\hat{e}) + \beta_3 e + \beta_4 e^3 \tag{5.15}$$

where the parameters $\beta_1,\ \beta_2,\ \beta_3,\ \beta_4$ are positive constants, and the parameters $\gamma_1,\ \gamma_2$ can be selected as $0 < \gamma_1 < 1,\ \gamma_2 = 2\gamma_1/(1+\gamma_1)$.

According to the SMC theory, the following conditions are satisfied when the robot system reaches the sliding mode:

$$\begin{aligned} \hat{s} &= 0 \\ \dot{\hat{e}} &= 0 \end{aligned} \tag{5.16}$$

Thus, the sliding mode dynamics can be acquired as

$$\hat{e} = -\int \left[\beta_1 |e|^{\gamma_1} sign\,(e) + \beta_2 |\hat{e}|^{\gamma_2} sign\,(\hat{e}) + \beta_3 e + \beta_4 e^3\right] \tag{5.17}$$

Theorem 5.2. *For the sliding mode dynamics in (5.17), the origin is defined as the stable equilibrium point and the state trajectories converge to zero in the finite-time.*

Proof of Theorem 5.2

Taking the derivative of the tracking error in (5.3) respect to time yields

$$\begin{aligned} \dot{e} &= \dot{x}_1 - \dot{x}_d \\ &= x_2 - \dot{x}_d \end{aligned} \tag{5.18}$$

Based on the definition of the estimation errors in Section 5.3, the velocity error (5.14) is rewritten as

$$\begin{aligned} \hat{\dot{e}} &= \hat{x}_2 - \dot{x}_d \\ &= x_2 - \dot{x}_d - \tilde{x}_2 \end{aligned} \tag{5.19}$$

After convergence time of the estimation errors (5.7), the estimated velocity, $\hat{x}_2$, reaches the true velocity, x_2. Hence, the velocity error (5.19) becomes

$$\hat{\dot{e}} = x_2 - \dot{x}_d = \dot{e} \tag{5.20}$$

The sliding mode dynamics in (5.17) becomes

$$\dot{e} = -\int \left[\beta_1 |e|^{\gamma_1} sign\,(e) + \beta_2 |\dot{e}|^{\gamma_2} sign\,(\dot{e}) + \beta_3 e + \beta_4 e^3\right] \tag{5.21}$$

Then, the following sliding mode dynamics can be obtained

$$\ddot{e} = -\beta_1 |e|^{\gamma_1} sign\,(e) - \beta_2 |\dot{e}|^{\gamma_2} sign\,(\dot{e}) - \beta_3 e - \beta_4 e^3 \tag{5.22}$$

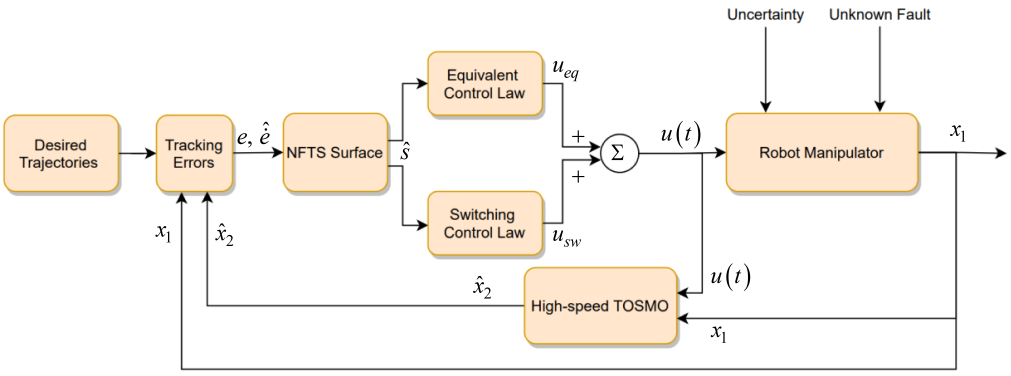

FIGURE 5.1: Overall structure of the proposed FTC approach

A Lyapunov function candidate is selected as

$$V_1 = \frac{\beta_1}{\gamma_1 + 1}|e|^{\gamma_1+1} + \frac{1}{2}\dot{e}^2 + \frac{\beta_3}{2}e^2 + \frac{\beta_4}{4}e^4 \tag{5.23}$$

Taking the time derivative of the Lyapunov function candidate (5.23) and substituting the result from (5.22) yields

$$\begin{aligned}\dot{V}_1 &= \beta_1|e|^{\gamma_1}sign(e)\dot{e} + \dot{e}\ddot{e} + \beta_3 e\dot{e} + \beta_4 e^3\dot{e} \\ &= \beta_1|e|^{\gamma_1}sign(e)\dot{e} + \dot{e}\left(-\beta_1|e|^{\gamma_1}sign\left(e\right) - \beta_2|\dot{e}|^{\gamma_2}sign\left(\dot{e}\right) - \beta_3 e - \beta_4 e^3\right) \\ &\quad + \beta_3 e\dot{e} + \beta_4 e^3\dot{e} \\ &= -\beta_2|\dot{e}|^{\gamma_2+1}\end{aligned} \tag{5.24}$$

From (5.23) and (5.24), it can be concluded that $V_1 > 0$ and $\dot{V}_1 < 0$, therefore, the origin of the sliding mode dynamics (5.17) is stable equilibrium point and the state trajectories e and $\hat{e}$ converge to zero in finite-time. Thus, the theorem 5.2 is successfully proven.

5.4.2 Observer-based NFTSMC design

To obtain the control law for the robot manipulator system (5.2), an observer-based NFTSMC as shown in Fig. 5.1 is proposed. The control input signal is design as follows

$$u = -M\left(x_1\right)\left(u_{eq} + u_{sw}\right) \tag{5.25}$$

Here, the equivalent control law, u_{eq}, plays the role to hold the error state variables on the sliding surface and is designed as follows:

$$u_{eq} = \Psi(x) + k_2|\tilde{x}_1|^{1/3} sign\left(\tilde{x}_1\right) + \Gamma\left(\dot{\hat{x}}_1 - \hat{x}_2\right) + \int k_3 sign(\tilde{x}_1) + A - \ddot{x}_d \quad (5.26)$$

where $A = \beta_1|e|^{\gamma_1} sign\left(e\right) + \beta_2|\hat{\dot{e}}|^{\gamma_2} sign\left(\hat{\dot{e}}\right) + \beta_3 e + \beta_4 e^3$.

The switching control law, u_{sw}, plays the role of driving the state variables to the sliding surface, is designed as following

$$u_{sw} = \left(\Delta_\delta + \mu\right) sign\left(\hat{s}\right) \quad (5.27)$$

The proposed control input is stated in the following Theorem 5.3:

Theorem 5.3. *Consider the robot manipulator system given by (5.2), if the NFTSMC is designed as (25-27), then the system (5.2) is stable. Additionally, the finite-time convergence of tracking errors is guaranteed.*

Proof of Theorem 5.3

Taking the derivative of both the sliding surface (5.15) and the tracking velocity error (5.14) respect to time, we obtain

$$\dot{\hat{s}} = \frac{d}{dt}\hat{\dot{e}} + A \quad (5.28)$$

$$\frac{d}{dt}\hat{\dot{e}} = \dot{\hat{x}}_2 - \ddot{x}_d \quad (5.29)$$

Substituting the second term of the proposed observer (5.6) into (5.29) yields

$$\begin{aligned} \tfrac{d}{dt}\hat{\dot{e}} &= -\ddot{x}_d + \Psi(\hat{x}) + M(x_1)^{-1}u + k_2|\tilde{x}_1|^{1/3} sign\left(\tilde{x}_1\right) + \Gamma\left(\dot{\hat{x}}_1 - \hat{x}_2\right) + \hat{z} \\ \dot{\hat{z}} &= k_3 sign(\tilde{x}_1) \end{aligned} \quad (5.30)$$

Substituting (5.30) into (5.28), we obtain

$$\begin{aligned} \dot{\hat{s}} &= -\ddot{x}_d + \Psi(\hat{x}) + M(x_1)^{-1}u + k_2|\tilde{x}_1|^{1/3} sign\left(\tilde{x}_1\right) + \Gamma\left(\dot{\hat{x}}_1 - \hat{x}_2\right) + \hat{z} + A \\ &= -\ddot{x}_d + \Psi(x) + \delta(x, \tilde{x}) + M(x_1)^{-1}u + k_2|\tilde{x}_1|^{1/3} sign\left(\tilde{x}_1\right) \\ &\quad + \Gamma\left(\dot{\hat{x}}_1 - \hat{x}_2\right) + \hat{z} + A \\ \dot{\hat{z}} &= k_3 sign\left(\tilde{x}_1\right) \end{aligned} \quad (5.31)$$

Applying control input in (5.25-5.27) to (5.31) gives

$$\dot{\hat{s}} = -\left(\Delta_\delta + \mu\right) sign\left(\hat{s}\right) + \delta(x, \tilde{x}) \tag{5.32}$$

Let define the Lyapunov function candidate as following

$$V_2 = \frac{1}{2}\hat{s}^T\hat{s} \tag{5.33}$$

With the result of (5.32), the time derivative of Lyapunov function candidate (5.33) yields

$$\begin{aligned}
\dot{V}_2 &= \hat{s}^T\dot{\hat{s}} \\
&= \hat{s}^T\left(-\left(\Delta_\delta + \mu\right) sign\left(\hat{s}\right) + \delta(x, \tilde{x})\right) \\
&= -\left(\Delta_\delta + \mu\right)\sum_{i=1}^{n}|\hat{s}_i| + \delta(x, \tilde{x})^T\hat{s} \leq -\mu\sum_{i=1}^{n}|\hat{s}_i| \\
&\leq -\mu\left\|\hat{s}\right\| = -\sqrt{2}\mu {V_2}^{1/2} < 0,\ \forall \hat{s} \neq 0
\end{aligned} \tag{5.34}$$

Remark 5.5. *In equivalent control law (5.26), we can see that the estimated lumped unknown input, $\int k_3 sign(\tilde{x}_1)$, which is obtained from the high-speed TOSMO in Eq. (5.6), is included. Consequently, the switching control law now is utilized to handle the effects of the estimation errors, therefore, a small value of sliding gain can be chosen. By this way, the high-frequency chattering phenomenon will be significantly decreased in control input signal.*

Remark 5.6. *In combining of observer and controller, the convergence speed of controller is depended on the convergence speed of the designed observer. Therefore, the proposed high-speed TOSMO not only supports in early fault detection but also helps the controller to achieve a faster convergence speed than when combining with the TOSMO.*

Remark 5.7. *Although the NFTS surface is selected according to [63], the proposed equivalent control law in (5.26) is different. Therefore, it can be considered as a contribution of this chapter.*

5.5 Numerical Simulations

To validate the efficiency of the suggested algorithm, in this section, we use the PUMA560 robot manipulator with the last three joints are blocked for computer simulation. The structure of the PUMA560 robot is shown in Fig. 5.2. The specific parameter values of the PUMA560 robot dynamic model are provided in

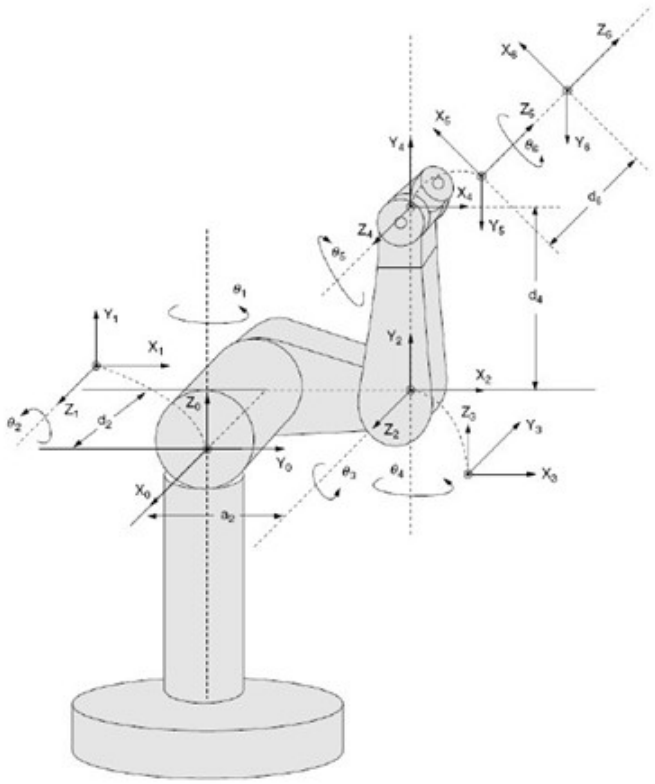

FIGURE 5.2: Structure of the PUMA560 robot manipulator

[104]. In the simulation analysis, the MATLAB/Simulink program is performed with sampling time is 10^{-3}second.

In the simulation, the desired trajectories of the three are assumed as

$$q_d = \begin{bmatrix} q_{d_1} \\ q_{d_2} \\ q_{d_3} \end{bmatrix} = \begin{bmatrix} \cos(\pi t/5) - 1 \\ \sin(\pi t/5 + \pi/2) - 1 \\ \sin(\pi t/5 + \pi/2) - 1 \end{bmatrix} \tag{5.35}$$

The initial states of the robot are selected as $q_1(0) = q_2(0) = q_3(0) = -0.5$ and $\dot{q}_1(0) = \dot{q}_2(0) = \dot{q}_3(0) = 0$.

The friction vector and external disturbance vector are assumed as

$$F_r = \begin{bmatrix} F_{r1} \\ F_{r2} \\ F_{r3} \end{bmatrix} = \begin{bmatrix} 1.9\sin(\dot{q}_1) \\ 2.03\sin(\dot{q}_2) \\ 1.76\sin(\dot{q}_3) \end{bmatrix} \tag{5.36}$$

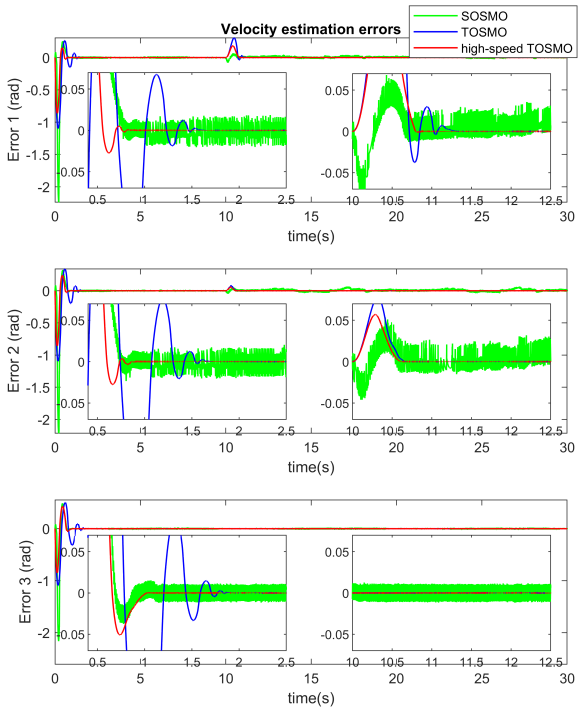

FIGURE 5.3: Velocity estimation errors at each joint

$$\tau_d = \begin{bmatrix} \tau_{d_1} \\ \tau_{d_2} \\ \tau_{d_3} \end{bmatrix} = \begin{bmatrix} 1.1\dot{q}_1 + 1.2\sin(3q_1) \\ 1.65\dot{q}_2 + 2.14\sin(2q_2) \\ -3.01\dot{q}_3 + 1.3\sin(q_3) \end{bmatrix} \tag{5.37}$$

The fault is assumed to occur at $T_f = 10s$ with the fault signal is as following

$$\Phi = \begin{bmatrix} \Phi_1 \\ \Phi_2 \\ \Phi_3 \end{bmatrix} = \begin{bmatrix} 10\sin(q_1q_2) + 3.7\cos(\dot{q}_1q_2) + 5.2\cos(\dot{q}_1\dot{q}_2) \\ 15\sin(q_1q_2) + 3.6\cos(\dot{q}_1q_2) + 2.7\cos(\dot{q}_1\dot{q}_2) \\ 0 \end{bmatrix} \tag{5.38}$$

The parameters of the controllers and observers are selected as follows: $\gamma_1 = 1/2$, $\gamma_2 = 2/3$, $\beta_1 = diag(15, 15, 15)$, $\beta_2 = diag(10, 10, 10)$, $\beta_3 = diag(10, 10, 10)$, $\beta_4 = diag(5, 5, 5)$, $\Delta_\delta = 0.5$, $\bar{\Delta} = 22$, and $\Gamma = 5$.

The simulation consists of two parts. First, the estimation results of the proposed high-speed TOSMO are compared with that of the TOSMO and the SOSMO which are designed as in [52]. Second, the proposed FTC technique is compared with three controllers: 1) NFTSMC without compensation; 2) NFTSMC with SOSMO compensation (NFTSMC-SOSMO); 3) NFTSMC with TOSMO compensation (NFTSMC-TOSMO).

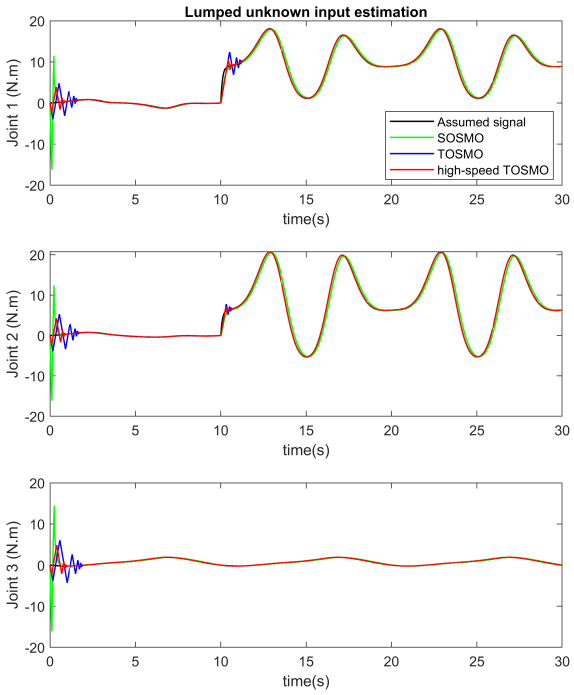

FIGURE 5.4: Lumped unknown input estimation

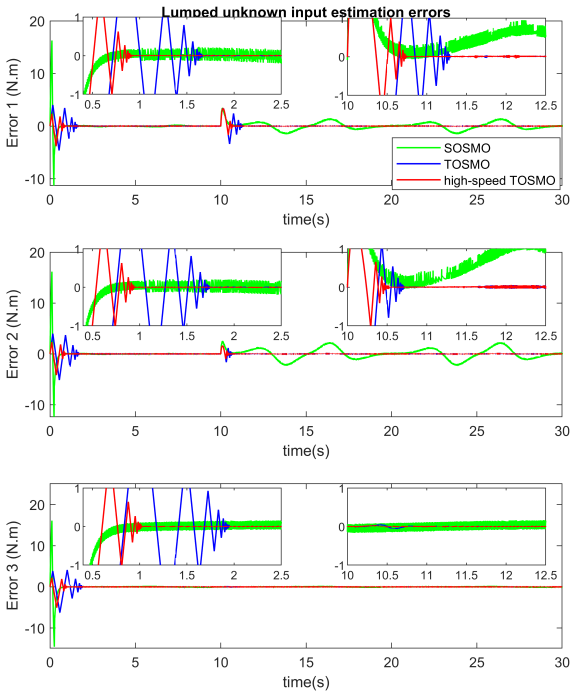

FIGURE 5.5: Lumped unknown input estimation errors at each joint

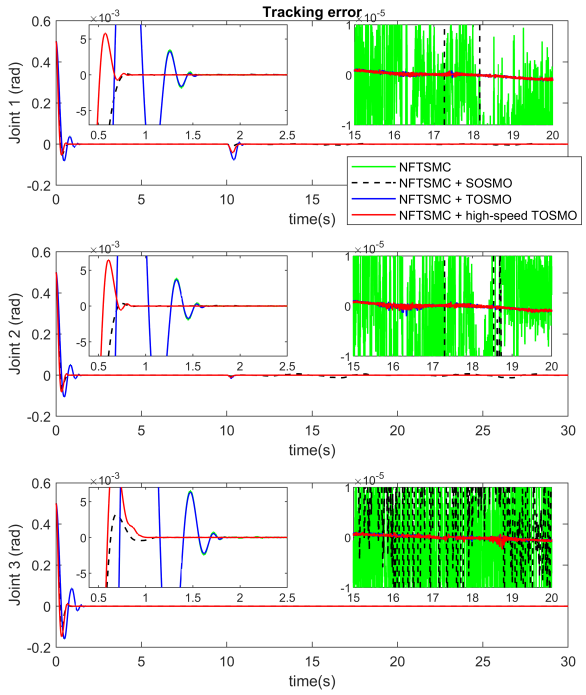

FIGURE 5.6: Comparison of tracking errors among controllers

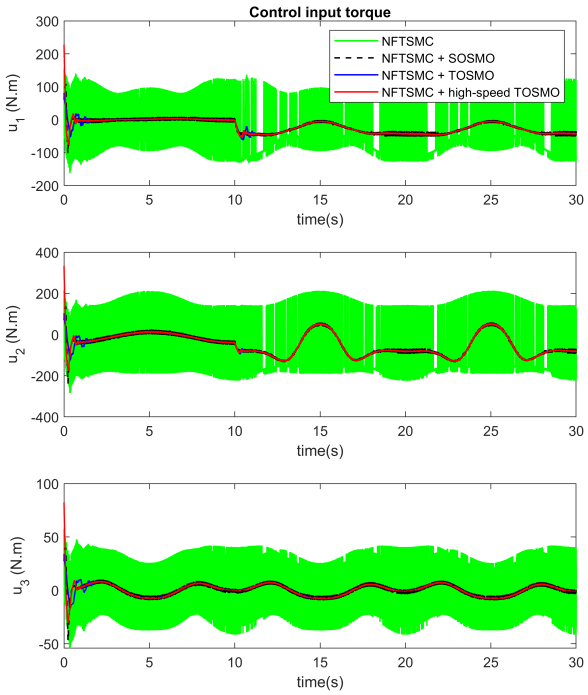

FIGURE 5.7: Comparison of control input torque among controllers

In the first part, the comparison results among three observers are shown in Fig. 5.3 to Fig. 5.5. The obtained velocity estimation errors are shown in Fig. 5.3. As in the results, the SOSMO (green solid line) provides a faster estimation of velocity compared to the TOSMO (blue solid line). In contrast, the TOSMO provides velocity estimation with higher precision, and less chattering compared to the SOSMO. The red solid line in the figure shows the estimation results of the high-speed TOSMO. It is easy to see that the estimated information of high-speed TOSMO maintains the higher precision, and less chattering characteristic of the TOSMO while the convergence speed is significantly increased and matches the speed of the SOSMO. The faster velocity estimation will help the controller reaches a faster convergence time. In terms of the lumped unknown input estimation, the results are shown in Fig. 5.4 and Fig. 5.5. As shown in the results, the SOSMO provides estimation information with lower accuracy compared the TOSMO and the proposed high-speed TOSMO due to the time delay when using lowpass filter to reconstruct the estimation signal. On the contrary, the TOSMO and the high-speed TOSMO can reconstruct the lumped unknown input directly without any filtration. However, the convergence time of the TOSMO is little slower. The same as in the velocity estimation results, the lumped unknown input estimation results of the high-speed TOSMO can maintain the high estimation performance of the TOSMO and reaches convergence speed of the SOSMO. It is worth mentioning that the faster estimation speed helps in early fault detection, thus, reduces the robot failure rate.

In the second part, the comparison results among four controllers are shown in Fig. 5.6 and Fig. 5.7. The Fig. 5.6 shows the results of tracking error at each joint. As in the figure, in terms of tracking performance, the NFTSMC without compensation (green solid line) and the NFTSMC-SOSMO (black dash line) provide quite good tracking precision. However, with a better approximation information, the NFTSMC-TOSMO (blue solid line) and the proposed FTC strategy (red solid line) provides higher control performance. The two controllers provide almost the same tracking accuracy due to the estimation accuracy of the TOSMO and the high-speed TOSMO are not much difference. In terms of convergence speed, the NFTSMC without compensation and the NFTSMC-TOSMO converge simultaneously because they use the same velocity signal in design process. According to the effect of the velocity signal, the proposed FTC strategy converges faster the above two controllers and almost the same with the NFTSMC-SOSMO. Therefore, it can be concluded that the proposed high-speed TOSMO not only obtains the faster estimation information

but also helps the designed controller achieves better control performance. The comparison of control input torque is shown in Fig. 5.7. As in the figure, the control input of the NFTSMC without compensation is under the effect of the chattering phenomenon because of using large sliding gain. After compensation, the sliding gain can be chosen with smaller value, therefore, the chattering phenomenon in control inputs of the NFTSMC-SOSMO, the NFTSMC-TOSMO, and the proposed FTC are significantly reduced.

5.6 Conclusions

This chapter proposed a novel FTC strategy for robot manipulator systems using only position measurement. Thanks to the linear characteristic of the added elements, the proposed high-speed TOSMO can estimate both the velocity signal and the lumped unknown input with faster convergence time comparing to the TOSMO. The obtained information from observer is combined with NFTSMC in designing the FTC. The proposed controller-observer tactic provides excellent properties such as fast convergence time, high position tracking precision, finite-time convergence, chattering phenomenon reduction, robust against the effects of the lumped unknown input, and velocity requirement elimination. The faster convergence characteristic of the observer also improves the convergence speed of the designed controller. The system stability and finite-time convergence have been proved using Lyapunov stability theory. Finally, the efficiency of the proposed algorithm is validated by simulations on the PUMA560 robot manipulator.

Chapter 6

Conclusion and Future Works

6.1 Conclusions

In this dissertation, the finite-time controller-observer strategies have been developed for uncertain and faulty robotic manipulators. The FTC techniques are mainly developed based on the NFTSMC with excellent characteristics such as fast convergence time, high position tracking precision, finite-time convergence, robust against the effects of the LUaF. The FD methods are developed based on the high-order sliding mode observers with the ability to provide the signal estimation with excellent accuracy, rapid convergence, and almost no chattering. The results in the thesis have been derived based on Lyapunov theory and finite-time control theory. The control performance of the closed-loop systems has been explicitly analyzed.

The Chapter 2 presents an FTC strategy using an A-NFTSMC based on a DO for uncertain and faulty robotic manipulators. The proposed DO demonstrated its capacity to estimate the LUaF with excellent accuracy, rapid convergence, and almost no chattering. The suggested FTC technique has advanced control characteristics of high positioning tracking accuracy with quick finite-time convergence, chattering phenomena minimization, and LUaF robustness. Especially, applying the adaptive law helps the FTC algorithm not depend on the estimation accuracy of the observer. However, the proposed controller-observer algorithm still requires velocity measurement in the designing process.

The Chapter 3 proposes a novel sliding function is proposed by combining the NFTSMC and the TOSMO for the robotic manipulator system. The ability to approximate system velocities of the TOSMO eliminates the requirement of tachometers in the system. This ability eliminates the aforementioned disadvantage of the proposed algorithm in Chapter 2. Especially, two stages of

time that before and after the convergence time, are carefully analyzed. The obtained LUaF from the TOSMO are utilized to compensate for their effects on the system. The novelty in designing improves the convergence speed of the FTC method. Further, the tracking performance of the proposed controller-observer method is improved.

The Chapter 4 proposes an effective FTC method for the class of second-order uncertain nonlinear systems. To improve the convergence speed of the proposed method in Chapter 3, the estimated velocity from the TOSMO is applied to propose an integral NFTSMC. In addition, the obtained LUaF from the TOSMO with high accuracy is applied to the FTC to compensate for their effects. Therefore, the control performance of the FTC method is increased. The proposed controller-observer algorithm has been successfully applied to robot manipulators.

In Chapter 5, the novel high-speed TOSMO is proposed by combining the high estimation accuracy ability of the TOSMO and the fast convergence characteristic of the linear elements. The high-speed TOSMO can estimate both the velocity signal and the LUaF with a faster convergence time compared to the TOSMO. The obtained information from the observer is combined with NFTSMC in designing the FTC. The faster convergence characteristic of the observer also improves the convergence speed of the designed controller.

6.2 Future works

The FD and FTC methods are very important for the application of modern robotic manipulator systems. Although the valuable FD and FTC methods are developed in this thesis, the research works still need to be studied in the future. Therefore, some possible future studies are suggested as follows.

1. In this thesis, the developed FD and FTC methods are finite-time convergence. Designing fixed-time controller-observer algorithms are promising and challenging.
2. Applying optimization methods for determining the optimal coefficients of observers and controllers. This is a promising approach to obtain the best tracking performance of the FTC algorithms.

3. Designing FTC algorithms by combining the sliding mode observer and computed torque control. This is a promising approach to increase tracking performance and to make it easier to apply the algorithm to real-time operating systems.

4. Along with the development of hardware, the computation ability of robotic systems has been increased significantly. Therefore, we can apply complicated algorithms to real-time operating systems. The deep neural network (DNN) with multiple non-linear hidden layers inside has its own potential power in the control system and signal processing to approximate the nonlinear systems.

5. The developed FD methods in this thesis are model-based approaches. The signal-based approaches using vibration signals and current signals are promising and challenging.

Publications

SCI(E) Journals

1. **Nguyen, Van-Cuong**, Anh-Tuan Vo, and Hee-Jun Kang. "A non-singular fast terminal sliding mode control based on third-order sliding mode observer for a class of second-order uncertain nonlinear systems and its application to robot manipulators." IEEE Access 8 (2020): 78109-78120. (**SCIE**)
2. **Nguyen, Van-Cuong**, Anh-Tuan Vo, and Hee-Jun Kang. "A finite-time fault-tolerant control using non-singular fast terminal sliding mode control and third-order sliding mode observer for robotic manipulators." IEEE Access 9 (2021): 31225-31235. (**SCIE**)
3. **Nguyen, Van-Cuong**, Phu-Nguyen Le, and Hee-Jun Kang. "An Active Fault-Tolerant Control for Robotic Manipulators Using Adaptive Non-Singular Fast Terminal Sliding Mode Control and Disturbance Observer." Actuators. Vol. 10. No. 12. (2021). (**SCIE**)
4. **Nguyen, Van-Cuong**, Hoang, D. T., Tran, X. T., Van, M., and Kang, H. J. "A Bearing Fault Diagnosis Method Using Multi-Branch Deep Neural Network." Machines 9.12 (2021): 345. (**SCIE**)
5. **Nguyen, Van-Cuong**, and Kang, H. J. "A Novel High-Speed Third-Order Sliding Mode Observer for Fault-Tolerant Control Problem of Robot Manipulators." IEEE Access. (**Under review**)

Conference Papers

1. **Nguyen, Van-Cuong**, and Hee-Jun Kang. "A Robust Fault Diagnosis for the Robot Manipulator using Third Order Sliding Mode Linear Observer." 12th International Forum on Strategic Technology (IFOST), pp.58, 2017.
2. **Nguyen, Van-Cuong**, Anh-Tuan Vo, and Hee-Jun Kang. "A Fault Tolerant Control for Robot Manipulators Using a Neural Network Observer and

a Third-Order Sliding Mode Observer." 21st International Conference on Mechatronics Technology (ICMT 2017), pp. 56-61, 2017.

3. Vo, Anh Tuan, Hee-Jun Kang, and **Nguyen, Van-Cuong**. "An output feedback tracking control based on neural sliding mode and high order sliding mode observer." 2017 10th International Conference on Human System Interactions (HSI). IEEE, 2017.

4. **Nguyen, Van-Cuong**, Anh-Tuan Vo, and Hee-Jun Kang. "Continuous PID sliding mode control based on neural third order sliding mode observer for robotic manipulators." International conference on intelligent computing. Springer, Cham, 2019.

5. **Nguyen, Van-Cuong**, and Hee-Jun Kang. "A fault tolerant control for robotic manipulators using adaptive non-singular fast terminal sliding mode control based on neural third order sliding mode observer." International Conference on Intelligent Computing. Springer, Cham, 2020.

6. **Nguyen, Van-Cuong**, Phu-Nguyen Le, and Hee-Jun Kang. "Model-Free Continuous Fuzzy Terminal Sliding Mode Control for Second-Order Nonlinear Systems." International Conference on Intelligent Computing. Springer, Cham, 2021.

7. **Nguyen, Van-Cuong**, Hee-Jun Kang, Anh-Tuan Vo, and Thanh-Nguyen Truong. "An Adaptive Supper Twisting Algorithm-based Terminal Sliding Mode Control for Robotic Manipulators." ICROS 2021, pp. 7-9, 2021.

8. Vo, Anh Tuan, Hee-Jun Kang, Thanh Nguyen Truong, and **Nguyen, Van-Cuong**. "A New Tracking Control Method of Maglev Systems." ICROS 2021, pp. 40-43, 2021.

9. Truong, Thanh-Nguyen, Hee-Jun Kang, Anh Tuan Vo, and **Nguyen, Van-Cuong**. "A Disturbance Observer-Based Control for Robotic Manipulators." ICROS 2021, pp. 3-6, 2021.

Bibliography

[1] Dechao Chen, Yunong Zhang, and Shuai Li. "Tracking control of robot manipulators with unknown models: A jacobian-matrix-adaption method". In: *IEEE Transactions on Industrial Informatics* 14.7 (2017), pp. 3044–3053.

[2] Long Jin et al. "Robot manipulator control using neural networks: A survey". In: *Neurocomputing* 285 (2018), pp. 23–34.

[3] Meng Zhou et al. "Zonotoptic fault estimation for discrete-time LPV systems with bounded parametric uncertainty". In: *IEEE Transactions on Intelligent Transportation Systems* 21.2 (2019), pp. 690–700.

[4] Hamed Kazemi and Alireza Yazdizadeh. "Optimal state estimation and fault diagnosis for a class of nonlinear systems". In: *IEEE/CAA Journal of Automatica Sinica* (2017).

[5] Iván Salgado and Isaac Chairez. "Adaptive unknown input estimation by sliding modes and differential neural network observer". In: *IEEE Transactions on Neural Networks and Learning Systems* 29.8 (2018), pp. 3499–3509. ISSN: 21622388. DOI: 10.1109/TNNLS.2017.2730847. URL: https://ieeexplore.ieee.org/abstract/document/8010905/.

[6] Farzaneh Abdollahi, H Ali Talebi, and Rajnikant V Patel. "Stable identification of nonlinear systems using neural networks: Theory and experiments". In: *IEEE/ASME Transactions On Mechatronics* 11.4 (2006), pp. 488–495.

[7] Quang Dan Le and Hee-Jun Kang. "Implementation of Fault-Tolerant Control for a Robot Manipulator Based on Synchronous Sliding Mode Control". In: *Applied Sciences* 10.7 (2020), p. 2534.

[8] Jorge Davila, Leonid Fridman, and Arie Levant. "Second-order sliding-mode observer for mechanical systems". In: *IEEE transactions on automatic control* 50.11 (2005), pp. 1785–1789.

[9] Jaime A Moreno and Marisol Osorio. "A Lyapunov approach to second-order sliding mode controllers and observers". In: *2008 47th IEEE conference on decision and control*. IEEE. 2008, pp. 2856–2861.

[10] Maolin Jin, Jinoh Lee, and Kyung Kwan Ahn. "Continuous nonsingular terminal sliding-mode control of shape memory alloy actuators using time delay estimation". In: *IEEE/ASME Transactions on Mechatronics* 20.2 (2014), pp. 899–909.

[11] Mien Van, Shuzhi Sam Ge, and Hongliang Ren. "Finite Time Fault Tolerant Control for Robot Manipulators Using Time Delay Estimation and Continuous Nonsingular Fast Terminal Sliding Mode Control". In: *IEEE Transactions on Cybernetics* 47.7 (2017), pp. 1681–1693. ISSN: 21682267. DOI: 10.1109/TCYB.2016.2555307. URL: https://ieeexplore.ieee.org/abstract/document/7462227/.

[12] Mien Van et al. "Output feedback tracking control of uncertain robot manipulators via higher-order sliding-mode observer and fuzzy compensator". In: *Journal of Mechanical Science and Technology* 27.8 (2013), pp. 2487–2496.

[13] Anh Tuan Vo, Hee-Jun Kang, and Van-Cuong Nguyen. "An output feedback tracking control based on neural sliding mode and high order sliding mode observer". In: *2017 10th International Conference on Human System Interactions (HSI)*. IEEE. 2017, pp. 161–165.

[14] Van-Cuong Nguyen, Anh-Tuan Vo, and Hee-Jun Kang. "A Finite-Time Fault-Tolerant Control Using Non-Singular Fast Terminal Sliding Mode Control and Third-Order Sliding Mode Observer for Robotic Manipulators". In: *IEEE Access* 9 (2021), pp. 31225–31235.

[15] Qikun Shen et al. "Novel neural networks-based fault tolerant control scheme with fault alarm". In: *IEEE Transactions on Cybernetics* 44.11 (2014), pp. 2190–2201. ISSN: 21682267. DOI: 10.1109/TCYB.2014.2303131. URL: https://ieeexplore.ieee.org/abstract/document/6849489/.

[16] Mien Van, Shuzhi Sam Ge, and Hongliang Ren. "Finite time fault tolerant control for robot manipulators using time delay estimation and continuous nonsingular fast terminal sliding mode control". In: *IEEE transactions on cybernetics* 47.7 (2016), pp. 1681–1693.

[17] Qingsong Xu. "Continuous integral terminal third-order sliding mode motion control for piezoelectric nanopositioning system". In: *IEEE/ASME Transactions on Mechatronics* 22.4 (2017), pp. 1828–1838.

[18] Xuan-Toa Tran et al. "Attitude stabilization of flapping micro-air vehicles via an observer-based sliding mode control method". In: *Aerospace Science and Technology* 76 (2018), pp. 386–393.

[19] Mien Van, Pasquale Franciosa, and Dariusz Ceglarek. "Fault diagnosis and fault-tolerant control of uncertain robot manipulators using high-order sliding mode". In: *Mathematical Problems in Engineering* 2016 (2016).

[20] Mouhacine Benosman and K-Y Lum. "Passive actuators' fault-tolerant control for affine nonlinear systems". In: *IEEE Transactions on Control Systems Technology* 18.1 (2009), pp. 152–163.

[21] Jovan D Stefanovski. "Passive fault tolerant perfect tracking with additive faults". In: *Automatica* 87 (2018), pp. 432–436.

[22] Iman Sadeghzadeh et al. "Active fault tolerant control of a quadrotor uav based on gainscheduled pid control". In: *2012 25th IEEE Canadian Conference on Electrical and Computer Engineering (CCECE)*. IEEE. 2012, pp. 1–4.

[23] Qiang Shen et al. "Active fault-tolerant control system design for spacecraft attitude maneuvers with actuator saturation and faults". In: *IEEE Transactions on Industrial Electronics* 66.5 (2018), pp. 3763–3772.

[24] Anh Tuan Vo and Hee-Jun Kang. "A novel fault-tolerant control method for robot manipulators based on non-singular fast terminal sliding mode control and disturbance observer". In: *IEEE Access* 8 (2020), pp. 109388–109400.

[25] Yongduan Song, Xiucai Huang, and Changyun Wen. "Robust adaptive fault-tolerant PID control of MIMO nonlinear systems with unknown control direction". In: *IEEE Transactions on Industrial Electronics* 64.6 (2017), pp. 4876–4884.

[26] Jinke Zhang and Lei Guo. "Theory and design of PID controller for nonlinear uncertain systems". In: *IEEE Control Systems Letters* 3.3 (2019), pp. 643–648.

[27] Bo Zhao and Yuanchun Li. "Local joint information based active fault tolerant control for reconfigurable manipulator". In: *Nonlinear dynamics* 77.3 (2014), pp. 859–876.

[28] Alain Codourey. "Dynamic modeling of parallel robots for computed-torque control implementation". In: *The International Journal of Robotics Research* 17.12 (1998), pp. 1325–1336.

[29] Mingming Li et al. "Adaptive control of robotic manipulators with unified motion constraints". In: *IEEE Transactions on Systems, Man, and Cybernetics: Systems* 47.1 (2016), pp. 184–194.

[30] Yuxiang Wu et al. "Adaptive neural network control of uncertain robotic manipulators with external disturbance and time-varying output constraints". In: *Neurocomputing* 323 (2019), pp. 108–116.

[31] Fujin Luan et al. "Adaptive neural network control for robotic manipulators with guaranteed finite-time convergence". In: *Neurocomputing* 337 (2019), pp. 153–164. ISSN: 18728286. DOI: 10.1016/j.neucom.2019.01.063. URL: https://www.sciencedirect.com/science/article/pii/S0925231219300906.

[32] Liangyong Wang, Tianyou Chai, and Lianfei Zhai. "Neural-network-based terminal sliding-mode control of robotic manipulators including actuator dynamics". In: *IEEE Transactions on Industrial Electronics* 56.9 (2009), pp. 3296–3304.

[33] M Roopaei and M. Zolghadri Jahromi. "Chattering-free fuzzy sliding mode control in MIMO uncertain systems". In: *Nonlinear Analysis, Theory, Methods and Applications* 71.10 (2009), pp. 4430–4437. ISSN: 0362546X. DOI: 10.1016/j.na.2009.02.132. URL: https://www.sciencedirect.com/science/article/pii/S0362546X09004143.

[34] Song Ling, Huanqing Wang, and Peter X. Liu. "Adaptive fuzzy dynamic surface control of flexible-joint robot systems with input saturation". In: *IEEE/CAA Journal of Automatica Sinica* 6.1 (2019), pp. 97–106. ISSN: 23299274. DOI: 10.1109/JAS.2019.1911330. URL: https://ieeexplore.ieee.org/abstract/document/8600792/.

[35] Mien Van, Xuan Phu Do, and Michalis Mavrovouniotis. "Self-tuning fuzzy PID-nonsingular fast terminal sliding mode control for robust fault tolerant control of robot manipulators". In: *ISA Transactions* 96 (2020), pp. 60–68. ISSN: 00190578. DOI: 10.1016/j.isatra.2019.06.017. URL: https://www.sciencedirect.com/science/article/pii/S0019057819302782.

[36] Quang Phuc Ha, David C Rye, and Hugh F Durrant-Whyte. "Fuzzy moving sliding mode control with application to robotic manipulators". In: *Automatica* 35.4 (1999), pp. 607–616.

[37] Shuanghe Yu et al. "Continuous finite-time control for robotic manipulators with terminal sliding mode". In: *Automatica* 41.11 (2005), pp. 1957–1964.

[38] Shuping He and Jun Song. "Finite-time sliding mode control design for a class of uncertain conic nonlinear systems". In: *IEEE/CAA Journal of Automatica Sinica* 4.4 (2017), pp. 809–816.

[39] Christopher Edwards and Sarah Spurgeon. *Sliding mode control: theory and applications*. Crc Press, 1998.

[40] Vadim I Utkin. *Sliding modes in control and optimization*. Springer Science & Business Media, 2013.

[41] Halim Alwi and Christopher Edwards. "Fault detection and fault-tolerant control of a civil aircraft using a sliding-mode-based scheme". In: *IEEE Transactions on Control Systems Technology* 16.3 (2008), pp. 499–510.

[42] Van-Cuong Nguyen, Anh-Tuan Vo, and Hee-Jun Kang. "Continuous PID Sliding Mode Control Based on Neural Third Order Sliding Mode Observer for Robotic Manipulators". In: *International Conference on Intelligent Computing*. Springer. 2019, pp. 167–178.

[43] Man Zhihong, Andrew P Paplinski, and Hong Ren Wu. "A robust MIMO terminal sliding mode control scheme for rigid robotic manipulators". In: *IEEE transactions on automatic control* 39.12 (1994), pp. 2464–2469.

[44] Hai Wang et al. "Design and implementation of adaptive terminal sliding-mode control on a steer-by-wire equipped road vehicle". In: *IEEE Transactions on Industrial Electronics* 63.9 (2016), pp. 5774–5785.

[45] Van-Cuong Nguyen, Phu-Nguyen Le, and Hee-Jun Kang. "Model-Free Continuous Fuzzy Terminal Sliding Mode Control for Second-Order Nonlinear Systems". In: *International Conference on Intelligent Computing*. Springer. 2021, pp. 245–258.

[46] Saleh Mobayen. "Fast terminal sliding mode controller design for nonlinear second-order systems with time-varying uncertainties". In: *Complexity* 21.2 (2015), pp. 239–244.

[47] Cesar U Solis, Julio B Clempner, and Alexander S Poznyak. "Fast terminal sliding-mode control with an integral filter applied to a Van Der Pol oscillator". In: *IEEE Transactions on Industrial Electronics* 64.7 (2017), pp. 5622–5628.

[48] Tarek Madani, Boubaker Daachi, and Karim Djouani. "Modular-controller-design-based fast terminal sliding mode for articulated exoskeleton systems". In: *IEEE Transactions on Control Systems Technology* 25.3 (2016), pp. 1133–1140.

[49] Chuan-Kai Lin. "Nonsingular terminal sliding mode control of robot manipulators using fuzzy wavelet networks". In: *IEEE Transactions on Fuzzy Systems* 14.6 (2006), pp. 849–859.

[50] Samira Eshghi and Renuganth Varatharajoo. "Nonsingular terminal sliding mode control technique for attitude tracking problem of a small satellite with combined energy and attitude control system (CEACS)". In: *Aerospace science and technology* 76 (2018), pp. 14–26.

[51] Mien Van, Michalis Mavrovouniotis, and Shuzhi Sam Ge. "An adaptive backstepping nonsingular fast terminal sliding mode control for robust fault tolerant control of robot manipulators". In: *IEEE Transactions on Systems, Man, and Cybernetics: Systems* 49.7 (2018), pp. 1448–1458.

[52] Van-Cuong Nguyen, Anh-Tuan Vo, and Hee-Jun Kang. "A Non-singular Fast Terminal Sliding Mode Control Based on Third-Order Sliding Mode Observer for a Class of Second-Order Uncertain Nonlinear Systems and Its Application to Robot Manipulators". In: *IEEE Access* (2020).

[53] Vo Anh Tuan and Hee-Jun Kang. "A new finite time control solution for robotic manipulators based on nonsingular fast terminal sliding variables and the adaptive super-twisting scheme". In: *Journal of Computational and Nonlinear Dynamics* 14.3 (2019).

[54] Van-Cuong Nguyen and Hee-Jun Kang. "A Fault Tolerant Control for Robotic Manipulators Using Adaptive Non-singular Fast Terminal Sliding Mode Control Based on Neural Third Order Sliding Mode Observer". In: *International Conference on Intelligent Computing*. Springer. 2020, pp. 202–212.

[55] Mohammad Hossein Hamedani et al. "Recurrent Fuzzy Wavelet Neural Network Variable Impedance Control of Robotic Manipulators with Fuzzy Gain Dynamic Surface in an Unknown Varied Environment". In: *Fuzzy Sets and Systems* (2020).

[56] S N Huang, Kok Kiong Tan, and Tong Heng Lee. "Automated fault detection and diagnosis in mechanical systems". In: *IEEE Transactions on Systems, Man, and Cybernetics, Part C (Applications and Reviews)* 37.6 (2007), pp. 1360–1364.

[57] Mien Van et al. "A robust fault diagnosis and accommodation scheme for robot manipulators". In: *International Journal of Control, Automation and Systems* 11.2 (2013), pp. 377–388.

[58] Youmin Zhang and Jin Jiang. "Bibliographical review on reconfigurable fault-tolerant control systems". In: *Annual reviews in control* 32.2 (2008), pp. 229–252.

[59] Chengxi Zhang et al. "Fault-Tolerant Attitude Stabilization for Spacecraft with Low-Frequency Actuator Updates: An Integral-Type Event-Triggered Approach". In: *IEEE Transactions on Aerospace and Electronic Systems* (2020).

[60] Chenguang Yang et al. "Finite-time convergence adaptive fuzzy control for dual-arm robot with unknown kinematics and dynamics". In: *IEEE Transactions on Fuzzy Systems* 27.3 (2018), pp. 574–588.

[61] Thanh Nguyen Truong, Anh Tuan Vo, and Hee-Jun Kang. "Implementation of an Adaptive Neural Terminal Sliding Mode for Tracking Control of Magnetic Levitation Systems". In: *IEEE Access* 8 (2020), pp. 206931–206941.

[62] F. Abdollahi, H. A. Talebi, and R. V. Patel. "A stable neural network observer with application to flexible-joint manipulators". In: *ICONIP 2002 - Proceedings of the 9th International Conference on Neural Information Processing: Computational Intelligence for the E-Age* 4 (2002), pp. 1910–1914. DOI: 10.1109/ICONIP.2002.1199006. URL: https://ieeexplore.ieee.org/abstract/document/1593697/.

[63] Xuan-Toa Tran and Hee-Jun Kang. "A Novel Adaptive Finite-Time Control Method for a Class of Uncertain Nonlinear Systems". In: *INTERNATIONAL JOURNAL OF PRECISION ENGINEERING AND MANUFACTURING* 16.13 (2015), pp. 2647–2654. DOI: 10.1007/s12541-015-0339-z. URL: https://link.springer.com/article/10.1007/s12541-015-0339-z.

[64] Zhenyu Gao and Ge Guo. "Fixed-time sliding mode formation control of AUVs based on a disturbance observer". In: *IEEE/CAA Journal of Automatica Sinica* 7.2 (2020), pp. 539–545.

[65] Arun T Vemuri and Marios M Polycarpou. "Neural-network-based robust fault diagnosis in robotic systems". In: *IEEE Transactions on neural networks* 8.6 (1997), pp. 1410–1420.

[66] Luis Angel Castañeda, Alberto Luviano-Juárez, and Isaac Chairez. "Robust Trajectory Tracking of a Delta Robot Through Adaptive Active Disturbance Rejection Control". In: *IEEE Transactions on Control Systems Technology* 23.4 (2015), pp. 1387–1398. ISSN: 10636536. DOI: 10.1109/TCST.2014.2367313. URL: https://ieeexplore.ieee.org/abstract/document/6960100/.

[67] Huanqing Wang, Wen Bai, and Peter Xiaoping Liu. "Finite-time adaptive fault-tolerant control for nonlinear systems with multiple faults".

In: *IEEE/CAA Journal of Automatica Sinica* 6.6 (2019), pp. 1417–1427. ISSN: 23299274. DOI: 10.1109/JAS.2019.1911765. URL: https://ieeexplore.ieee.org/abstract/document/8894752/.

[68] Wei He et al. "Adaptive neural network control of a robotic manipulator with unknown backlash-like hysteresis". In: *IET Control Theory & Applications* 11.4 (2016), pp. 567–575.

[69] Mou Chen and Wen-Hua Chen. "Sliding mode control for a class of uncertain nonlinear system based on disturbance observer". In: *International Journal of Adaptive Control and Signal Processing* 24.1 (2010), pp. 51–64.

[70] Xuan-Toa Tran and Hee-Jun Kang. "Adaptive hybrid high-order terminal sliding mode control of MIMO uncertain nonlinear systems and its application to robot manipulators". In: *International Journal of Precision Engineering and Manufacturing* 16.2 (2015), pp. 255–266.

[71] Mien Van. "An enhanced robust fault tolerant control based on an adaptive fuzzy PID-nonsingular fast terminal sliding mode control for uncertain nonlinear systems". In: *IEEE/ASME Transactions on Mechatronics* 23.3 (2018), pp. 1362–1371.

[72] Anh Tuan Vo and Hee-Jun Kang. "An adaptive neural non-singular fast-terminal sliding-mode control for industrial robotic manipulators". In: *Applied Sciences* 8.12 (2018), p. 2562.

[73] Zhiqiang Ma, Zhengxiong Liu, and Panfeng Huang. "Fractional-order Control for Uncertain Teleoperated Cyber-physical System with Actuator Fault". In: *IEEE/ASME Transactions on Mechatronics* (2020).

[74] Yuqiang Wu, Xinghuo Yu, and Zhihong Man. "Terminal sliding mode control design for uncertain dynamic systems". In: *Systems & Control Letters* 34.5 (1998), pp. 281–287.

[75] Xinghuo Yu and Man Zhihong. "Fast terminal sliding-mode control design for nonlinear dynamical systems". In: *IEEE Transactions on Circuits and Systems I: Fundamental Theory and Applications* 49.2 (2002), pp. 261–264.

[76] Shuanghe Yu, Xinghuo Yu, and Russel Stonier. "Continuous finite-time control for robotic manipulators with terminal sliding modes". In: *Proceedings of the 6th International Conference on Information Fusion, FUSION 2003*. Vol. 2. 2003, pp. 1433–1440. ISBN: 0972184449. DOI: 10.1109/ICIF.2003.177408. URL: https://www.sciencedirect.com/science/article/pii/S000510980500227X.

[77] Yong Feng, Xinghuo Yu, and Zhihong Man. "Non-singular terminal sliding mode control of rigid manipulators". In: *Automatica* 38.12 (2002), pp. 2159–2167. ISSN: 00051098. DOI: 10.1016/S0005-1098(02)00147-4. URL: https://www.sciencedirect.com/science/article/pii/S0005109802001474.

[78] Sendren Sheng Dong Xu, Chih Chiang Chen, and Zheng Lun Wu. "Study of nonsingular fast terminal sliding-mode fault-tolerant control". In: *IEEE Transactions on Industrial Electronics* 62.6 (2015), pp. 3906–3913. ISSN: 02780046. DOI: 10.1109/TIE.2015.2399397. URL: https://ieeexplore.ieee.org/abstract/document/7031407/.

[79] Xiaoyuan Zhu et al. "Cloud-based shaft torque estimation for electric vehicle equipped with integrated motor-transmission system". In: *Mechanical Systems and Signal Processing* 99 (2018), pp. 647–660.

[80] Xiaoyuan Zhu and Wei Li. "Takagi–Sugeno fuzzy model based shaft torque estimation for integrated motor–transmission system". In: *ISA transactions* 93 (2019), pp. 14–22.

[81] Jaemin Baek et al. "A widely adaptive time-delayed control and its application to robot manipulators". In: *IEEE Transactions on Industrial Electronics* 66.7 (2019), pp. 5332–5342. ISSN: 02780046. DOI: 10.1109/TIE.2018.2869347. URL: https://ieeexplore.ieee.org/abstract/document/8464677/.

[82] Fernando A Ortiz-Ricardez, Tonámetl Sánchez, and Jaime A Moreno. "Smooth Lyapunov function and gain design for a second order differentiator". In: *2015 54th IEEE Conference on Decision and Control (CDC)*. IEEE. 2015, pp. 5402–5407.

[83] Yong Feng, Fengling Han, and Xinghuo Yu. "Chattering free full-order sliding-mode control". In: *Automatica* 50.4 (2014), pp. 1310–1314. ISSN: 00051098. DOI: 10.1016/j.automatica.2014.01.004. URL: https://www.sciencedirect.com/science/article/pii/S0005109814000375.

[84] Mien Van, Shuzhi Sam Ge, and Hongliang Ren. "Robust fault-tolerant control for a class of second-order nonlinear systems using an adaptive third-order sliding mode control". In: *IEEE Transactions on Systems, Man, and Cybernetics: Systems* 47.2 (2016), pp. 221–228.

[85] Xuan-Toa Tran and Hee-Jun Kang. "Continuous adaptive finite-time modified function projective lag synchronization of uncertain hyperchaotic systems". In: *Transactions of the Institute of Measurement and Control* 40.3 (2018), pp. 853–860.

[86] Arie Levant. "Higher-order sliding modes, differentiation and output-feedback control". In: *International journal of Control* 76.9-10 (2003), pp. 924–941.

[87] Sanjay P Bhat and Dennis S Bernstein. "Finite-time stability of continuous autonomous systems". In: *SIAM Journal on Control and Optimization* 38.3 (2000), pp. 751–766.

[88] Minh-Duc Tran and Hee-Jun Kang. "Nonsingular terminal sliding mode control of uncertain second-order nonlinear systems". In: *Mathematical Problems in Engineering* 2015 (2015).

[89] Youyi Wang, Lihua Xie, and Carlos E De Souza. "Robust control of a class of uncertain nonlinear systems". In: *Systems & control letters* 19.2 (1992), pp. 139–149.

[90] Bin Xian et al. "A continuous asymptotic tracking control strategy for uncertain nonlinear systems". In: *IEEE Transactions on Automatic Control* 49.7 (2004), pp. 1206–1211.

[91] Marcelo C M Teixeira and Stanislaw H Zak. "Stabilizing controller design for uncertain nonlinear systems using fuzzy models". In: *IEEE Transactions on Fuzzy systems* 7.2 (1999), pp. 133–142.

[92] Jing Zhou, Changyun Wen, and Ying Zhang. "Adaptive backstepping control of a class of uncertain nonlinear systems with unknown backlash-like hysteresis". In: *IEEE transactions on Automatic Control* 49.10 (2004), pp. 1751–1759.

[93] Changyun Wen et al. "Robust adaptive control of uncertain nonlinear systems in the presence of input saturation and external disturbance". In: *IEEE Transactions on Automatic Control* 56.7 (2011), pp. 1672–1678.

[94] Wenxiang Deng, Jianyong Yao, and Dawei Ma. "Adaptive control of input delayed uncertain nonlinear systems with time-varying output constraints". In: *IEEE Access* 5 (2017), pp. 15271–15282.

[95] Hak-Keung Lam, F H Frank Leung, and Peter Kwong-Shun Tam. "Stable and robust fuzzy control for uncertain nonlinear systems". In: *IEEE Transactions on Systems, Man, and Cybernetics-Part A: Systems and Humans* 30.6 (2000), pp. 825–840.

[96] Mien Van, Hee-Jun Kang, and Young-Soo Suh. "A novel neural second-order sliding mode observer for robust fault diagnosis in robot manipulators". In: *International Journal of Precision Engineering and Manufacturing* 14.3 (2013), pp. 397–406.

[97] Liangyong Wang, Tianyou Chai, and Chunyu Yang. "Neural-network-based contouring control for robotic manipulators in operational space". In: *IEEE Transactions on Control Systems Technology* 20.4 (2011), pp. 1073–1080.

[98] Anh Tuan Vo and Hee-Jun Kang. "Adaptive neural integral full-order terminal sliding mode control for an uncertain nonlinear system". In: *IEEE Access* 7 (2019), pp. 42238–42246.

[99] Liang Yang and Jianying Yang. "Nonsingular fast terminal sliding-mode control for nonlinear dynamical systems". In: *International Journal of Robust and Nonlinear Control* 21.16 (2011), pp. 1865–1879.

[100] Maolin Jin, Sang Hoon Kang, and Pyung Hun Chang. "Robust compliant motion control of robot with nonlinear friction using time-delay estimation". In: *IEEE Transactions on Industrial Electronics* 55.1 (2008), pp. 258–269.

[101] Qi Zhou et al. "Observer-based adaptive neural network control for nonlinear stochastic systems with time delay". In: *IEEE Transactions on Neural Networks and Learning Systems* 24.1 (2012), pp. 71–80.

[102] Asif Chalanga et al. "Implementation of super-twisting control: Super-twisting and higher order sliding-mode observer-based approaches". In: *IEEE Transactions on Industrial Electronics* 63.6 (2016), pp. 3677–3685.

[103] Hocine Imine et al. "Rollover risk prediction of heavy vehicle using high-order sliding-mode observer: Experimental results". In: *IEEE Transactions on Vehicular Technology* 63.6 (2013), pp. 2533–2543.

[104] Brian Armstrong, Oussama Khatib, and Joel Burdick. "The explicit dynamic model and inertial parameters of the PUMA 560 arm". In: *Proceedings. 1986 IEEE international conference on robotics and automation*. Vol. 3. IEEE. 1986, pp. 510–518.

[105] Shuang Zhang et al. "Adaptive neural control for robotic manipulators with output constraints and uncertainties". In: *IEEE transactions on neural networks and learning systems* 29.11 (2018), pp. 5554–5564.

[106] Emil Madsen et al. "Adaptive feedforward control of a collaborative industrial robot manipulator using a novel extension of the Generalized Maxwell-Slip friction model". In: *Mechanism and Machine Theory* 155 (2021), p. 104109.

[107] Julian Nubert et al. "Safe and fast tracking on a robot manipulator: Robust mpc and neural network control". In: *IEEE Robotics and Automation Letters* 5.2 (2020), pp. 3050–3057.

[108] Naji Alibeji and Nitin Sharma. "A PID-Type Robust Input Delay Compensation Method for Uncertain Euler–Lagrange Systems". In: *IEEE Transactions on Control Systems Technology* 25.6 (2017), pp. 2235–2242.

[109] Jean-Jacques E Slotine, Weiping Li, and Others. *Applied nonlinear control*. Vol. 199. 1. Prentice hall Englewood Cliffs, NJ, 1991.

[110] Hua O Wang, Kazuo Tanaka, and Michael F Griffin. "An approach to fuzzy control of nonlinear systems: Stability and design issues". In: *IEEE transactions on fuzzy systems* 4.1 (1996), pp. 14–23.

[111] Yongduan Song and Junxia Guo. "Neuro-adaptive fault-tolerant tracking control of Lagrange systems pursuing targets with unknown trajectory". In: *IEEE Transactions on Industrial Electronics* 64.5 (2017), pp. 3913–3920.

[112] D. S. Broomhead and David Lowe. "Multivariable functional interpolation and adaptive networks". In: *Complex Systems* 2 (1988), pp. 321–355.

[113] Shafiqul Islam and Xiaoping P Liu. "Robust sliding mode control for robot manipulators". In: *IEEE Transactions on industrial electronics* 58.6 (2010), pp. 2444–2453.

[114] Qingsong Xu. "Piezoelectric nanopositioning control using second-order discrete-time terminal sliding-mode strategy". In: *IEEE Transactions on industrial electronics* 62.12 (2015), pp. 7738–7748.

[115] Saeed Zaare and Mohammad Reza Soltanpour. "Continuous fuzzy nonsingular terminal sliding mode control of flexible joints robot manipulators based on nonlinear finite time observer in the presence of matched and mismatched uncertainties". In: *Journal of the Franklin Institute* 357.11 (2020), pp. 6539–6570.

[116] Mien Van, Xuan Phu Do, and Michalis Mavrovouniotis. "Self-tuning fuzzy PID-nonsingular fast terminal sliding mode control for robust fault tolerant control of robot manipulators". In: *ISA Transactions* 96 (2020), pp. 60–68. ISSN: 00190578. DOI: 10.1016/j.isatra.2019.06.017. URL: https://www.sciencedirect.com/science/article/pii/S0019057819302782.

[117] Vadim Utkin, Jürgen Guldner, and Jingxin Shi. *Sliding mode control in electro-mechanical systems*. CRC press, 2009.

[118] DONG Ya-Li and M E I Sheng-Wei. "Adaptive observer for a class of nonlinear systems". In: *Acta Automatica Sinica* 33.10 (2007), pp. 1081–1084.

[119] Bin Jiang, Marcel Staroswiecki, and Vincent Cocquempot. "Fault diagnosis based on adaptive observer for a class of non-linear systems with unknown parameters". In: *International Journal of Control* 77.4 (2004), pp. 367–383.

[120] Xingjian Wang et al. "Linear extended state observer-based motion synchronization control for hybrid actuation system of more electric aircraft". In: *Sensors* 17.11 (2017), p. 2444.

[121] Amir Saleki and Mohammad Mehdi Fateh. "Model-free control of electrically driven robot manipulators using an extended state observer". In: *Computers & Electrical Engineering* 87 (2020), p. 106768.